

## All-Sky spectrally matched UBVRI-ZY and u'g'r'i'z' magnitudes for stars in the Tycho2 catalog

A. Pickles and É. Depagne

*Las Cumbres Observatory Global Telescope, Goleta, CA 93117, USA*

apickles@lcogt.net

### ABSTRACT

We present fitted UBVRI-ZY and  $u'g'r'i'z'$  magnitudes, spectral types and distances for 2.4 M stars, derived from synthetic photometry of a library spectrum that best matches the Tycho2  $B_T V_T$ , NOMAD  $R_N$  and 2MASS  $JHK_{2/S}$  catalog magnitudes. We present similarly synthesized multi-filter magnitudes, types and distances for 4.8 M stars with 2MASS and SDSS photometry to  $g < 16$  within the Sloan survey region, for Landolt and Sloan primary standards, and for Sloan Northern (PT) and Southern secondary standards.

The synthetic magnitude zeropoints for  $B_T V_T$ ,  $UBVRI$ ,  $Z_V Y_V$ ,  $JHK_{2/S}$ ,  $JHK_{MKO}$ , Stromgren  $uvby$ , Sloan  $u'g'r'i'z'$  and  $ugriz$  are calibrated on 20 *calspec* spectrophotometric standards. The  $UBVRI$  and  $ugriz$  zeropoints have dispersions of 1–3%, for standards covering a range of color from  $-0.3 < V - I < 4.6$ ; those for other filters are in the range 2–5%.

The spectrally matched fits to Tycho2 stars provide estimated  $1\sigma$  errors per star of  $\sim 0.2$ , 0.15, 0.12, 0.10 and 0.08 mags respectively in either  $UBVRI$  or  $u'g'r'i'z'$ ; those for at least 70% of the SDSS survey region to  $g < 16$  have estimated  $1\sigma$  errors per star of  $\sim 0.2$ , 0.06, 0.04, 0.04, 0.05 in  $u'g'r'i'z'$  or  $UBVRI$ .

The density of Tycho2 stars, averaging about 60 stars per square degree, provides sufficient stars to enable automatic flux calibrations for most digital images with fields of view of 0.5 degree or more. Using several such standards per field, automatic flux calibration can be achieved to a few percent in any filter, at any airmass, in most workable observing conditions, to facilitate inter-comparison of data from different sites, telescopes and instruments.

*Subject headings:* Stars, Data Analysis and Techniques

## 1. Introduction

Reliable flux calibration is important for accurate photometry, and to compare observations taken by different observers, at different times or different sites, with different equipment and possibly different filter bandpasses.

Ground based optical calibration is traditionally achieved by observing with the same equipment both standard stars and at least some stars in the field of interest, during periods known to be photometric. In principle this permits calibration of program stars on a standard photometric system to better than 1%, but in practice filter and instrumental mismatches, atmospheric and other variations during this process often limits effective calibration to 2% or worse.

Internal relative flux calibration of single or repeated data sets are routinely achieved to 0.2% or better, including during non-photometric conditions, by reference to non-variable stars in the observed field. But significant questions arise about effective cross calibration of observations from different epochs. The situation is particularly complicated for time-domain science, where multiple sites, telescope apertures, filters and sets of instrumentation become involved, or when time constraints or observing conditions preclude traditional calibrations. Offsets between otherwise very accurate data sets can be much larger than expected. This can introduce significant uncertainty in multi-observation analysis, or obscure real variations.

Cross comparisons can be facilitated by parallel wide-field observations along the line of sight to each image, as in the CFHT skyprobe facility (Cuillandre et al 2004)<sup>1</sup>, or other “context” camera systems. But having multi-filter standards within each digital image offers many simplifying advantages. The ideal scenario for calibration of optical imaging data would be if there were all-sky stars of adequately known brightness on standard photometric systems, and present in sufficient numbers to provide a few in every digital image.

Precursors to such standards include i) the Sloan Digital Sky Survey (SDSS) of 360 million objects, observed with a 2.5m telescope to about 22 mag in *ugriz* filters and covering about 1/4 of the sky (Gunn et al 1998)<sup>2</sup>, ii) the 2MASS whole sky survey of about 300 million stars observed with two 1.3m telescopes to about 15 mag in *JHK<sub>2/S</sub>* filters (Cutri 1998)<sup>3</sup>, and iii) the USNO NOMAD catalog (Zacharias et al 2004)<sup>4</sup>, which contains over 1

---

<sup>1</sup><http://www.cfht.hawaii.edu/Instruments/Skyprobe/>

<sup>2</sup><http://www.sdss.org/dr7/>

<sup>3</sup><http://www.ipac.caltech.edu/2mass/overview/about2mass.html>

<sup>4</sup><http://www.nofs.navy.mil/nomad/>

billion stars covering the whole sky. It is often used for automatic astrometric fits, and has calibrated photographic  $R_N$ -band photometry (on the Landolt system) with a dispersion of about 0.25 mag.

The Tycho2 catalog (Høg et al 2000) provides a consistent set of all-sky optical standards, observed with the *Hipparcos*<sup>5</sup> satellite. It provides  $\sim 2.5$  million stars to about 13.5 & 12.5 mag in  $B_T$  &  $V_T$  filters. While this catalog contains less than 1% of the stars in the 2MASS catalog, and has large photometric errors at the faint end, it forms the basis along with 2MASS and NOMAD for an effective and consistent all-sky photometric catalog, that can be used now by many optical telescopes to achieve reasonable automatic flux calibration.

The average density of Tycho2 stars varies from  $\sim 150$  stars per square degree at galactic latitude  $b = 0$  deg, through  $\sim 50$  stars per square degree at  $|b| = 30$  deg to  $\sim 25$  stars per square degree at  $|b| = 90$  deg (Høg et al 2000), so it is typically possible to find 5–15 Tycho2 stars within a 30-arcmin field of view. These numbers obviously decrease for smaller fields of view, and become uninteresting for fields of view much smaller than 15-arcmin. The footprints in equatorial coordinates of several catalogs discussed here are shown in figure 1.

Ofek (2008) described how to produce synthetic  $g'r'i'z'$  magnitudes for about 1.6 M Tycho2 stars brighter than 12 mag in  $V_T$  and 13 mag in  $B_T$ . The present paper extends this to 2.4 M Tycho2 stars, with synthetic magnitudes on both the Landolt and Sloan standard photometric systems, and to other filter systems calibrated here such as Stromgren and UKIRT  $ZY$  &  $JHK_{MKO}$ <sup>6</sup>. The methodology permits *post facto* extrapolation to other filter systems of interest, and can be applied to future all-sky catalogs of greater depth and accuracy.

In section 2 we describe our calculations of synthetic magnitudes and fluxes from flux calibrated digital spectra.

In section 3 we describe the zeropoint calibration of our synthetic photometry against the *de facto* standard: 20 spectrophotometric standards with photometric data and covering a significant color range, taken from the Hubble Space Telescope (HST) *calspec*<sup>7</sup> project.

In section 4 we describe the spectral matching library and calibrated magnitudes in different filter systems:  $B_T V_T$ ,  $UBVRI$ ,  $J_2 H_2 K_{2/S}$ , UKIRT  $ZY$  and  $JHK_{MKO}$ , Stromgren *uvby* and Sloan filter sets, both primed and unprimed system bandpasses.

---

<sup>5</sup><http://www.rssd.esa.int/index.php?project=HIPPARCOS>

<sup>6</sup>[http://www.jach.hawaii.edu/UKIRT/astronomy/calib/phot\\_cal/](http://www.jach.hawaii.edu/UKIRT/astronomy/calib/phot_cal/)

<sup>7</sup><http://www.stsci.edu/hst/observatory/cdbs/calspec.html>

In section 5 we describe the spectral matching process, chi-square optimization and distance constraints.

In section 6 we illustrate the spectral matching and flux fitting methodology with results fitted with different combinations of optical and infrared colors for Landolt and Sloan primary standards.

In section 7 we further illustrate the strengths and limitations of the spectral fitting method with  $\sim 16000$  Southern Sloan standards (Smith et al 2005),  $\sim 1$  M SDSS PT secondary patch standards (Tucker et al 2006; Davenport et al 2007) with 2MASS magnitudes, and  $\sim 11000$  of those which also have Tycho2  $B_T V_T$  magnitudes and NOMAD  $R_N$  magnitudes.

In section 8 we describe online catalogs with fitted types, distances and magnitudes in UBVRI-ZY and u'g'r'i'z' for: i) Landolt and Sloan primary standards, ii) Sloan secondary North and South standards, iii) 2.4 M Tycho2 stars and iv) 4.8 M stars within the Sloan survey region to  $g < 16$ .

## 2. Synthetic Photometry

Bessell (2005) describes the preferred method for convolving an  $F(\lambda)$  digital spectrum with filter/system bandpass sensitivity functions to obtain synthetic magnitudes that take account of the photon-counting nature of modern detectors.

$$N_{photons} = \int (F(\lambda)/h\nu) \cdot S_b(\lambda) \cdot d\lambda = \int (\lambda \cdot F(\lambda)/hc) \cdot S_b(\lambda) \cdot d\lambda$$

which can be normalized by the filter/system bandpass to form the weighted mean photon flux density

$$\langle \lambda \cdot F(\lambda)_b \rangle = \int \lambda \cdot F(\lambda) \cdot S_b(\lambda) \cdot d\lambda / \int (\lambda \cdot S_b(\lambda) \cdot d\lambda)$$

As Bessell (2005) notes, this weights the fluxes by the wavelength, and shifts the effective wavelength of the bandpass to the red. This is the basic convolution methodology used in the HST *synphot*<sup>8</sup> package. From the Synphot User's Guide we can form:

$$mag_\lambda(b) = -2.5 * \log_{10} \langle \lambda \cdot F(\lambda)_b \rangle - 21.1$$

where the numerical factor for the nominal  $F(\lambda)$  at  $V=0$  brings the resultant magnitudes

---

<sup>8</sup>[http://www.stsci.edu/resources/software\\_hardware/stsdas/synphot](http://www.stsci.edu/resources/software_hardware/stsdas/synphot)

close to standard values<sup>9</sup>. Additionally, as discussed in the “Principles of Calibration” section of the Synphot User’s Guide, we can form the effective wavelength

$$\langle \text{efflam} \rangle = \int F(\lambda).S_b(\lambda).\lambda^2.d\lambda / \int F(\lambda).S_b(\lambda).\lambda.d\lambda$$

and the source-independent pivot wavelength

$$\lambda_{pivot} = \sqrt{\frac{\int S_b(\lambda).\lambda.d\lambda}{\int S_b(\lambda).d\lambda/\lambda}}$$

and form a magnitude system based on  $F(\nu)$  as

$$mag_\nu(b) = mag_\lambda(b) - 5 * \log_{10}\lambda_{pivot} + 18.692 - ZeroPoint_b \quad (1)$$

where the numeric constant, as derived in Sirianni et al (2005), has the advantage of bringing  $mag_\nu$  close to the AB79 system of Oke & Gunn (1983). The bandpass zeropoints in equation 1 are to be determined.

Pickles (1998) adopted a different approach based on mean flux per frequency in the bandpass  $\langle F(\nu) \rangle$ . The differences between this and the *synphot* methods for calculating magnitudes are typically of order 0.02 to 0.04 mag over most of the color range, but for very red stars with non-smooth spectra can become as large as 0.1 mag in  $R$ , which has an extended red tail. Importantly, the *synphot* approach produces less zeropoint dispersion for stars covering a wide range of type and color, and is adopted here.

### 3. Filters and zeropoints based on spectrophotometric standards

All the filter-bands discussed here (except the medium-band Stromgren filters) are illustrated in figure 2. Only the wavelength coverage and particularly the *shape* of the system bandpass matters, not the height, which is taken out in the filter normalization.

Our approach is similar to that presented by Holberg & Bergeron (2006) but deliberately attempts to calibrate a large number of filters with standards covering a wide range of color and spectral type. The small zeropoint dispersions achieved here demonstrate the validity of this approach over a wide variety of spectral types and colors. They reinforce the advances that have been made in accurate flux calibration, as the result of careful work by Bohlin (1996); Colina & Bohlin (1997); Bohlin et al (2001); Bohlin (2010).

---

<sup>9</sup>21.0999 =  $-2.5 * \log_{10}(3631e^{-12}erg.cm^{-2}.s^{-1}.A^{-1})$

### 3.1. Calspec standards

There are 13 standards with STIS\_NIC\_003 calibrated spectrophotometry covering 0.1 to  $2.5\mu$ , which include the latest HST *calspec* calibration enhancements, and the 2010 corrections to STIS gain settings. The spectra are mainly of white dwarfs, but include four G dwarfs and VB8(=LHS 429, a late M dwarf) so provide significant color range:  $-0.3 < V - I < 4.6$ .

There are two K giants (KF08T3, KF06T1) with low reddening which were observed with NICMOS to provide IRAC calibration (Reach et al 2005). There is little optical standard photometry for these two K giants, so they are only included in the 2MASS  $JHK_{2/S}$  zeropoint averages, but optical colors estimated from their types are shown to be consistent with the derived optical zeropoints.

There are three additional *calspec* white dwarfs with coverage to  $\sim 1\mu$  (G93-48, GD 50, Feige 34), and two subdwarfs (G158-100, BD +26 2606) observed by Oke (1990) and Oke & Gunn (1983) for which fairly extensive photometric data are available in the literature. The latter 5 spectra calibrated from the uv to  $\sim 1\mu$ , were extended to  $2.5\mu$  for illustrative purposes. Their synthetic infrared magnitudes are computed and shown for comparison, but only their optical zeropoints are combined in the averages.

### 3.2. Standard Catalog Magnitudes

The matching “catalog” photometric data for *calspec* standards comes from i) the Tycho2 catalog for  $B_T V_T$ , ii) the 2MASS catalog for  $J_2 H_2 K_{2/S}$ , iii)  $UBVRI$  data from Landolt (2009) for GD 71 (DA1), G93-48 (DA3) & GD 50 (DA2), and Landolt & Uomoto (2007) for G191-B2B (DA0), BD +17 4708 (sdF8), BD +26 2606 (sdF), AGK +81 266 (sdO), GRW +70 5824 (DA3), LDS 749B (DBQ4), Feige 110 (DOp), Feige 34 (DA) & G158-100 (sdG), iv) from Bessell (1991) for optical and infrared photometry of VB8 (M7V), v) from the UKIRT standards listed on the JAC/UKIRT website<sup>10</sup> for  $JHK_{MKO}$  and their WFCAM  $ZY_{MKO}$  data, and vi) from Wegner (1983), Lacombe & Fontaine (1981) and Hauck & Mermilliod (1998) for Stromgren standards (white dwarfs). All the above catalog data are on the “vega” system where the magnitudes of Vega are nominally zero in all bands.

Sloan catalog (vii) data on the AB system are from Smith et al (2002) for primary standards, from the SDSS\_PT catalog (Tucker et al 2006; Davenport et al 2007) and Southern

---

<sup>10</sup>[http://www.jach.hawaii.edu/UKIRT/astrometry/calib/phot\\_cal/](http://www.jach.hawaii.edu/UKIRT/astrometry/calib/phot_cal/)

SDSS standards (Smith et al 2005), from the SDSS DR7 database<sup>11</sup> for LDS 749B, VB8, GD 50, and in 2 cases (G191-B2B & GD 71) from Holberg & Bergeron (2006) for  $u'g'r'i'z'$  magnitudes.

Additional  $UBVRI$  and  $ugriz$  photometric data for GD 153 (DA0) are from Holberg & Bergeron (2006). Additional  $BV$  data for P041C, P177D, P330E (G0 V), KF08T3 (K0.5 III) and KF06T1 (K1.5 III) are from the *calspec* website.

Photometric data for the *calspec* standards are summarized in tables 1 and 2.

In electronic table *AllFlx* we have computed mean fluxes and synthetic magnitudes by equation 1 in the system bandpasses of all the filters for up to 20 standards which have both accurate digital spectra available from *calspec*, and measured photometry from the literature. Table *AllFlx* lists for each spectrum and filter all the digitally measured spectrophotometric data including: average wavelengths  $\langle \lambda \rangle$ , effective wavelengths  $\langle \text{efflam} \rangle$ , pivot wavelengths (which are the same for each star), mean fluxes  $\langle F(\lambda) \rangle$ ,  $\langle \lambda.F(\lambda) \rangle$  and  $\langle F(\nu) \rangle$ , and catalog magnitudes from the literature where available, with quoted errors.

For each standard and each filter, magnitudes have been computed via equation 1, and the zeropoints calculated to match synthetic to observed magnitudes. The calculated values are listed in electronic table *SynZero*.

### 3.3. Zeropoint means and dispersions

In table 3 we summarize for each filter the synthesized pivot wavelengths, zeropoint means and dispersions, adopted zeropoints, measured magnitudes and fluxes of the STIS\_005 *calspec* spectrum of Vega, and our derived values of  $\langle F(\nu) \rangle$  for 0-magnitude in all filters.

Figure 3 shows the filter bands over-plotted on the the STIS\_005 *calspec* spectrum of Vega, plotted as  $F(\nu)$  vs. wavelength. The spectrum illustrates the nominal 0-mag definition for filters on the *vega* system, and the horizontal line at 3631 Jy illustrates the AB=0 mag reference. The points show our synthesized Vega magnitudes from column 7 of table 3, and the error bars show our zeropoint  $\pm 2\sigma$  dispersion errors from column 5 of table 3. The electronic versions of these figures are in color.

Some uncertain zeropoint values in electronic table *SynZero* are marked with a colon “xxx:” to indicate they are derived from catalog photometry (in tables 1, 2 & electronic table

---

<sup>11</sup><http://www.sdss.org/dr7/>

*AllFlt*) which is uncertain by 0.1 mag or more. Zeropoint values enclosed in parentheses indicate values which are *not* used to form the final zeropoints. Either they are photometric estimates, or literature values which are out of range, as discussed in the text. The number of standards included in each filter zeropoint calculation ranges from 5 for  $V_T$  to 17 for  $B$  and  $V$ .

The 2MASS and SDSS coordinates of VB8 differ by 7.4-arcsec, corresponding to the large proper motion (-0.77, -0.87 arcsec/year) for this star between the epochs of the two surveys. We obtain good VB8 zeropoint fits for  $BVRI$ ,  $J_2H_2K_2/S$  and  $HK_{MKO}$  and  $grz$ , but not for  $J_{MKO}$ ,  $u$  or  $i$  bands (see also section 3.6). There is no U-band photometry for VB8.

### 3.4. Choice of Landolt synthetic filter bandpasses

For  $UBVRI$  we tested several possible synthetic system bandpass profiles from the literature. We have made an empirical choice of the best system bandpass(es) that minimize zeropoint scatter in the fitted mean zeropoints for each filter, over the full color range.

In table 3, we list zeropoints for  $UBVRI$  using both Landolt (system) filter response functions convolved with a typical atmosphere and detector response (Cohen et al 2003a), and synthetic system bandpasses for  $U_MB_MV_M$  from Maiz Apellániz (2006) and  $V_C R_C I_C$  from Bessell (1979).

It may seem that the Landolt system response curves would provide the optimum synthetic matches to Landolt photometry, but this is not necessarily the case, and not shown by our results in table 3 and illustrated in figure 4.

Both Landolt and Kron-Cousins measurements seek to emulate the original Johnson system for UB $V$ . Both apply calibrating steps in terms of color to their instrumental magnitudes, to bring them into correspondence with standard system values extending back several decades. These steps are summarized in Landolt (2007) for example, and in Landolt (1983, 1992a,b, 2009) to illustrate how equipment changes over time have required slightly different color corrections to maintain integrity with the original system definition. These calibration steps are further reviewed in Sung & Bessell (2000).

Real photometry is done with bandpasses that can vary with evolving instrumentation. We could measure synthetic magnitudes in the Landolt bandpasses and apply color corrections to achieve “standard” values. But synthetic photometry of flux calibrated spectra has the advantage of being able to select bandpass profiles that minimize dispersion and color

effects. We have not attempted to optimize any bandpasses here, but have selected among those available from the literature. For *UBVRI*, the results in table 3 indicate that these are best provided by the  $U_M B_M V_C R_C I_C$  bandpasses.

The zeropoint dispersions are 0.027, 0.020, 0.008, 0.014 and 0.016 mag for  $U_M B_M V_C R_C I_C$  respectively in table 3, for the full color range from White Dwarfs to VB8 ( $-0.3 < V - I < 4.6$ ). The effective wavelengths vary from 355 to 371 nm, 432 to 472 nm, 542 to 558 nm, 640 to 738 nm and 785 to 805 nm for  $U_M B_M V_C R_C I_C$  respectively, between White Dwarfs and VB8. Figure 4 illustrates that the selected bands show much less zeropoint dispersion than do  $U_L B_L V_L R_L I_L$ , with negligible trend with color. In figure 4 (and for other zeropoint figures) the ordinate is inverted so that zeropoints that appear vertically higher result in larger (fainter) magnitudes.

This is *not* a criticism of Landolt system response curves, which enable accurate photometry with appropriate calibration and color corrections, but indicates that the selected  $U_M B_M V_C R_C I_C$  system profiles are best for deriving synthetic spectrophotometry of flux calibrated spectra to properly match Landolt photometry.

The zeropoint dispersions for  $U_3 B_3$  from Azusienis & Straizys (1969); Buser (1978) are worse, at 0.050 and 0.024 mag respectively. The dispersion for  $V_M$  is marginally worse than for  $V_C$ , where  $V_C$  has a slightly more elongated red tail than  $V_M$ .

The zeropoint dispersions for *UBVRI* and *ugriz* (primed and unprimed) in table 3, typically closer to 0.02 mag than 0.01 mag, indicate both the accuracy and the limitations of comparing synthetic photometry of well calibrated spectra with good standard photometry. Tighter fits can be obtained by restricting the selection of comparison stars, for instance to only WD standards, but such zeropoints can then be a function of color and lead to synthesized magnitude errors for other stellar types much larger than the nominal dispersion for a restricted set of standards.

We are gratified that these comparisons match so well over a large range of color and standard types, confirming the increasing correspondence (currently at the 1–3% level) between spectrophotometric and photometric standards. This sets the basis for enabling synthetic magnitudes of an extended spectral library to be calibrated on standard photometric systems.

### 3.5. Other synthetic filter zeropoints on the Vega system

The system transmission functions for  $B_T V_T$  have been taken from Maiz Apellániz (2006). The zeropoint dispersions for  $B_T V_T$  are 0.045 and 0.020 respectively, which is acceptable given the typical errors in the photometric values for fainter stars, and several stars included here. There are a total of 7 values covering a color range from white dwarfs to G dwarfs for  $B_T$ , but only 5 with accurate  $V_T$  information, with HD209458 (G0 V – out of planet occultation) being the reddest comparison standard for  $B_T V_T$ .

The filter transmission functions for  $ZY$  have been taken from the *Vista* website<sup>12</sup>. In what follows we refer to (upper case)  $Z_V Y_V$  for these filter bandpasses, where we are using the subscript “V” to refer to both the VISTA/UKIDSS consortium and the fact that these are *vega* based magnitudes. The UKIRT WFCAM detector QE is not included in the system bandpass but, unlike a CCD, is roughly flat over these wavelengths<sup>13</sup>. The dispersions for  $Z_V Y_V$  zeropoints, compared to only 5 and 4 UKIRT standards measured with the WFCAM filters, are 0.038 and 0.031 mag respectively. The  $Y_V$  zeropoint for G158-100 is suspect as its *calspec* spectrum is not well defined at  $1\mu$ .  $Z_V Y_V$  zeropoint determinations may improve as more photometric standards in common with spectrophotometric standards are measured. The zeropoint results and somewhat restricted color ranges for  $B_T V_T Z_V Y_V$  are illustrated in figure 5.

Having a wider color range here for comparison would clearly be advantageous, but there are several mitigating factors. The  $B_T$  and  $Z_V Y_V$  bandpasses are more “rectangular” in shape than are the  $B$  and  $z$  bandpasses for example. They have effective wavelengths that vary less with color, and are therefore less susceptible to color effects suffered by filters with extended “tails”. The range of effective wavelengths from white dwarfs to VB8 are 416.3 to 440.4 nm, 524.3 to 543.1 nm, 875.1 to 884.9 nm, and 1018.8 to 1023.2 nm for  $B_T V_T Z_V Y_V$  respectively. Also the  $B_T - V_T$  colors derived from our synthesized *LibMags* flux library (see section 4) follow the standard Tycho2 conversion formulas<sup>14</sup>, with standard deviations less than 0.02 & 0.03 mag respectively over a large color range.

$$V = V_T - 0.09 * (B_T - V_T)$$

$$B - V = 0.85 * (B_T - V_T)$$

Similarly, as shown in section 6.1.1, the synthesized  $Z_V$  and  $z'$  data fit well over a wide

---

<sup>12</sup><http://www.vista.ac.uk/Files/filters>

<sup>13</sup><http://www.ukidss.org/technical/technical.html>

<sup>14</sup><http://heasarc.nasa.gov/W3Browse/all/tycho2.html>

color range, indicating an extended range of validity beyond that illustrated in figure 5.

The  $Y_V$  data are included because several survey cameras (PanStarrs<sup>15</sup>, SkyMapper<sup>16</sup>, Dark Energy Survey (DES)<sup>17</sup>, UKIDSS/VISTA<sup>18</sup> and our LCOGT<sup>19</sup> monitoring cameras are using or plan to use a Y filter at  $\sim 1$  micron. This is further discussed in section 6.1.1.

The transmission functions of the 2MASS filters, including detector and typical atmosphere, have been taken from the *IPAC* website<sup>20</sup>. The zeropoint dispersions for  $J_2H_2K_{2/S}$ , indicated graphically in figure 6, are about 0.02 mag, quite comparable to the typical (low) 2MASS errors for these stars, and the zeropoints show no trend with color.

The transmission functions for the JHK filters on the Mauna Kea Observatory (MKO) system have been taken from Tokunaga et al (2002). Unlike the 2MASS system bandpasses, these do not include detector QE or atmosphere. The zeropoint dispersions for  $JHK_{MKO}$  are 0.02, 0.02 and 0.04 respectively, for relatively few standards, but they do show trends with color. We indicate the  $J_{MKO}$  zeropoint for VB8 in figure 6 but, due to uncertainty with its catalog magnitude, have not included it in the  $J_{MKO}$  zeropoint average.

The transmission functions for the Stromgren filters (not illustrated) are from Maiz Apellániz (2006). The zeropoints derived in table 3 are  $-0.29 \pm 0.04$ ,  $-0.32 \pm 0.01$ ,  $-0.18 \pm 0.02$  and  $-0.04 \pm 0.03$  for Stromgren *uvby* respectively. These are averaged over 7 *calspec* white dwarfs for which Stromgren photometry was found in the literature. The validity of these zeropoints for redder stars is not demonstrated, but the effective wavelength variations with color are small for medium band filters with “rectangular” profiles, so zeropoint variations with color should not be large for the Stromgren filter bandpasses.

### 3.5.1. Mould R-band

The  $R_p$  filter system profile shown in figure 2 is a “Mould” R-band interference filter with rectangular profile, of the type used at many observatories to measure R on the Landolt

---

<sup>15</sup><http://pan-starrs.ifa.hawaii.edu/public/>

<sup>16</sup><http://rsaa.anu.edu.au/skymapper/>

<sup>17</sup><https://www.darkenergysurvey.org/>

<sup>18</sup><http://www.vista.ac.uk>

<sup>19</sup><http://lcogt.net>

<sup>20</sup><http://www.ipac.caltech.edu/2mass/overview/about2mass.html>

system. In this case it is the CFH12K 7603 filter originally from CFHT<sup>21</sup> and now used by PTF<sup>22</sup>. The  $R_p$  system profile includes the CCD response and atmospheric transmission appropriate to 1.7 km and Airmass 1.3, although both of these are roughly flat in this region. The zeropoint (table 3) for this filter profile excludes VB8, since the lack of a red-tail results in magnitudes which are too faint for stars redder than  $R - I > 0.6$ .

Figure 8 shows (upper panel) the comparison of  $R_p - R_C$  with Landolt  $R - I$  color, which results in a tight 2-segment curved fit. The lower two panels show  $R_p - R_C$  and  $R_p - r'$  against the Sloan  $r' - i'$  color, both of which show reasonable 2-segment linear fits, confirming that rectangular-shaped “Mould” R observations can be reliably converted to standard R magnitudes.

$$R_p \sim R_C - 0.022 - 0.092 * (r' - i') \quad (r' - i') < 0.56$$

$$R_p \sim R_C - 0.202 - 0.227 * (r' - i') \quad (r' - i') > 0.56$$

$$R_p \sim r' - 0.198 - 0.318 * (r' - i') \quad (r' - i') < 0.36$$

$$R_p \sim r' - 0.227 - 0.220 * (r' - i') \quad (r' - i') > 0.36$$

### 3.5.2. NOMAD R-band

The USNO NOMAD catalog (Zacharias et al 2004) contains BVR and JHK data for many stars. The NOMAD  $BV$  data for brighter stars are typically derived from Tycho2  $B_T V_T$  using standard conversion formulas referenced in section 3.5. It is possible to compare these converted values with synthesized BV magnitudes, but it is better and more accurate to compare as we have done the Tycho2  $B_T V_T$  values directly with their synthesized values in the  $B_T V_T$  system bandpasses. The NOMAD JHK magnitudes are from 2MASS, so do not provide additional information.

The NOMAD R-band data are derived from the USNO-B catalog which was photometrically calibrated against Tycho2 stars at the bright end, and two fainter catalogs as described in Monet et al (2003), with a typical standard deviation of 0.25 mag.

Figure 9 illustrates our comparison of NOMAD R-band data against Landolt standards, and 16 *calspec* standards. The data are plotted as the differences  $R_{Nomad} - R_{Landolt}$  vs.  $R_{Landolt}$ . A  $3\sigma$  clip has been applied which excludes about 10 stars plotted as black crosses,

---

<sup>21</sup><http://www.cfht.hawaii.edu/Instruments/Filters/>

<sup>22</sup><http://www.astro.caltech.edu/ptf/>

but retains more than 98% plotted as grey (red in electronic color version) crosses. The dashed histogram of all the stars shows the distribution of these differences plotted with increasing number to the right against the magnitude delta on the ordinate. This shows a good one-to-one fit, with zero mean offset and a  $1\sigma$  dispersion of 0.25 mag for sigma clipped Landolt stars. The equivalent dispersion is 0.17 mag for the *calspec* stars excluding VB8. The location of the red M dwarf VB8 is indicated: the photographic R band, like the “Mould” type R-band above lacks the red-tail of the Kron/Cousins/Landolt R filter, so measures magnitudes which are too faint for extremely red stars where the flux is rising rapidly through the bandpass.

It would be preferable to compare digitized photographic R-magnitudes with synthesized values in the appropriate system bandpass, but this is clearly impossible, and probably would not improve this calibration. The NOMAD R-band calibration is linear over a significant magnitude range and the dispersion is roughly constant with magnitude, probably indicating the difficulties of measuring digitized plates rather than any linearity or systemic calibration issues.

In section 5 we include the NOMAD  $R_N$  band data together with Tycho2 and 2MASS magnitudes to provide 6-band spectral matching of the Tycho2 stars, where the catalog  $R_N$  is matched to our synthesized  $R_C$  magnitude, because inclusion does improve the fits slightly over just Tycho2/2MASS fits. We adopt a photometric error of 0.25 mag for all NOMAD  $R_N$  magnitudes.

### 3.6. Sloan filters on the AB system

The system transmission functions of the unprimed *ugriz* filters used in the imaging camera, including typical atmosphere and detector response, have been taken from the *sky-service* website<sup>23</sup> at Johns Hopkins University (JHU). Those for the primed  $u'g'r'i'z'$  filters used for standard observations have been taken from the United States Naval Observatory (USNO) website<sup>24</sup>, for 1.3 airmasses.

In order to compute zeropoints for the imaging survey (unprimed) Sloan bandpasses *ugriz*, we computed conversion relations between the primed and unprimed Sloan system values by comparing synthetic magnitudes of digital library spectra from Pickles (1998), as listed in electronic table *LibMags* (section 4). This approach avoids many complexities

---

<sup>23</sup><http://skyservice.pha.jhu.edu>

<sup>24</sup><http://www-star.fnal.gov/ugriz/Filters/response.html>

detailed in Tucker et al (2006); Davenport et al (2007), but produces tight correspondence between synthetically derived Sloan primed and unprimed magnitudes, over a wide color range.

With the exception of two zeropoint adjustments for  $g$  and  $r$ , these relations are identical to those listed on the SDSS site<sup>25</sup>, and are summarized here.

$$\begin{aligned}
 u &= u' & (\sigma = 0.011) \\
 g &= 0.037 + g' + 0.060 * (g' - r' - 0.53) & (\sigma = 0.012) \\
 r &= 0.010 + r' + 0.035 * (r' - i' - 0.21) & (\sigma = 0.007) \\
 i &= i' + 0.041 * (r' - i' - 0.21) & (\sigma = 0.015) \\
 z &= z' & (\sigma = 0.003)
 \end{aligned}$$

These relations were used to convert SDSS standard values on the primed system to unprimed values (and *vice versa* when only DR7 data was available, eg. for LDS 749B, P177D, P330E & GD 50) then compared with synthetic magnitudes computed in the unprimed bandpasses to derive their zeropoints and dispersions.

The SDSS DR7 u-band data for VB8 appears too bright, likely because of the known red leak. The DR7 i-band magnitude is close to the r-band magnitude, and appears too faint for such a red star. As mentioned in section 3.2 we have omitted the  $u$  and  $i$  band data for VB8 from our zeropoint averages.

The zeropoint dispersions for  $u'g'r'i'z'$  and  $ugriz$  listed in table 3 are about 0.02 mag (slightly worse for the g-band) for up to 14 standards covering a wide color range.

There is little evidence for non-zero zeropoints in  $griz$ ; they are zero to within our measured dispersions, and we have chosen to set them zero. We find a zeropoint for both  $u'$  and  $u$  of  $-0.03 \pm 0.02$  mag. The zeropoint results for  $u'g'r'i'z'$  and  $ugriz$  are illustrated in figure 7, and show essentially no trend with color.

We find synthetic spectrophotometry with the published Sloan system transmission functions ( $u'g'r'i'z'$  &  $ugriz$ ) matches Sloan standard values well, with the quoted zeropoints and no color terms. We note however that there are commercial ‘‘Sloan’’ filters available that have excellent throughput, but which do not match the bandpasses of the Sloan filters precisely, for instance with an  $i'/z'$  break close to 800 nm. We checked synthetic spectrophotometry of our library spectra with a measured set of such filters (and standard

---

<sup>25</sup>[http://www.sdss.org/dr5/algorithms/jeg\\_photometric\\_eq\\_dr1.html](http://www.sdss.org/dr5/algorithms/jeg_photometric_eq_dr1.html)

atmosphere & CCD response) against standard Sloan values. We obtain good fits to standard values for these commercial filters but with the addition of color terms, particularly in  $i'$ .

### 3.7. V-band magnitude of Vega

We note that our  $V_C$  zeropoint derivation based on 17 standards (including VB8) results in a Landolt V magnitude for Vega of  $0.021 \pm 0.008$ , with Vega colors of  $U - B = -0.007 \pm 0.031$ ,  $B - V = -0.009 \pm 0.022$ ,  $V - R = -0.002 \pm 0.016$  and  $V - I = -0.010 \pm 0.018$ . These values, the same as in Pickles (2010), are based on 13–17 standards and fall within quoted errors of those derived in Maiz Apellániz (2007).

We further note that using the Cohen et al (2003a) filter definition results in a zeropoint ( $ZP_{VL} = -0.014 \pm 0.021$ ) which leads to  $V_L(Vega) = 0.013 \pm 0.021$  using all 17 standards, or a zeropoint based solely on the first 3 DA white dwarfs ( $ZP_{VL} = -0.024 \pm 0.002$ ), which leads to  $V_L(Vega) = 0.023 \pm 0.002$ . The latter value is closer to the recently adopted *calspec* value of Landolt  $V(Vega) = 0.025$  mag. However the  $V_L$  zeropoint is clearly a function of color, as seen in figure 4. In figure 4 (and for other zeropoint figures) the ordinate is inverted so that zeropoints that appear vertically higher result in larger (fainter) magnitudes, so  $V_L$  magnitudes are indicated fainter for bluer  $V - I$  color. The effect is fairly small, but for the appropriate color for Vega ( $V - I = -0.01$  vs.  $V - I \sim -0.3$  for WDs), the color-corrected zeropoint ( $ZP_{VL} = -0.022$ ), leads to  $V_L(Vega) = 0.021$ , ie. the *same* as our  $V_C(Vega) = 0.021$  derivation when color effects are taken into account.

We argue that our  $V_C(Vega)$  magnitude of  $0.021 \pm 0.008$  represents a realistic mean value and error for the Landolt V magnitude of the STIS\_005 spectrum of Vega. The zeropoint dispersion could probably be improved by standard photometric measurements of more red stars, including the IRAC K giants, which are shown in the diagram but not used here, as they lack optical standard photometry.

The further question of the small differences between Landolt, Kron-Cousins (SAAO) and Johnson V magnitudes are discussed in Landolt (1983, 1992a) and Menzies et al (1991), and summarized again in Sung & Bessell (2000), but is sidestepped here. For *UBVRI* we are comparing synthetic spectrophotometry of *calspec* standards to available published photometry on the Landolt system.

### 3.8. Vega and Zero magnitude fluxes

Columns 7 and 8 of table 3 show for each bandpass: our synthesized magnitudes of Vega with the adopted zeropoints and the  $\langle F(\nu) \rangle$  fluxes measured on the STIS\_005 spectrum of Vega. Column 9 shows our inferred fluxes ( $F(\nu)$  in Jy) for a zero-magnitude star (ie. zero *vega* mag for  $B_T V_T, UBVRI, Z_V Y_V, JHK$ , Stromgren *uvby*; and zero AB mag for Sloan  $u'g'r'i'z'$  and *ugriz* filters).

The zero magnitude fluxes can be compared with other values given for instance by Bessell (1979); Bessell & Brett (1988), Cohen et al (2003b), Hewett et al (2006), and the IPAC<sup>26</sup>, SPITZER<sup>27</sup> and Gemini<sup>28</sup> websites. The largest discrepancy is for U, where our 0-mag U-band flux is about 4% less than the IPAC value for example, compared to our measured sigma of 2.7%.

We obtain zero magnitude fluxes for *griz* and  $g'r'i'z'$  close to 3631 Jy, and close to 3680 Jy for *u* and  $u'$ .

With our adopted Stromgren zeropoints, we derive Vega magnitudes of 1.431, 0.189, 0.029 and 0.046 in Stromgren *uvby* respectively, compared to values of 1.432, 0.179, 0.018 and 0.014 derived in Maiz Apellániz (2007).

### 3.9. Absolute and Bolometric magnitudes

Electronic table *LibMags* (section 4) lists in the last column a nominal absolute magnitude  $M_V$  for each spectrum, mainly taken from Pickles (1998). The absolute magnitudes of the white dwarf spectra, in the range  $M_V=12.2$  to 12.6, were estimated from the tables of cooling curves in Chabrier et al (2000), using their  $V - I$  colors and hence temperature. Absolute magnitudes are used to calculate distances from spectral fits, as described in section 5.2. Absolute magnitudes in other bands can be formed as (eg)  $M_K=M_V - (V - K)$ .

Also in table *LibMags* and table 3 we have included a digital “bolometric” magnitude  $Emag$ , with unit throughput over the full spectral range ( $0.115 \mu$  to  $2.5 \mu$ ). The “E” zeropoint, on the *vega* system, was adjusted to give approximately correct bolometric corrections for solar type stars. Bolometric corrections in the V and K bands can be computed as  $BC_V =$

---

<sup>26</sup>[http://www.ipac.caltech.edu/2mass/releases/allsky/doc/sec6\\_4a.html](http://www.ipac.caltech.edu/2mass/releases/allsky/doc/sec6_4a.html)

<sup>27</sup><http://casa.colorado.edu/~ginsbura/filtersets.htm>

<sup>28</sup><http://www.gemini.edu/?q=node/11119>

$E - V$  and  $BC_K = E - K$ , and bolometric magnitudes can be formed as  $M_{bol} = M_V - (V - E) = M_V + BC_V$  or  $M_{bol} = M_K - (K - E) = M_K + BC_K$ . Thus it is possible to derive HR diagrams for the fitted catalog stars in different magnitude vs. color combinations.

#### 4. Spectral Matching Library and calibrated Magnitudes

Electronic table *LibMags* shows the magnitudes computed by the *synphot*  $\langle \lambda.F(\lambda) \rangle$  method for all the filters described, using the zeropoints listed in table 3, for 141 digital spectra: Vega, 131 library spectra from Pickles (1998), eight additional *calspec* spectra, and one *DA1/K4V* double star spectrum, discussed in section 6.1

The additional spectra from *calspec* added to extend coverage are: G191-B2B (DA0), GD 153 (DA0), GD 71 (DA1), GRW +70 5824 (DA3), LDS 749B (DBQ4), Feige 110 (D0p), AGK +81 266 (sdO) and VB8 (M7V).

In table *LibMags* the magnitudes listed for Vega are those derived from the STIS\_005 spectrum, but scaled to zero mag in V. All the flux calibrated library spectra, which are available from the quoted sources, have been *multiplied* by the scaling factor indicated to produce synthetic  $V_C$  magnitudes of zero, ie. the Pickles (1998) spectra have been scaled down and the *calspec* spectra have been scaled up to achieve this normalization to  $V_C = 0$ .

In later sections, library spectra are referred to by number and name, together with the V-mag scaling necessary for the matched spectrum to fit the program star photometry. Magnitudes in other bandpasses, including *JHK<sub>MKO</sub>* or Stromgren *wby* can be derived by adding the appropriate filter magnitude from table *LibMags* for the fitted library spectrum, to the fitted V-mag for the program star.

### 5. Spectral Matching

#### 5.1. Spectral scaling and Chi-square optimization

For each star with catalog magnitudes (CM) to be fitted, and for each library spectrum (0...140) with measured synthetic magnitudes (SM), we form the weighted magnitude difference between the catalog and program magnitudes:

$$wmag = \Sigma(w_i * (CM_i - SM_i)) / \Sigma(w_i)$$

$$w_i = 1 / (eCM_i * fac_i)$$

where the weights are the inverse of the catalog errors ( $eCM$ ) in magnitudes, scaled by factors determined empirically to optimize the fits. After experimentation with data sets where cross checks are available, we chose factors of  $\{6,4,3,4,4\}$  for  $UBVRI$ ,  $\{6,4,2,3,3\}$  for  $u'g'r'i'z'$ , and  $\{1,1,1.5,1,1.3,1.3\}$  for  $B_TV_TR_NJ_2H_2K_2/S$ . All the filter bands display broad, shallow minima of *synthetic–catalog* error with factor, and there is some cross-talk between bands. The results are *not* critically dependent on these factors, they are much more dependent on the catalog photometric errors themselves. But the factors were selected within these broad minima to minimize the RMS errors in each band and to improve the consistency of spectral type fitting between different fits.

Smaller factors imply higher weights, although the weighting also depends on the catalog magnitude errors, so the weighting for NOMAD  $R_N$  (dispersion 0.25 mag, factor 1.5) is usually least. Larger factors are necessary for data with small intrinsic errors, because the library spectra cannot achieve milli-mag fits to the data. The factors are not completely independent, but are inter-connected by the library spectra themselves. Fitted magnitudes in U/u' or B/g' for instance can be improved slightly by reducing the scale factor for these bands, but at the expense of slightly worse fits in redder bands. This tends to indicate spectral library calibration errors in the U/u' region.

For each filter band to be fitted, we then form:

$$dM_i = (CM_i - SM_i - wmag)$$

and form a chi-square normalized by the number of filters:

$$chi2 = \Sigma(w_i * dM_i)^2 / nbands$$

The resultant *chi2* will be dominated by those bands where  $dM_i$  exceeds  $eCM_i$ .

Additionally we can form RMS magnitude error values for the 6 Tycho2/NOMAD  $R_N/2MASS$  bands, the 5 Landolt, 5 Sloan and three 2MASS bands when they are available, as:

$$RTM = \sqrt{\Sigma(dM_{Tycho2/R_N/2MASS}^2)/6}$$

$$RUI = \sqrt{\Sigma(dM_{Landolt}^2)/5}$$

$$RuZ = \sqrt{\Sigma(dM_{Sloan}^2)/5}$$

$$R2M = \sqrt{\Sigma(dM_{2MASS}^2)/3}.$$

RMS values without the influence of U/u' can also be formed, eg.  $RBI$  and  $Rgz$ .

The spectral matching process also computes a distance modulus using the adopted absolute V magnitude from table *LibMags* and the fitted (apparent) V magnitude, and

hence a distance estimate in parsec for each fit.

$$D(pc) = 10^{(1-0.2*(M_V-SM_V))}$$

For each program star we get an ordered list of 141 values of *chi2*, one for each spectrum, where the optimum spectrum has the lowest *chi2*. Good fits normally have  $chi2 \leq 1$  because of the normalization by photometric errors and number of filters, but higher values are possible when there are significant differences between catalog and synthetic magnitudes in one or more bands

Several fits at the top of the ordered list may have close, and good fits. These typically represent uncertainty between close spectral types, metal-rich spectra of slightly earlier type, metal-weak spectra of later type, or confusion between dwarf, giant or even supergiant spectra of similar colors.

Additional constraints used to discriminate between these cases are described below. The predicted magnitudes of fits with similar *chi2* values are themselves similar to within 1–3%. The predicted distances however can vary widely, particularly when there are close dwarf and giant matches.

## 5.2. Distance Constraints

We can use the (J-H, H-K) color-color diagram as in fig. 5 of Bessell & Brett (1988) to discriminate between late-type dwarfs and giants. We have adopted the simple criterion that an M-star fitted type must be a dwarf if the 2MASS colors  $(H_2 - K_2) > 0.23$  and  $(J_2 - H_2) < 0.75$ .

Luminosity class discrimination can also be based on any available distance information, including Proper Motions listed in the Tycho2 catalog. The Hipparcos catalog displays a fairly good relation between parallax and Proper Motion:

$$Parallax(mas) \sim 0.065 * PM(mas.yr^{-1}) \quad \sigma = 130 mas$$

$$\text{where } PM = \sqrt{PMra^2 + PMdec^2} \quad mas.yr^{-1}$$

Expressed as a limit, where we adopt the outer boundary of the relation, this is

$$Parallax(mas) > 0.015 * PM(mas.yr^{-1}) \quad \text{or} \quad Distance(pc) < 67000/PM$$

The proper motions listed in the Tycho2 catalog can therefore be used, with some caution, to check derived distances. Small measured proper motions do not provide a significant limit to distance, but large measured proper motions can be used to discriminate between

giant fits at many kpc or nearer subgiants or dwarfs. We did not use parallax measurements directly to determine distance, as they are not available for most catalog stars.

For catalog stars with low or no known proper motion, we set a somewhat arbitrary Galactic upper distance limit of 20 pc. Usually this excludes supergiants, except where the catalog star is bright, but does not exclude giant fits. We do not make any allowance for reddening in our spectral fits, or in our distance estimates.

We also adopt a lower distance limit of 3 pc, which excludes some very nearby dwarf fits (eg. at a distance of 0 pc) in favor of brighter candidates. There are however several nearby stars in the Tycho2 catalog, including Barnard’s star (BD +04 3561a fitted as an M3 V at a distance of 5 pc; an M4.2 V fit at 2.9 pc was excluded by our lower distance limit), Lalande 21185 (BD +36 2147 fitted as an M1.9 V at 4 pc), Ross 154 (fitted as an M4.2 V at 5 pc), Epsilon Eridani (BD -09 697 fitted erroneously as a G5 III at 12 pc; a K2 V fit at 3 pc occurs at a lower rank), Groombridge 34 (GJ 15 fitted as an M 1.9 V at 5 pc), Epsilon Indi (CPD -57 10015 fitted as a K4 V at 3 pc), Luyten’s star (BD +05 1668 fitted as an M3 V at 6 pc), Kapteyn’s star (CD -45 1841 fitted as an M2.5 V at 7 pc), Wolf 1061 (fitted as an M4.2 V at 4 pc), Gliese 1 (fitted as an M1.9 V at 6 pc), GJ 687 (BD +68 946 fitted as an M3 V at 5 pc), GJ 674 (fitted as an M3 V at 5 pc), GJ 440 (WD 1142-645 fitted as an L749-DBQ4 type WD at 5 pc), Groombridge 1618 (GJ 380 fitted as an M1 V at 3 pc), and AD Leonis (fitted as an M3 V at 5 pc).

We always accept the highest ranked spectrum (lowest  $\chi^2$ ) unless we have proper motion, distance limit or color information to exclude a top-ranked giant or supergiant fit.

In the case that the top-ranked spectral fit contravenes one of the above four criteria, our process descends the list of rank-ordered chi-squared fits to the first fit compliant with our distance constraints. This additional test increases the  $\chi^2$  value, but often not by very much. In checks of Tycho2/NOMAD/2MASS (TNM) fits where we also have Sloan or Landolt information, it increases the  $RTM$  values, but can reduce the  $RUI$  or  $Ruz$  values.

Our checks indicate that the (relatively noisy) TNM fits can select giant fits over dwarf fits more often than do fits with better optical data. Nevertheless for TNM fits we have set our proper motion/distance limit very conservatively, modifying the selected fit only when the predicted distance is clearly too large. There is therefore some residual bias in the TNM fits towards giants over dwarfs. The rank of each accepted fit is listed in the results, and the predicted distances can be checked against the Tycho2 proper motions.

We have used SM<sup>29</sup> and Enthought Python<sup>30</sup> for most of the data processing; these scripts are available on request. By judicious use of *numpy* arrays we can fit  $\sim 1$ M stars in eight bands with 141 sets of library magnitudes in about 10 minutes on a typical single CPU, so processing time is not a limiting factor.

### 5.3. Accuracy of the Spectral Matching process

The Library spectra typically have relatively high S/N, but are limited by their own flux calibration uncertainties particularly in the U-band which, unlike the uv, was observed from the ground. In approximate order of decreasing uncertainty, the accuracy of our spectrally fitted magnitudes are limited by the accuracies of:

1. the input catalog magnitudes,
2. the spectral matching process, discussed below,
3. the adopted system transmission functions, discussed in section 3,
4. our derived zeropoints listed in table 3, discussed in sections 3.4 to 3.6,
5. our library spectra particularly in U and, to a much lesser extent,
6. the *calspec* spectra.

The first item is usually largest but it is noteworthy that our fits to catalog values, where they can be properly checked, approach (and sometimes exceed) the accuracy of catalogs themselves.

The methodology presented here can not (yet) approach the goal of sub 1% photometry, and is fundamentally limited by the accuracy of the *calspec* spectra, currently to about 2%. In some ways it avoids the end-to-end calibration of telescopes and detectors, discussed for instance in Stubbs & Tonry (2006), but complements it by offering an easy way to monitor total system throughput by enabling automatic pipelined measurements for wider-field images.

The issues of atmospheric variability in nominally photometric conditions are discussed in Sung & Bessell (2000) and McGraw et al (2010). The methodology presented here is

---

<sup>29</sup><http://www.astro.princeton.edu/~rhl/sm/>

<sup>30</sup><http://www.enthought.com/>

currently less accurate than the expected atmospheric changes for field-to-field comparisons. But using standards in each digital field, rather than transferring them, offers the advantage of both monitoring and consistently removing such variability within the same field, even during known non-photometric conditions.

## 6. Primary Standards

### 6.1. Landolt Standards with 2MASS

We illustrate the spectral matching process by matching library spectra to 594 Landolt standards with accurate *UBVRI* magnitudes, for which we also have 2MASS *JHK<sub>2/S</sub>* magnitudes.

We took the updated Landolt coordinates, magnitudes, uncertainties and proper motions from Landolt (2009). We used the `find2mass` tool in the `cdsclient` package from Centres de Données (CDS)<sup>31</sup> to check 2MASS matches within 3 arcsec to these coordinates and found good correspondence to Landolt (2009) for all except SA92-260 and SA109-956. For these last two stars we have adjusted the coordinates, and matching 2MASS magnitudes, checking them with Landolt finding charts and DSS images. As indicated in Landolt (2009) the star 'E' near the T-Phe variable has a NOMAD entry but no 2MASS entry within 30 arcsec; it has been excluded from our list here.

The catalog data for the Landolt standards: sexagesimal coordinates, *UBVRI* magnitudes and errors, 2MASS magnitudes, errors and coordinates in degrees, together with UKIRT *ZY* & *JHK<sub>MKO</sub>* data where available are listed in the online table *LandoltCat*. Where Landolt (2009) photometric errors were left blank, indicating one or few standard observations, we have set them to 0.009 mag for the purpose of our fitting process.

For each standard, we compute the *chi2* value for each of 141 library spectral magnitudes as described in section 5 for the eight L2M bands: Landolt *UBVRI* and 2MASS *JHK<sub>2/S</sub>*. We then order them by *chi2*, check against our distance constraints, and select the one that satisfies the constraints with the best match to the eight catalog magnitudes,

The results are listed in the online table *LandoltFit*, which lists the standard name, coordinates, Landolt magnitudes and colors, number of observations, and spectral type from Drilling & Landolt (1979), then fitted rank, *chi2* values, two RMS error in Landolt magnitudes *RUI* & *RBI*, fitted spectral library number and type, and fitted magnitudes in *B<sub>T</sub>V<sub>T</sub>*,

---

<sup>31</sup><http://cdsarc.u-strasbg.fr/doc/cdsclient.html>

$JHK_{2/S}$ ,  $UBVRI$ , UKIRT  $Z_V Y_V$ , Sloan  $u'g'r'i'z'$ , and distance in parsec. Magnitude values in other bandpasses can be derived by adding the library magnitude from *LibMags* for the appropriate band and spectral type to the fitted V magnitude.

There is reasonably good correspondence between the objective prism spectral types from Drilling & Landolt (1979) and those fitted here; about 123 close matches, *versus* 13 discrepant types – the worst two being SA110-499 and SA110-450.

Figure 10 shows the 8-band L2M fitted magnitudes plotted as *Fit* – *Landolt* magnitudes against their Landolt standard values for  $BVRI$ . The display range excludes a few outliers discussed below. The dashed histograms of number (to the right) vs. delta magnitude (ordinate) illustrate that most stars lie close to the zero-delta line. The clipped  $1\sigma$  dispersions are 0.05, 0.03, 0.04 and 0.05 mag for  $BVRI$  respectively. In order to compute these dispersions we formed a sigma for each of  $BVRI$  separately, performed a  $3\sigma$  clip, then repeated a second (tighter)  $3\sigma$  clip to arrive at the quoted  $1\sigma$  dispersions. This typically clips 4–8% of the values, or 25–45 of the values here, but retains about 95% of the values.

Of the clipped values, almost 2/3 have been observed only once or twice in table *LandoltCat*; the others are mainly white dwarfs, very red stars, or perhaps double stars. A few poor fits with large values of  $chi^2$  and  $RUI$  include some late giants and supergiants where the spectral library coverage is weak and Feige 24, a double star, which is fairly well fit with a double-star spectrum constructed from a 68:32% mix at V-band of DA1 (GD 71) and K4 V spectra. PG1530+057 is listed as a uv-emission source, and is also best fit with this DA/K4 dwarf double star spectrum, as is SA107-215. No effort was made to optimize these coincidental double-spectrum fits, but they emphasize that double stars are likely to be present among Landolt standards, as among other catalog stars.

In many cases of multiple stars within the observing aperture, including known doubles like BD +26 2606, the spectral flux will be sufficiently dominated by one spectrum at all wavelengths that fitting to a single spectral type is valid. But some data do show the predominant influence of one spectrum in the blue and another in the red. Most stars here (~94% or 560) are very well fit by the (single) spectral matching process.

The clipped  $1\sigma$  dispersion for  $U$  shown in figure 11 is 0.16 mags; 0.12 mags to  $U < 16$  and increasing for fainter magnitudes. The four faintest  $U$  standards were not observed often in Landolt (2009). Our fits for these find brighter  $U$  values, but have fairly large  $chi^2$  and  $RUI$ .

The distribution of spectrally fitted types and luminosities for Landolt standards is shown graphically as an HR diagram in figure 12. The fitted types are plotted as absolute V magnitudes vs.  $V - I$  color, with different symbols for different Luminosity classes and

metallicities. The area of each symbol is proportional to the number of fitted stars of that type. The truncation of the lower main sequence is of course a brightness selection effect. The Landolt primary standards cover a wide range of colors, types and metallicities, with most MK types well represented.

### 6.1.1. $Z_V$ on Vega and AB systems

Table *LandoltCat* also contains  $Z_V Y_V$  data from UKIRT for 14 standards, and  $JHK_{MKO}$  for 17 Landolt standards (see section 1). The  $1\sigma$  dispersions (not shown) for both  $Z_V$  and  $Y_V$  are 0.06 mag for 14 stars with standard values (including two calspec standards: GD 50 fit with a GD 153 DA0 type spectrum & GD 71 fit with its own Library GD 71 DA1 spectrum).

Despite the fact that the  $Z_V$  bandpass terminates shortward of  $z$  or  $z'$ , and because of the falling long-wavelength response of CCDs, the pivot wavelengths of  $Z_V$  &  $z'$  in table 3 are similar. It is therefore not surprising that there is a simple one-to-one relation between fitted values for  $Z_V$  on the *vega* system and  $z'$  and  $z$  on the AB system, which holds for 14 Landolt/Sloan standards and also for 594 fitted values for Landolt Standards and for the spectral library magnitude data in table *LibMags*, both of which cover a wide color range:

$$0.58 + Z_V \simeq z_{AB} \simeq z'_{AB} \quad \sigma = 0.014$$

where the additive constant is simply the derived zeropoint for  $Z_V$  (and that for  $z_{AB}$  is zero). This is equivalent to the magnitude difference between the *vega* and AB system 0-mag fluxes at  $Z_V$ :  $0.58 = -2.5 * \log_{10}(2128/3631)$  from table 3.

For AB magnitudes measured with a bandpass similar to  $Y_V$  used by UKIRT/WFCAM, the relation between the  $Y_V$  *vega* and AB system magnitudes should also be the *vega* to AB zeropoint offset at this bandpass, ie.

$$K_Y + Y_V \simeq y_{AB}$$

where  $K_Y$  should be close to  $0.61 - 0.0$ , or alternatively to the difference in magnitudes between the 0-mag flux at  $Y_V$  on the *vega* system and 0-mag (3631 Jy) for the AB system, ie.  $0.61 = -2.5 * \log_{10}(2072/3631)$  from table 3.

Care must be taken however, particularly with Y-band measurements made with CCDs, because CCD QEs fall very fast in the  $1.0-1.1 \mu$  region, and CCD Y-bandpass profiles are necessarily quite different from the rectangular UKIRT WFCAM HgCdTe  $Y_V$  bandpass, see figure 2. Many CCDs have little or no sensitivity at Y-band. Deep depletion CCDs can have significant QE out to the Silicon bandgap at  $1.1\mu$ , but CCDs even of the same type may

have varying QE curves and system bandpasses at Y, and hence also have different effective and pivot wavelengths.

At LCOGT we use the PanStarrs-type  $Z_S$  (for Z-short) and Y filters with our Merope E2V 42-40 2K CCDs on Faulkes Telescopes North and South (FTN & FTS). Our LCOGT  $Z_S Y_E$  system bandpasses including filter, atmosphere and detector are illustrated in fig 2. We refer to  $Y_E$  to specifically reference the PanStarrs-type Y bandpass with our E2V system QE curve, and 1.3 airmasses of extinction at a typical elevation of 2100m. The measured pivot wavelengths for  $Z_V$  and  $Z_S$  are 877.6 and 865.1 nm respectively; those for  $Y_V$  and  $Y_E$  are 1020.8 and 989.9 nm respectively. The effective wavelengths for either type of Z and Y bandpasses vary by less than 1% and 0.5% respectively however, from white dwarf to M-dwarf spectra, so Z/Y band measurements can provide convenient near infrared flux and temperature measurements, enabling quite good dwarf/giant discrimination for M stars, somewhat insulated from atmospheric and stellar spectral features.

For the same (few) standards shown in table 3 we obtain zeropoints (on the *vega* system):  $Z_S = 0.56 \pm 0.04$  and  $Y_E = 0.55 \pm 0.03$ . We can form  $Z_S Y_E$  filter system magnitudes for all the spectral library stars, and form linear relationships with  $Z_V Y_V$  of the same stars, but because of the bandpass differences they are no longer simply one-to-one relationships of unit slope. For synthetic measurements with LCOGT  $Z_S Y_E$  of our 141 spectral library standards in table *LibMags* we obtain:

$$1.05 * (0.56 + Z_S) \simeq z = z' \quad \sigma = 0.024, \text{ and}$$

$$1.04 * (Y_E - 0.03) \simeq Y_V \quad \sigma = 0.022$$

Where  $Z_S Y_E$  &  $Y_V$  are on the *vega* system. These relations are dependent on the particular bandpasses used here, but indicate that CCD based Y-band magnitudes (on either the *vega* or AB systems) can be successfully tied to the UKIRT/WFCAM Y-band standard system, with CCD-system-dependent equations.

### 6.1.2. $JHK_{MKO}$ fits

Our fitted values of  $JHK_{MKO}$  on the *vega* system match 17 Landolt stars with standard UKIRT values<sup>32</sup>, which further supports our derivation of their zeropoints.

$$J_{MKO}(fit) \simeq J_{MKO} \quad \sigma = 0.04$$

---

<sup>32</sup>[http://www.jach.hawaii.edu/UKIRT/astrometry/calib/phot\\_cal/fs\\_izyjhklm.dat](http://www.jach.hawaii.edu/UKIRT/astrometry/calib/phot_cal/fs_izyjhklm.dat)

$$H_{MKO}(fit) \simeq H_{MKO} \quad \sigma = 0.05$$

$$K_{MKO}(fit) \simeq K_{MKO} \quad \sigma = 0.07$$

$J - H$  and  $H - K$  fitted colors form linear relationships with  $J - H_{MKO}$  &  $H - K_{MKO}$  for these same 17 stars with sigmas of 0.04 & 0.03 mag respectively, but with little color range. There are color terms between the  $JHK_{MKO}$  and 2MASS  $JHK_{2/S}$  systems.

## 6.2. Sloan Standards

There are 158 Sloan Standards listed in electronic table *SloanCat*, together with UKIRT values of  $Z_V Y_V$  and  $JHK_{MKO}$  where available, and 2MASS values of  $JHK_{2/S}$ . These have been spectrally matched with eight S2M bands of  $u'g'r'i'z' J_2 H_2 K_2$ , and their fitted values of Landolt and Sloan magnitudes and distances in parsec are listed in electronic table *SloanFit*. The comparisons with standard data are discussed below.

## 6.3. Landolt/Sloan/Tycho2/2MASS Standards

There are 96 standards in common between the Landolt and Sloan lists; they all have 2MASS  $J_2 H_2 K_2/S$  and NOMAD  $R_N$  magnitudes; 65 of these also have Tycho2  $B_T V_T$  magnitudes. This very small sample with cross-referenced data provides useful illustrations of the strengths and limitations of the spectral matching process.

Electronic table *LanSloCat*, lists Landolt, Sloan, NOMAD, 2MASS and Tycho2 magnitudes, errors, coordinates and proper motions. In this case the proper motions are from Tycho2; they are similar to but slightly different from proper motions listed in electronic table *LandoltCat* which are from Landolt (2009). The proper motions are only used to discriminate distance limits here.

These stellar magnitudes have been fitted four ways: i) they were fitted with  $UBVRI$ ,  $u'g'r'i'z'$  and  $B_T V_T J_2 H_2 K_2/S$ , a total of 15 bands, ii) they were fitted with Landolt and 2MASS data (L2M, 8-bands), iii) they were fitted with Sloan and 2MASS data (S2M, 8-bands), and iv) they were fitted with Tycho2, NOMAD  $R_N$  and 2MASS data (TNM, 6 bands).

The fits are listed in electronic table *LanSloFit* where the results are listed in full for the first method, then only for those stars with different matching spectra for subsequent fits.

In each case the fitting process produces synthesized magnitudes at all bands, together

with library types and distances. The synthesized magnitudes were compared with the standard values, and the fitted library types checked for consistency between fits.

### 6.3.1. Examples of spectral matching

Figure 13 shows the S2M 8-band fit for SA93-424, a K1 III at 768 pc, with  $F(\nu)$  plotted against wavelength. The same K1 III fit is obtained with the 15-band fit and the L2M 8-band fit; ie. the fits have the same type and the scale is different by less than 0.2%. For this fit, RUI, Ruz and RTM rms values are 0.02, 0.03 & 0.16 mag respectively. Over-plotted (black dashed line) is the best-fit rK0 III type at 393 pc obtained with the TNM fit (6 bands). The 6-band fit is forced a bit brighter in the optical region by the  $B_T V_T$  data, but matches the  $K_{2/S}$  point better. This latter fit gives synthesized Landolt/Sloan magnitudes with RUI, Ruz and RTM of 0.16, 0.09 and 0.18 mag respectively. Drilling & Landolt (1979) list a G8 III spectral type for SA93-424, from objective prism spectra.

Figure 14 shows the L2M fit for BD +02 2711, a B3 III at 5.2 kpc, plotted as a blue dotted line, with RUI, Ruz and RTM values of 0.04, 0.05 and 0.08 mag. The S2M and 15-band fits are similar. The 6-band TNM fit of a GRW +70 5824 (DA3) type White Dwarf at 4 pc is shown as the over-plotted black dashed line, with RUI, Ruz and RTM values of 0.13, 0.14 and 0.07 mag respectively. The latter fit is a better match to the Tycho2 bands, but is unconstrained at wavelengths shorter than  $B_T$ , and is a poorer fit to the Landolt and Sloan bands. There is no objective prism type for BD +02 2711 from Drilling & Landolt (1979), but SIMBAD lists a type of B5 V at a distance (from its Hipparcos parallax) of 1.3 kpc. An early B dwarf type was selected as a high, but not top-ranked fit by all the spectral matches.

These examples were chosen to illustrate both the successes and limitations of the spectral matching method. They emphasize that color or spectral type are matched better than luminosity class, particularly when the input photometric errors are larger, but that good magnitude fits can be obtained in most cases.

Figure 15 shows the first ranked S2M fit for SA102-620, a K4 V at 38 pc. The K4 V fit is also obtained as the second ranked fits with the 15 band and the 8-band L2M fits, where a slightly higher ranked K2 III fit at 540 pc was rejected in these two cases as being beyond a calculated proper-motion-limited distance of 285 pc. For the S2M fit, RUI, Ruz and RTM values are 0.06, 0.08 & 0.05 mag respectively. Over-plotted (black dashed line) is the second ranked 6-band TNM fit rK1 III at 200 pc, which is a bit bluer in the optical region because of the  $B_T V_T R_N$  data. This latter fit has RUI, Ruz and RTM values of 0.11, 0.13 and 0.06 mag respectively; Drilling & Landolt (1979) list an M0 III type for SA102-620. SIMBAD

lists a K5 III but with a parallax (from Hipparcos) of 22 mas, implying a distance of 45 pc; ie. the star must be a dwarf. The K4 V L2M and S2M fits are best, but the TNM rK1 III fit still matches the magnitudes quite well.

Figure 16 compares three types of fit for the *LanSloCat* sample. The fitted *BVRI* magnitudes are plotted as *Fit – Landolt* on the ordinate vs. Landolt catalog values on the abscissa. The electronic version of this figure is in color. A plot of *Fit – Sloan* vs. Sloan catalog magnitudes shows similar dispersions. The clipped sigmas, typically containing more than 92% of the points, are: 0.12, 0.03, 0.02, 0.03, 0.03 & 0.13, 0.03, 0.03, 0.03, 0.04 mag for *UBVRI* & *u'g'r'i'z'* bands respectively for the 8-band L2M fits. They are: 0.14, 0.06, 0.03, 0.02, 0.03 & 0.15, 0.03, 0.02, 0.02, 0.03 mag for *UBVRI* & *u'g'r'i'z'* bands respectively for the 8-band S2M fits, and are: 0.21, 0.15, 0.12, 0.10, 0.08 & 0.19, 0.15, 0.11, 0.09, 0.07 mag for *UBVRI* & *u'g'r'i'z'* bands respectively for the 6-band TNM fits. These latter TNM sigmas, combined and averaged for *UBVRI* and *u'g'r'i'z'* as  $\sim 0.2$ , 0.15, 0.12, 0.10 & 0.08 mag, are what are reported as the typical  $1\sigma$  error per Tycho2 star per band in the abstract, and can be compared to the TNM *g'r'i'z'* fits reported in section 7.

### 6.3.2. Accuracy and consistency of the fits

It can be seen that there is good correspondence between the *UBVRI* and *u'g'r'i'z'* bandpass sigmas where we are able to compare them directly. This is natural because the fits depend primarily on the catalog errors and the spectral library errors, not on any mismatch between Landolt and Sloan systems, see section 5.3. In other cases we are only able to measure the quality of fit in either Landolt or Sloan bands, but can infer that the quality of fit for the other system will be quantitatively similar.

Landolt *UBVRI* magnitudes can also be derived in this simple case with accurate Sloan *u'g'r'i'z'* magnitudes, using the formulas from Jester et al (2005). For these 65 stars this results in sigmas of 0.06, 0.05, 0.03, 0.04 and 0.04 for *UBVRI* respectively. The spectral matching method for L2M and S2M methods are therefore comparable to or better than the Jester et al (2005) method for *BVRI* and *griz* bands, but *worse* for *U/u*. The TNM fits are less accurate, but generally fit better at BVR bands than the  $B_T V_T R_N$  errors themselves. They therefore offer a reliable fitting method in the absence of more accurate optical data.

Note that the Jester formulas are susceptible to errors in just one filter, that can propagate to several fitted filter bands. The spectral matching process is not immune to input catalog errors but, by giving lower weight to discrepant points with larger photometric errors, can provide more robust synthetic fits in all bands.

The fitted spectral types can vary according to the input data matched, but the results are generally consistent. Figure 17 illustrates our derived distributions of stellar types and luminosities for 65 Landolt/Sloan standards, binned into 141 library spectral types, and plotted as adopted absolute  $V$  magnitudes against their  $V - I$  colors. The same symbols for different Luminosity classes and different metallicities are used from figure 12, and the symbol area is proportional to the number of stars in each library type bin.

The first fit on the left is for all 15 Landolt, Sloan & Tycho2/2MASS bands. The second fit is for the 8-band L2M fits, third for the 8-band S2M fits, and fourth on the right for the 6-band TNM fits.

These fits and their distributions of selected spectral types and luminosities are different in detail, but similar statistically, and produce closely similar magnitude fits.

The HR diagram on the right illustrates that TNM fits show a slight preference for giant rather than dwarf types. The TNM fits also select one supergiant for SA97-351, an F0 I at a distance of 19 kpc (just inside our distance limit), rather than an A7 V at 342 pc (L2M) or F0 III at 553 pc (S2M). Drilling & Landolt (1979) list an objective prism spectral type of A0 for SA97-351.

There are 27 matches and 19 close matches between the L2M and S2M fits. There are 14 matches and 21 close matches between the S2M and TNM fits. In all cases the fitted spectra and derived magnitudes are similar, as shown in figure 16.

The difference in optimal fits, depending on the number and accuracy of filter photometry available, illustrates both the strengths and limitations of the spectral matching process, and of the spectral library. The library quantization is too fine for this purpose in some places, and insufficiently sampled in others. In general, the spectral matching process is better at determining the spectral type than the luminosity class.

The differences between accurate and lower quality photometric data are apparent. Nevertheless the spectral matching process works well even for poorly determined optical photometry, where the more accurate 2MASS data help constrain the fitted spectra in both type and magnitude scale.

Better spectral type discrimination is possible when more accurate filter data are available, but the fitted magnitudes are similar in all these cases, within the quoted errors. Fitted spectral types are more accurate than Luminosity class. The fitted distance estimates can be used as a sanity check on the derived fit.

## 7. Secondary SDSS Standards

### 7.1. SDSS PT observations

Tucker et al (2006) & Davenport et al (2007) have published lists of almost 3.2 M SDSS observations in  $g'r'i'z'$ <sup>33</sup>. These were observed on the US Naval Observatory photometric telescope (PT), and used to calibrate the SDSS survey scans<sup>34</sup>. They are more accurate than survey data, as evidenced by the consistency of their repeated observations and (small) errors. We use them here as secondary standard calibrators. We first combined the lists to produce a list of  $\sim 1$  M repeated observations, with photometric errors being the maximum of any single observation, or the rms of the average if that was greater. These were matched against 2MASS stars within 3-arcsec to produce a slightly shorter list of stars which reach as faint as  $g' \sim 21$  mag, and are discussed in section 8.2.

This list was further matched against the Tycho2 and NOMAD catalogs, to produce a smaller list of 10,926 SDSS-PT standards with  $B_T V_T R_N$  and reaching as faint as  $g' \simeq 13.5$  mag. These were fitted two ways: i) S2M with 7-bands  $g'r'i'z'$  &  $JHK_{2/S}$ , and ii) TNM with 6-bands  $B_T V_T R_N J_2 H_2 K_{2/S}$ , and their results compared with the PT standard values.

Figure 18 shows the S2M  $g'r'i'z'$  fits to the  $\sim 11,000$  SDSS-PT/2MASS stars with Tycho2/Nomad data, with sigmas of 0.03, 0.02, 0.02 and 0.03 in  $g'r'i'z'$  respectively, after clipping outliers, but retaining more than 96% of the points in each band. The sigma in  $g'$  is 0.07 mag for  $\sim 11,000$  stars, but the grey (red) dots show a sigma of 0.03 mag after clipping about 400 outliers. This illustrates typical  $1\sigma$  errors for accurate SDSS data coupled with 2MASS data. The histograms illustrate the number distributions of errors about the mean for all the points where they become overlapped and blurred.

From section 6.3.2 we infer that the errors for  $BVRI$  are similar. The sigmas for fitted  $JHK_{2/S}$  are 0.04, 0.04 & 0.03 mag respectively.

Figure 19 shows the corresponding TNM fits to these stars, with clipped and unclipped sigmas of 0.15/0.25, 0.12/0.16, 0.09/0.13 and 0.07/0.15 mag in  $g'r'i'z'$  respectively, after clipping outliers (shown in black) but leaving 78% of the grey (red) points in  $g'$  and more than 88% of the grey (red) points in the other three colors. We again infer that these illustrate typical  $1\sigma$  errors for both  $griz$  and  $BVRI$  fits to the Tycho2 catalog when coupled with NOMAD and 2MASS magnitudes, and note their similarity to typical TNM errors quoted in section 6.3.1 and the abstract. The histograms show the number distribution of

---

<sup>33</sup><http://das.sdss.org/pt/>

<sup>34</sup>[http://www.sdss.org/tour/photo\\_telescope.html](http://www.sdss.org/tour/photo_telescope.html)

errors about the mean for all the TNM fits to  $\sim 11,000$  SDSS-PT/2MASS/Tycho2 stars.

The TNM fit errors quoted here for  $r'i'z'$  are similar to those found by Ofek (2008), but for a larger magnitude range. The error quoted for  $g'$ -band is slightly larger than previously reported, but for a wider fitted magnitude range. The sigmas for fitted  $JHK_{2/S}$  are 0.03, 0.02 & 0.02 mag respectively.

## 7.2. Southern SDSS standards

Smith et al (2005)<sup>35</sup> have published a list of  $\sim 16,000$  southern SDSS standards, which includes some repetition. We matched 15,673 of these to 2MASS catalog values and fitted them in eight S2M bands:  $u'g'r'i'z'$  and  $JHK_{2/S}$ . The clipped and unclipped  $1\sigma$  fits are 0.22/0.51, 0.08/0.22, 0.04/0.07, 0.07/0.16 and 0.11/0.25 mag for  $u'g'r'i'z'$  respectively, for all Sloan Southern stars ranging up to  $g \sim 19$  mag, as shown in figure 20. The vertical histograms show the number distribution of errors about the mean for all these Southern Sloan stars, and indicate that our fits produce an excess of rejected fits *fainter* than the catalog values in  $z'$  and, to a lesser extent, in  $i'$ .

The  $JHK_2$  fits are not shown, but the  $J_2$  fit shows a corresponding excess of fitted points *brighter* than the catalog values, whereas the  $HK_2$  fits are symmetrically distributed about the mean-delta (zero) line. Thus our fits to southern Sloan  $i'z'$  are being pushed slightly fainter at the red end by the usually reliable 2MASS data.

There are  $\sim 6000$  stars with  $g' < 16$ : for these stars the clipped sigmas are 0.13, 0.07, 0.04, 0.06 and 0.09 in  $u'g'r'i'z'$  respectively, ie. not as good as for the SDSS-PT stars in figure 18, but for a larger magnitude range in this case.

The HR diagram for this fit is shown in figure 21. Compared with the Landolt distribution in figure 12, this shows a slightly less populated lower main sequence, more stars near the main sequence turnoff, a slightly better defined red giant branch out to M8 III, some “horizontal branch” type giants but no supergiants.

We have further matched this list to Tycho2  $B_T V_T$  and NOMAD  $R_N$  magnitudes, resulting in a list of only 201 Southern stars as most of the Southern SDSS standards are too faint to have Tycho2 matches. The comparison of fitted  $griz$  magnitudes to standard values for fits using 6 TNM bands is shown in figure 22, with sigmas of 0.23, 0.16, 0.12, 0.11 and 0.09 mags in  $ugriz$  respectively, and comparable to the TNM fits to SDSS PT stars above

---

<sup>35</sup><http://www-star.fnal.gov/>

for a similar magnitude range.

## 8. Catalogs

### 8.1. Landolt and Sloan Fitted data

Landolt standards including updated coordinates, magnitudes and errors,  $JHK_{2/S}$  2MASS data and UKIRT  $Z_V Y_V JHK_{MKO}$  data where known are listed for 594 stars in electronic table *LandoltCat*. Table *LandoltFit* contains the spectrally fitted rank,  $\chi^2$ , RUI, RBI, library number and type, fitted magnitudes  $B_T V_T J_2 H_2 K_2 UBVRI Z_V Y_V$ ,  $u'g'r'i'z'$ , and distances in parsec.

Similar data are contained in tables *SloanCat* and *SloanFit* for Sloan standards, and in tables *LanSloCat* and *LanSloFit* for stars common to both lists, as described in section 6.

### 8.2. Secondary standard fitted data

Electronic table *SDSSPTFit* contains coordinates, standard magnitudes and errors in  $g'r'i'z'$ , number of repeated PT observations, merged  $J_2 H_2 K_2$  2MASS data, and fitted Rgz, R2M (2MASS), library types,  $UBVRI - Z_V Y_V$  and  $u'g'r'i'z'$  magnitudes and distances for  $\sim 1$  M SDSS-PT stars.

Figure 23 shows the 7-band S2M fits for these stars. The outer, black dots show all the rejected stars, and the lighter grey, narrower band (red in the electronic version) contain more than 90% of the stars after sigma clipping. The sigma-clipped bands widen somewhat with magnitude, particularly for  $g'$  and  $z'$ . The number distributions of these points are strongly peaked to the center (zero) line, and are shown as dashed histograms. The sigmas are 0.04, 0.03, 0.03 & 0.07 to a limiting magnitude of 16 in  $g'r'i'z'$  bands respectively, and are 0.07, 0.03, 0.04 & 0.08, to the sample limiting magnitudes of about 19, 19, 18.5 and 18 in  $g'r'i'z'$  respectively. Infrared sigmas (not shown) are 0.04, 0.06 and 0.07 for  $JHK_2$  respectively.

Figure 24 shows the distribution of these stars as absolute magnitude against V-I color. The larger SDSS-PT sample shows a more heavily populated lower main sequence than for the Southern Sloan standards.

Electronic table *SDSSSouthFit* contains similar fitted data for 15,673 Sloan Southern standards, where the name contains the original sexagesimal coordinates. Missing input

magnitudes are listed as -9.999 with associated errors of +9.999

### 8.3. Spectrally matched Tycho2 catalog

The catalog of 2.4 M fitted Tycho2 stars is published in electronic table *Tycho2Fit*. It contains for each star: Tycho2 coordinates, proper motions in RA/DEC in mas/yr,  $B_T V_T$  catalog magnitudes and errors, NOMAD  $R_n$  magnitudes and 2MASS  $J_2 H_2 K_2/S$  magnitudes, mean errors and Quality Flag, followed by fitted values for rank,  $\chi^2$ , RTM (mag), number and type of matching spectrum, fitted  $B_T V_T$ ,  $UBVRI - ZY$  magnitudes on the *vega* system, fitted  $u'g'r'i'z'$  magnitudes on the AB system, and Distances in pc.

Because the Tycho2 catalog covers a wide range of optical magnitudes and colors, it also covers a wide range of 2MASS magnitudes. We have included bright 2MASS sources which have larger errors due to saturation effects, typically brighter than 5 mag in  $J$ ,  $H$  or  $K_S$ <sup>36</sup>. In these cases (about 40,000 entries with 2MASS quality flag 'C' or 'D') the fits tend to be dominated by the optical rather than the infrared bands. About 11,000 entries lack mean error information (quality flag 'U'); we assign 0.04, 0.05 and 0.06 mag mean errors for  $JHK_S$  respectively to enable our spectral matching procedure to work with the quoted 2MASS upper magnitude limits. About 570 entries lack magnitude information (quality flag 'X') in one or more 2MASS bands; for these entries our catalog shows -9.999 mag, with an error of +9.999. This permits the matching process to proceed with negligible input from the affected band. The 2MASS quality flags are included in the electronic catalogs, and most entries are 'AAA'.

The fitted optical and infrared magnitudes are compared to the catalog values in figure 25, which illustrates the magnitude range in the optical (+2.4 to  $\sim 15$  mag) and infrared (-4.5 to  $\sim 15$  mag). A  $3\sigma$  clip has been applied to all six bands, leaving 95%, 96%, 82%, 99%, 99% and 99% of values in  $B_T V_T$ ,  $R_N$  (matched to fitted Landolt R) and  $JHK_2$  bands respectively. The resulting sigmas are 0.19, 0.11, 0.26, 0.03, 0.03 and 0.03 mag in  $B_T V_T R_N JHK_2$  respectively, comparable with the quoted errors in these bands. The sigmas are 0.12 & 0.09 mag for  $B_T V_T$  to 13 and 12.5 mag respectively. Our fitted  $B_T V_T$  magnitudes may be more accurate than the catalog values, as they are tied to the more accurate 2MASS photometry via the spectral matching process. Both rejected and included points are shown, as described in the figure. The fitted values for  $B_T V_T$  are listed in electronic table *Tycho2Fit*; other values can be derived by adding the library magnitude from *LibMags* for the appropriate band and spectral type to the fitted V magnitude.

---

<sup>36</sup><http://www.ipac.caltech.edu/2mass/releases/allsky/doc/sec2.2.html>

Figure 26 shows the HR diagram derived for 2.4 M Tycho2 stars from these fits, which shows a less populated lower main sequence and a giant branch more dominated by solar metallicity stars than the Landolt, SDSS-PT or SDSS-Southern standards, and about 3,340 double star 'DA1/K4V' fits.

Figure 27 shows the same data plotted, where now the size of the symbols represent either the V-light or the K-light of the stellar types. The Tycho2 distribution is more dominated by solar-abundance types and by early giant branch types, than is the SDSS-PT standard population.

#### 8.4. Spectrally matched catalog of the SDSS survey region

The catalog of 4.8 M fitted Sloan survey stars with  $g < 16$  is published in electronic table *DR7Fit*, which contains the SDSS DR7 coordinates, unprimed *ugriz* (psf) magnitudes and errors for each star, matching 2MASS *JHK<sub>2/S</sub>* magnitudes, errors and quality flag, followed by fitted values of rank, *chi2*, Ruz, Rgz, R2M, number and type of fitted spectrum, fitted *UBVRI – ZY* magnitudes on the *vega* system, fitted *u'g'r'i'z'* magnitudes, fitted (unprimed) *ugriz* magnitudes and Distances in pc. Other fitted magnitudes can be obtained by reference to electronic table *LibMags*.

The catalog contains about 100 entries with 2MASS quality flag 'X', and about 43,000 entries with quality flag 'U', modified for magnitude and error as detailed above.

We found better fits to psf magnitudes and errors than to model magnitudes and errors, so have spectrally matched the psf magnitudes. The difference between psf and model magnitudes typically exceeds what would be expected from the DR7 quoted errors.

Figure 28 shows the comparison of DR7 *griz* magnitudes with our fitted unprimed *griz* magnitudes. There are quite a large number (about 30%) of discrepant points in one or more DR7 bands. In this case we have initially rejected points with large values of Rgz, and then performed the sigma clip to reduce the numbers only slightly. The sigmas after this process are 0.18, 0.06, 0.04, 0.04 and 0.05 for *ugriz* respectively, and by reference to section 6.3.2, are inferred to be similar for *UBVRI*. These S2M fits, for about 70% of the DR7 survey stars to  $g < 16$ , are what are reported as the typical  $1\sigma$  error per DR7 star per band in the abstract.

There are quite a large number of (black) points rejected by the above process at relatively bright magnitudes and near to the zero-delta line in each panel. This is because many of the  $\sim 30\%$  points rejected as having large Rgz values are seriously discrepant in one or

more color bands, but fit well in other colors. It is possible, but not verifiable here, that transparency variations during the drift scans have affected different color bands for different stars. Unfortunately the quoted psf errors are often quite low where the magnitudes appear to be severely discrepant, so our fitting process has trouble discriminating between accurate and doubtful data.

Note that the number of rejected points per histogram bin away from the peak are only 1–3% of those at the peak but, summed over  $\sim 20$  such bins contain about 30% of the (rejected) data points. The histogram bin size was increased from 0.05 to 0.1 mag here to emphasize the outlying values.

The R2M values in *DR7Fit* are based on the rms differences between 2MASS catalog and fitted values. Their sigma clipped values are 0.04, 0.05 & 0.06 mag for *JHK*<sub>2</sub> respectively.

Figure 29 shows the HR diagram derived for 4.8 M SDSS stars to  $g < 16$  from these fits, with symbol area is proportional to number of occurrences of each type.

Figure 30 shows the same data plotted as  $M_V$  and  $M_K$  vs.  $V - I$ , where the symbol area proportional to the V-light and K-light respectively.

Our fitted magnitudes may improve over discrepant points in individual filter bands in the input catalog values, since the spectral matching process associates fitted values in each band with additional, sometimes more accurate data.

## 9. Summary

We present online catalogs that provide synthetically calibrated & fitted magnitudes in several standard filter system bandpasses for several surveys, including the all-sky Tycho2 survey, and the Sloan survey region to  $g < 16$ . The errors of the synthesized magnitudes are mainly limited by the accuracy of the input data, but sufficient stars should be available in fields of view  $\geq 30$ -arcmin to average enough stars to provide flux calibrations to better than 10%, and often to better than 5%, in most bandpasses and most observing conditions. For instance with 9 Tycho2 stars in a typical 30 arcmin field of view, flux calibration to about 0.1, 0.05, 0.04, 0.03 & 0.03 mag should be possible in either *UBVRI* or *u'g'r'i'z'* systems. These are typically achievable field-to-field uncertainties on either standard system. Relative calibration of repeated images of the same field, with similar or different equipment, should be automatically possible to 2% or better, even during variable photometric conditions, but subject to the averaged systemic uncertainty (above).

The spectral matching technique provides a standard photometric system check on sur-

vey magnitudes and, because of matching to multiple filter bands, can be more accurate than individual measurements in some filter bandpasses. The accuracy of fitted magnitudes improves substantially with improving survey data accuracy, as does the reliability of fitted types, luminosity classes and distances. The method enables quick statistical analyses of stellar populations sampled by wide-field surveys.

Substantial improvements can be expected in terms of reliable types, multi-filter magnitudes and distances with realistic improvements in the spectral library definition, eg. the NGSL library Gregg et al (2006); Heap & Lindler (2010), and expected all-sky survey improvements but, importantly, only a few accurately determined survey bands (spanning optical and infrared bands) are typically necessary to derive accurate multi-filter fits. Spectral matching removes the necessity to accurately measure *all* desired filter bandpasses in all-sky surveys.

## 10. Acknowledgements

We acknowledge the referee who suggested several useful improvements. We would like to acknowledge the extensive standard system photometry referenced here, and the producers and maintainers of the *calspec* database at STScI. This research has made extensive use of the Tycho2, 2MASS, SDSS DR7 and NOMAD catalogs, and we gratefully acknowledge their producers. We have made use of the SIMBAD database operated at CDS, Strasbourg, France, and of several data access tools provided through the *cdsclient* package.

## REFERENCES

- Azusienis & Straizys, 1969, *Sov. Astron.* 13, 316
- Bessell M. S., 1979, *PASP*, 91, 589
- Bessell M. S., 1991, *AJ*, 101, 662
- Bessell M. S., 2005, *Ann. Rev. Astr. Astrophys.*, 43, 293
- Bessell M. S. & Brett J. M., 1988, *PASP*, 100, 1134
- Buser R., 1978, *Astr. Astrophys.*, 62, 411
- Bohlin, R. C., 1996, *AJ*, 111, 1743
- Bohlin, R. C., 2010, *AJ*, 139, 1515
- Bohlin, R. C., Dickinson M. E. & Calzetti D., 2001, *AJ*, 122, 2118
- Chabrier G., Brassard P., Fontaine G., & Saumon D., 2000, *ApJ*, 543, 216
- Cohen M., Megeath S.T., Hammersley P.L., Fabiola M-L. & Stauffer J., 2003a, *AJ*, 125, 2645
- Cohen M., Wheaton W. M. & Megeath S. T., 2003b, *AJ*, 126, 1090
- Colina L & Bohlin, R. C., 1997, *AJ*, 113, 1138
- Cuillandre, J.-C., Magnier, E. A., Isani, S., Sabin, D., Knight, W., Kraus, S. & Lai, K., 2004, *ASSL* 300, 287
- Cutri R. M., 1998, *AAS* 192, 6402
- Davenport J. R. A., Bochanski J. J., Covey K. R., Hawley S. L., West A. A. & Schneider D. P. 2007, *AJ*, 134, 2430
- Drilling J. S. & Landolt A. U., 1979, *AJ*, 84, 783
- Gregg M. D., Silva D., Rayner J., Worthey G., Valdes F., Pickles A., Rose J., Carney B. & Vacca W., 2006, *HSTC conf.*, 209

- Gunn, J. E., Carr, M., Rockosi, C., Sekiguchi, M., Berry, K., Elms, B., de Haas, E., Ivezić Z., Knapp, G., Lupton, R., Pauls, G., Simcoe, R., Hirsch, R., Sanford, D., Wang, S., York, D., Harris, F., Annis, J., Bartozek, L., Boroski, W., Bakken, J., Haldeman, M., Kent, S., Holm, S., Holmgren, D., Petravick, D., Prosapio, A., Rechenmacher, R., Doi, M., Fukugita, M., Shimasaku, K., Okada, N., Hull, C., Siegmund, W., Mannery, E., Blouke, M., Heidtman, D., Schneider, D., Lucinio, R., Brinkman, J., 1998, *AJ*, 116, 3040
- Hauck B. & Mermilliod M., 1998, *A&AS*, 129, 431
- Heap S. R. & Lindler D., 2010, *AAS*, 21546302H
- Hewett P.C., Warren S.J., Leggett S. K. & Hodgkin S. T., 2006, *MNRAS*, 367, 454
- Høg E., Fabricius C., Makarov V. V., Urban S., Corbin T., Wycoff G., Bastian U., Schwendiek P. & Wicenec A., 2000, *Astron. Astrophys.*, 355, 27
- Holberg J.B., & Bergeron P., 2006, *AJ*, 132, 1221
- Jester S., Schneider D. P., Richards G. T., Green R. F., Schmidt M., Hall P. B., Strauss M. A., Vanden Berk D. E., Stoughton C., Gunn J. E., Brinkman J., Kent S. E, Smith J. Allyn, Tucker D. L. & Yanny B., 2005, *AJ*, 130, 873
- Lacomb, P. & Fontaine G., 1981, *A&AS*, 43, 367
- Landolt A. U., 1983, *AJ*, 88, 439
- Landolt A. U., 1992a, *AJ*, 104, 340
- Landolt A. U., 1992b, *AJ*, 104, 372
- Landolt A. U., 2007, *AJ*, 133, 2502
- Landolt A. U., 2009, *AJ*, 137, 4186
- Landolt A. U. & Drilling J. S., 1979, *AJ*, 84, 783
- Landolt A. U. & Uomoto A. K., 2007, *AJ*, 133, 768
- Lu P. K., Demarque P., van Altena W., McAlister H. & Hartkopf W., 1987, *AJ*, 94, 1318
- Maiz Apellániz, J., 2006, *AJ*, 131, 1184
- Maiz Apellániz, J., 2007, *ASP Conference Series*, 364, 227

- McGraw J. T., Zimmer, P. C., Ackermann, M. R., Hines, D. C., Hull, A. B., Rossman, L., Zirzow D. C., Brown, S. W., Fraser, G. T., Lykke K. R., Smith A. W., Stubbs C. W. & Woodward J. T., *Astronomical Telescopes & Instrumentation*, 2010, SPIE, 7735E, 272
- Menzies J. W., Marang F., Laing J. D., Coulson I. M., Engelbrecht C. A. 1991, *MNRAS*, 248, 642
- Monet D. G., Levine S. E., Canzian B., Ables H. D., Bird A. R., Dahn C. C., Guetter H. H., Harris H. C., Henden A. A., Leggett S. K., Levison H. F., Luginbuhl C. B., Martini J., Monet A. K. B., Munn J. A., Pier J. R., Rhodes A. R., Riepe B., Sell S., Stone R. C., Vrba F. J., Walker R. L. & Westerhout G., 2003, *AJ*, 125, 984.
- Ofek, E. O., 2008, *PASP*, 120, 1128
- Oke J. B. 1990, *AJ*, 99, 1621
- Oke J. B. & Gunn J. E. 1983, *ApJ*, 266, 71
- Pickles A. J., 1998, *PASP*, 110, 863
- Pickles A. J., 2010 HST Calibration Workshop proceedings.
- Reach, William T., Megeath, S. T., Cohen, Martin, Hora, J., Carey, Sean, Surace, Jason, Willner, S. P., Barmby, P., Wilson, Gillian, Glaccum, William, Lowrance, Patrick, Marengo, Massimo & Fazio, Giovanni G. 2005, *PASP*, 117, 978
- Sirianni, M., Jee, M. J., Bentez, N., Blakeslee, J. P., Martel, A. R., Meurer, G., Clampin, M., De Marchi, G., Ford, H. C., Gilliland, R., Hartig, G. F., Illingworth, G. D., Mack, J. & McCann, W. J., 2005, *PASP*, 117, 1049
- Smith, J. Allyn, Tucker, Douglas L., Kent, Stephen, Richmond, Michael W., Fukugita, Masataka, Ichikawa, Takashi, Ichikawa, Shin-ichi, Jorgensen, Anders M., Uomoto, Alan, Gunn, James E., Hamabe, Masaru, Watanabe, Masaru, Tolea, Alin, Henden, Arne, Annis, James, Pier, Jeffrey R., McKay, Timothy A., Brinkmann, Jon, Chen, Bing, Holtzman, Jon, Shimasaku, Kazuhiro, York, Donald G., 2002, *AJ*, 123, 212
- Smith, J. Allyn, Allam, S. S., Tucker, Douglas L., Stute, J. L., Rodgers, C. T., Stoughton C., Beers, T. C., French R. S. & McGehee P. M., 2005, *BAAS*, 37, 1379
- Stubbs, C. W. & Tonry, J. L., 2006, *ApJ*, 646, 1436
- Sung H. & Bessell M. S., 2000, *PASA*, 17, 244

Tokunaga A. T., Simons D. A & Vacca W. D. 2002, *PASP*, 114, 180

Tucker D. L., Kent S., Richmond M. W., Annis J. A., Smith J. A., Allam S. S., Rodgers T., Stute J. L., Adelman-McCarthy J. K., Brinkmann J., Doi M., Finkbeiner D., Fukugita M., Goldston J., Greenway B., Gunn J. E., Hendry J. S., Hogg D. W., Ichikawa S.-I., Ivezić Z., Knapp G. R., Lampeitl H., Lee B. C., Lin H., McKay T. A., Merelli A., Munn J. A., Neilsen E. H., Newberg H. J., Richards G. T., Schlegel D. J., Stoughton C., Uomoto A. & Yanny B., 2006, *Astron. Nachr.*, 327, 821

Wegner G., 1983, *AJ*, 88, 109

Zacharias, N., Monet, D. G., Levine, S. E., Urban, S. E., Gaume, R. & Wycoff, G. L., 2004, *AAS*, 205, 4815

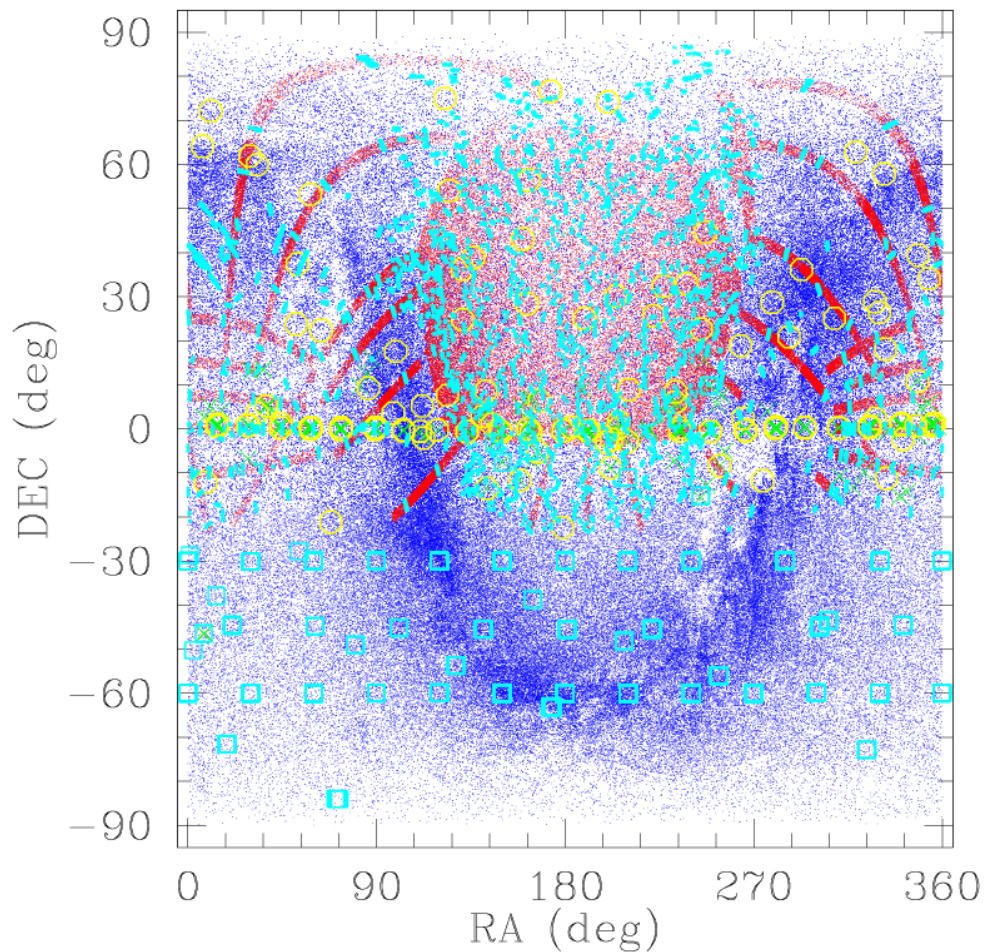


Fig. 1.— The footprint in equatorial coordinates of the various catalogs discussed here. The Tycho2 catalog (blue dots) covers the whole sky to  $B_T \sim 13.5$  mag. The Sloan survey grey (red in electronic version) dots covers less area but to a much fainter limiting magnitude, shown here to  $g < 16$  mag. The Landolt primary standards are marked with green crosses, the Sloan primary standards with yellow circles, the Southern Sloan secondary standards are marked with cyan squares, where each square represents many standards, and the Northern SDSS PT stars are marked with cyan dots.

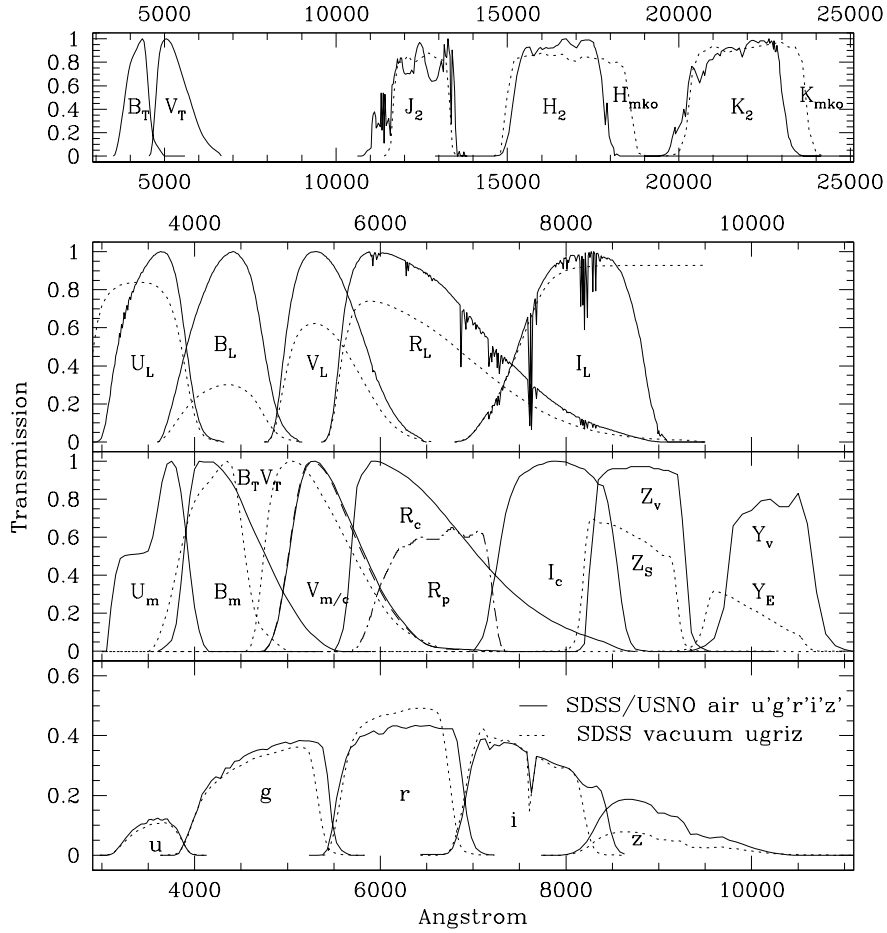


Fig. 2.— The filters discussed here are illustrated. In the first panel the Tycho2  $B_T V_T$  filter system transmissions are taken from Maiz Apellániz (2006), and over-plotted (dotted lines) in the third panel for convenient reference. The 2MASS  $J_2 H_2 K_2/S$  system total response curves are from the IPAC website; the  $JHK_{MKO}$  filter transmission curves (dotted) are from Tokunaga et al (2002). In the second panel the Landolt  $U_L B_L V_L R_L I_L$  transmission curves for the filters alone are shown – dotted, Landolt (1992a); their system response including typical atmosphere and detector QE are shown – solid, Cohen et al (2003a). In the third panel the synthetic  $U_M B_M V_M$  filters are from Maiz Apellániz (2006) ( $V_M$  plotted as dashed line); the  $V_C R_C I_C$  curves are from Bessell (1979) and the  $Z_V Y_V$  (solid) curves are from the UKIRT/VISTA collaboration. The PTF “Mould-type”  $R_p$  system response is also illustrated, as are the LCOGT  $Z_S Y_E$  system responses (dots) discussed in section 6.1.1. In the bottom panel the Sloan survey system bandpasses are shown for both the unprimed survey imaging bandpasses (dotted lines, where the filter interference red edges move bluer in the vacuum of the survey camera) and primed bandpasses used in air for PT and Southern standard observations ( $u'g'r'i'z'$  – solid lines); they are from the JHU skyservice and the USNO FNAL websites.

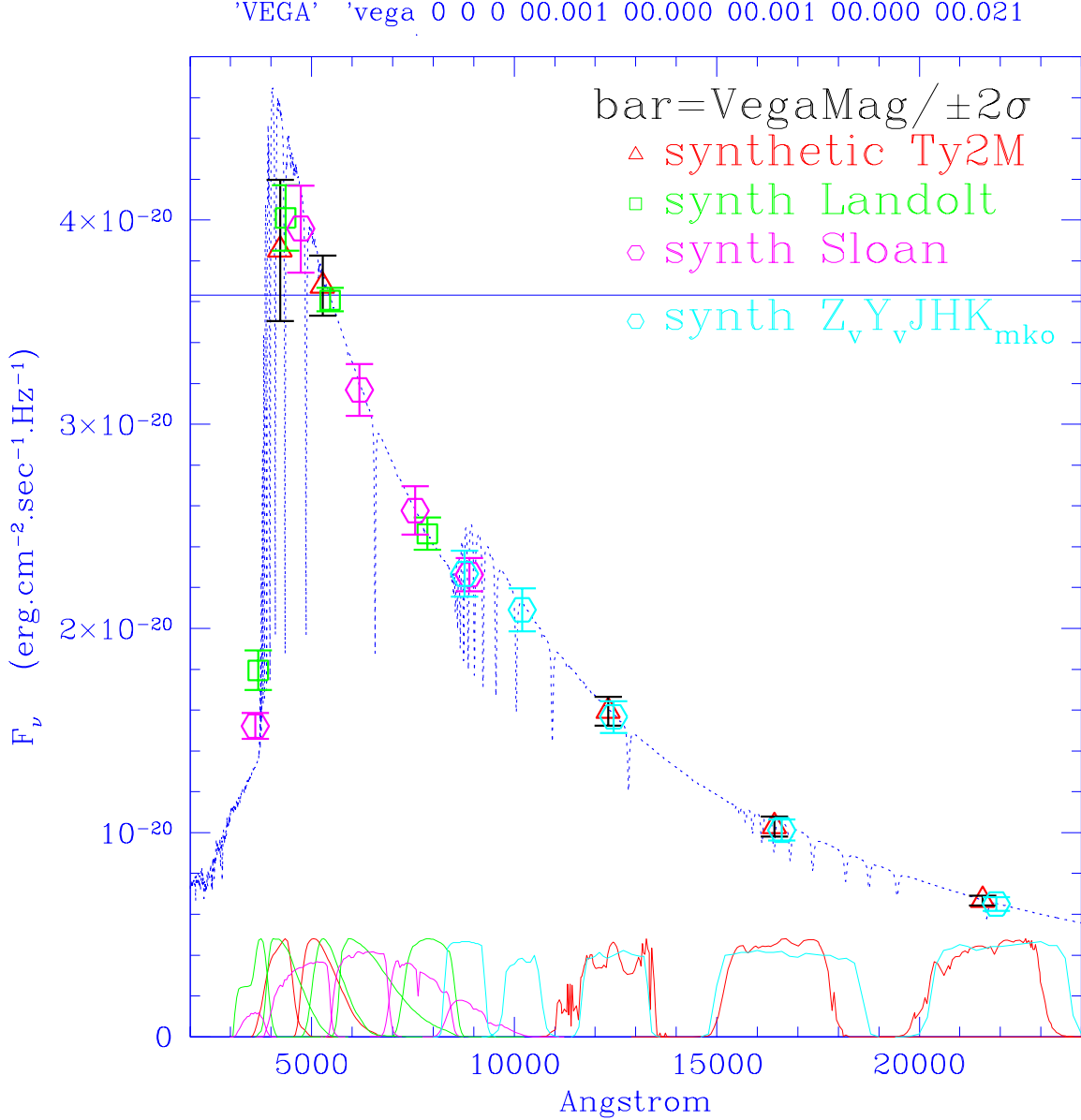


Fig. 3.— The bandpasses, zeropoints and synthetic measurements are illustrated for the *calspec* spectrum STIS\_005 spectrum of Vega (blue dotted trace), which defines the nominal 0-mag definition for filters on the *vega* system. The electronic version of this figure is in color. The horizontal line at  $3.631 \times 10^{-20} \text{ erg cm}^{-2} \text{ sec}^{-1} \text{ Hz}^{-1}$  (3631 Jy) illustrates the AB=0 mag reference. Tycho2/2MASS  $B_T V_T JHK_{2/s}$  bandpasses are indicated by red traces, synthetic flux measurements by red triangles and zeropoint dispersion values about them by error bars in black. All error bars here show  $\pm 2\sigma$  zeropoint dispersion for better visibility. Adopted Landolt  $U_M B_M V_C R_C I_C$  bandpasses are shown as green traces, synthetic flux measurements by green squares and zeropoint dispersion values by green bars. Sloan  $u'g'r'i'z'$  bandpasses are shown in magenta, synthetic measurements by magenta circles and zeropoint dispersion values by magenta bars. The UKIRT  $Z_V Y_V JHK_{MKO}$  bandpasses are shown as cyan traces, synthetic measurements as cyan circles and zeropoint dispersion values about them by cyan bars.

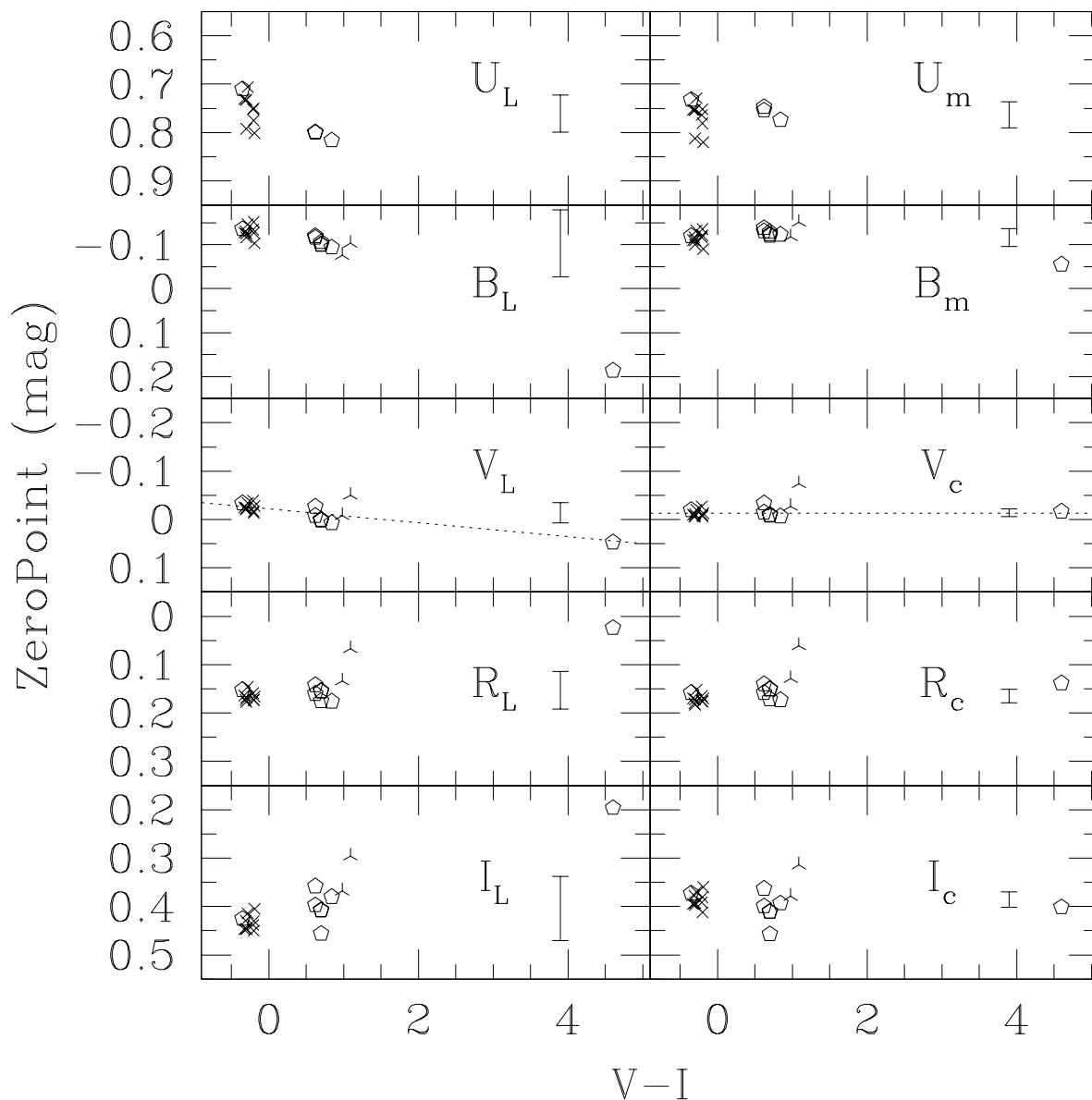


Fig. 4.— Zeropoints are shown for  $U_L B_L V_L R_L I_L$  (left) and  $U_M B_M V_C R_C I_C$  system band-passes (right) as a function of standard  $V-I$  color. The ordinate scale is set so that vertically higher zeropoints result in magnitudes which are larger (fainter). Vertical error bars indicate the average and  $\pm 1\sigma$  dispersion in each panel. Crosses indicate White Dwarfs, Pentagons indicate dwarfs. Three-point crosses indicate the two K giants, which are not included in these zeropoint averages or dispersions as they lack UBVRI photometry. The reddest point corresponding to the M7V VB8 lacks U-band data. The selected UBVRI system profiles on the right minimize zeropoint scatter and trend with color.

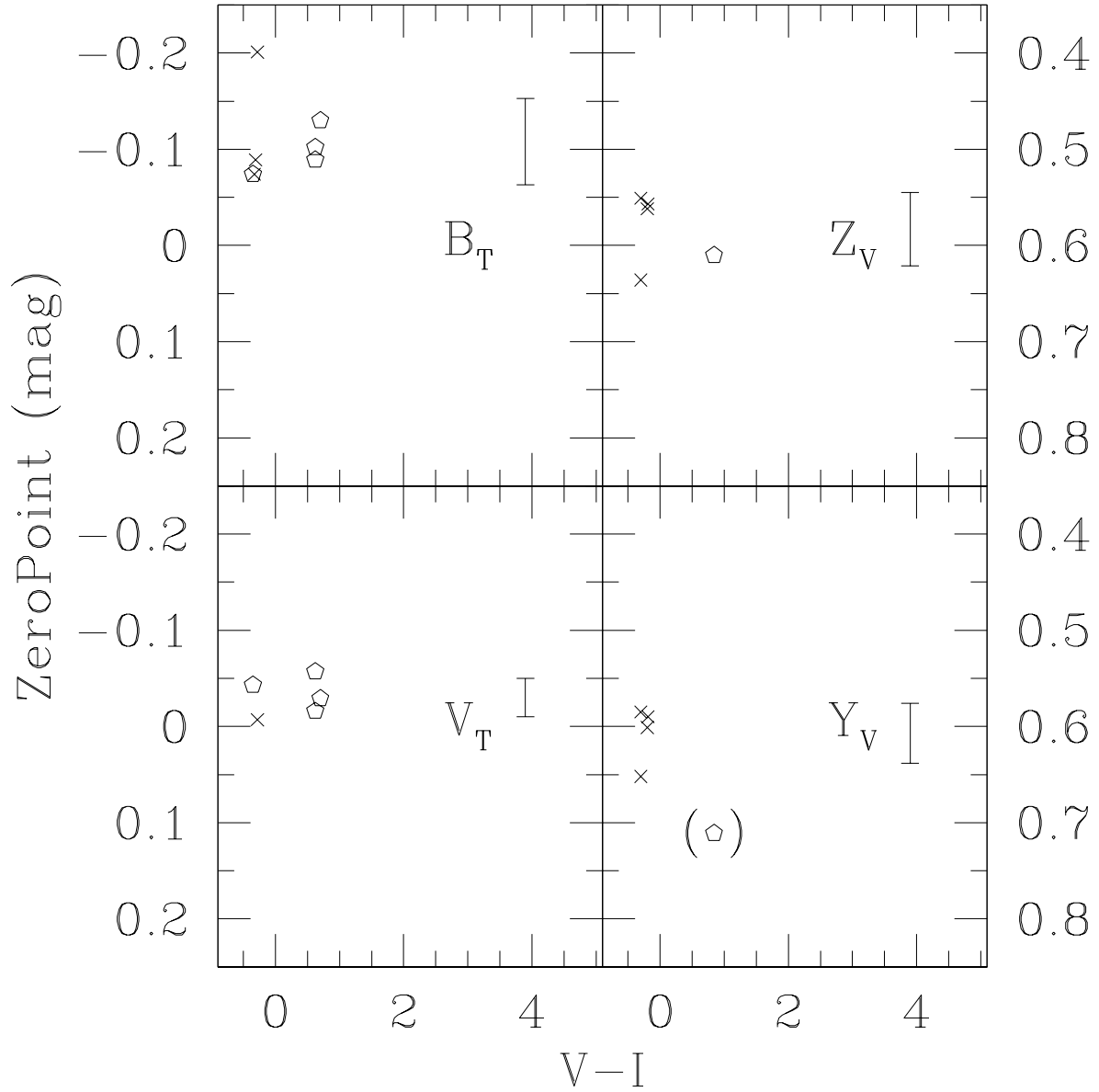


Fig. 5.— Zeropoints are shown for  $B_T V_T$  (left ordinate) and  $Z_V Y_V$  (right ordinate) as a function of standard  $V - I$  color, with averages and dispersions as vertical bars. The  $Y_V$  zeropoint for G158-100 is shown in parentheses but not included in the average. Symbols as before.

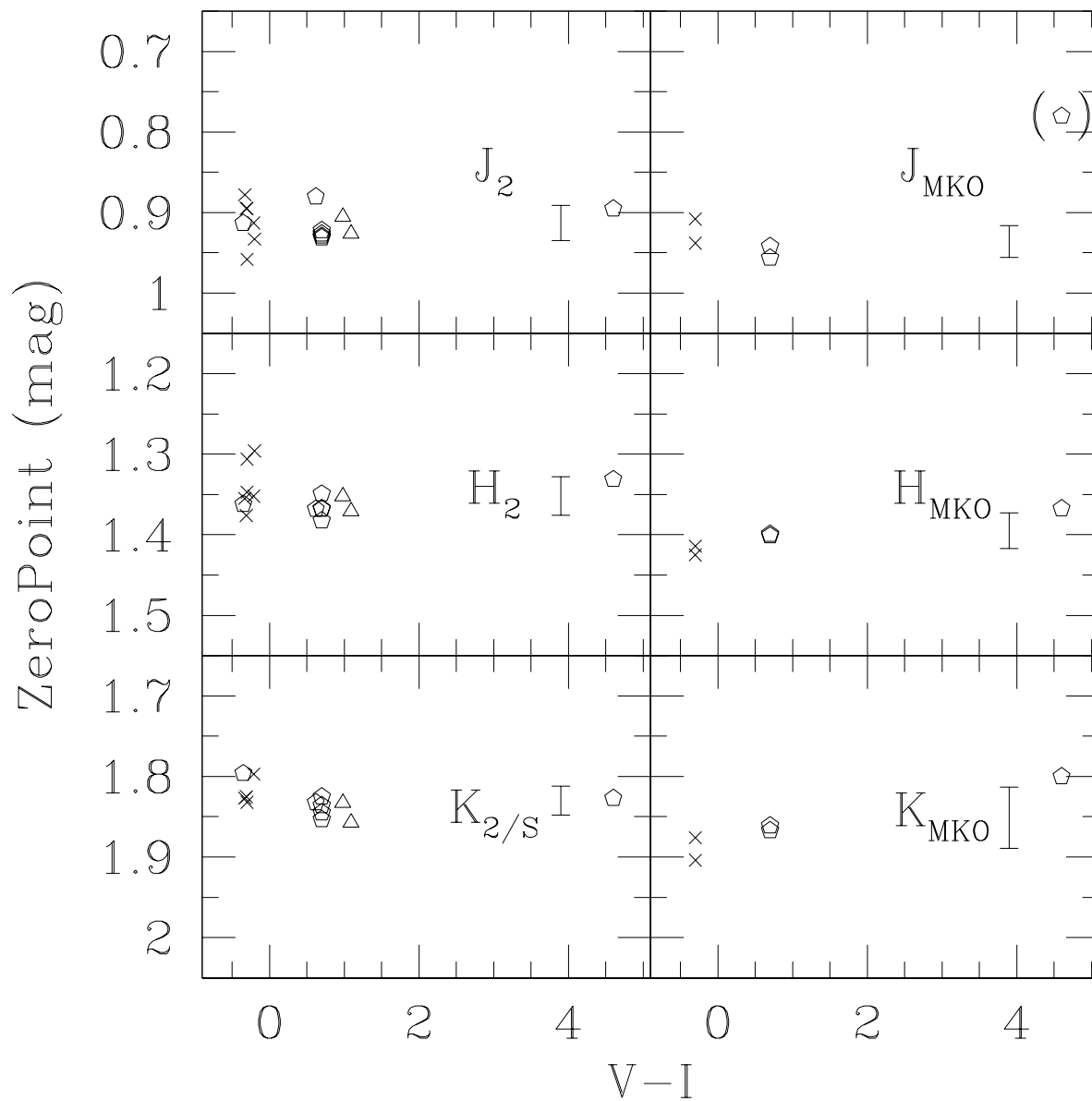


Fig. 6.— Zeropoints are shown for  $J_2H_2K_{2/S}$  (left) and  $JHK_{MKO}$  (right) as a function of standard  $V - I$  color, with averages and dispersions. Symbols as before. The KIII points (triangles) have been included for  $JHK_{2/S}$ . The zeropoints for  $JHK_{MKO}$  show some trend with color, but the  $J_{MKO}$  value for VB8 has been excluded due to uncertainty over its magnitude.

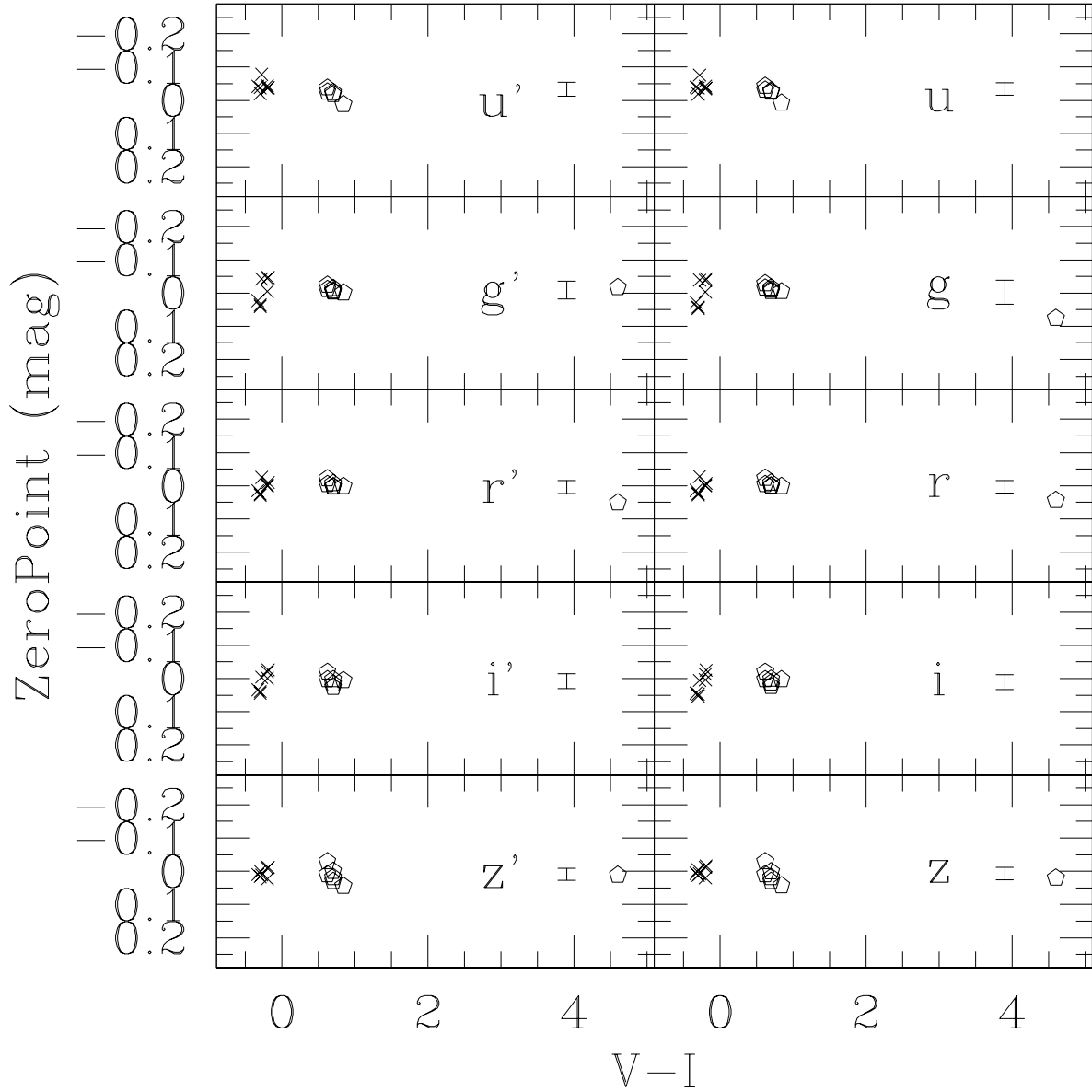


Fig. 7.— Zeropoints are shown for  $u'g'r'i'z'$  (left) and  $ugriz$  (right) as a function of standard  $V - I$  color, with averages and dispersions. VB8 is present in the  $grz$  plots, but has been omitted in the  $ui$  plots. Symbols as before.

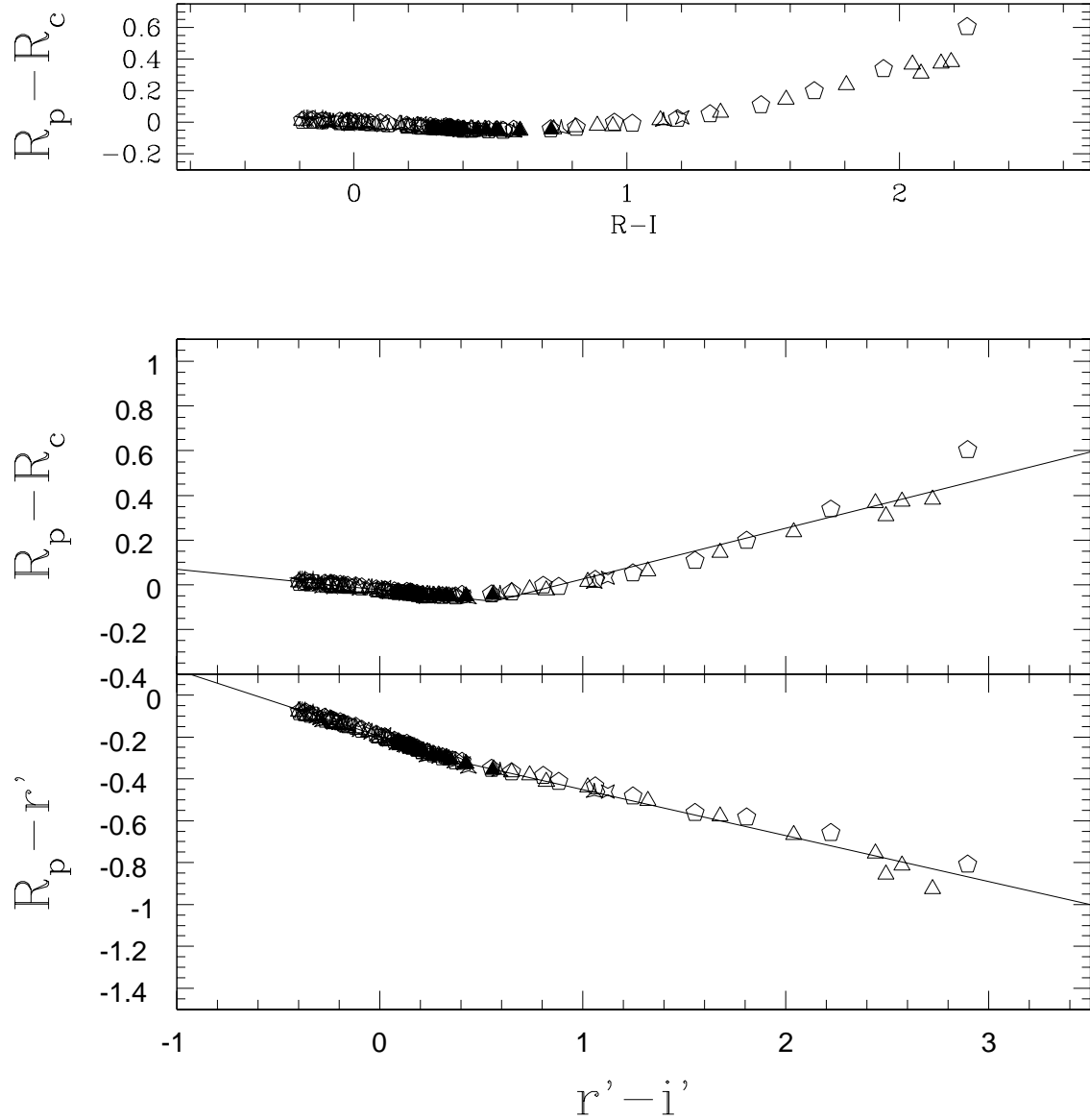


Fig. 8.— Upper panel shows the  $R_p - R_C$  color plotted against the Landolt  $R - I$  color. The fit is tight, but curved in both segments. Dwarfs are indicated as pentagons, subgiants as squares, giants as triangles and supergiants as crosses. The lower two panels show respectively the  $R_p - R_C$  and  $R_p - r'$  colors vs. Sloan  $r' - i'$ . Same symbols as before. In these cases there are good two-segment straight-line fits.

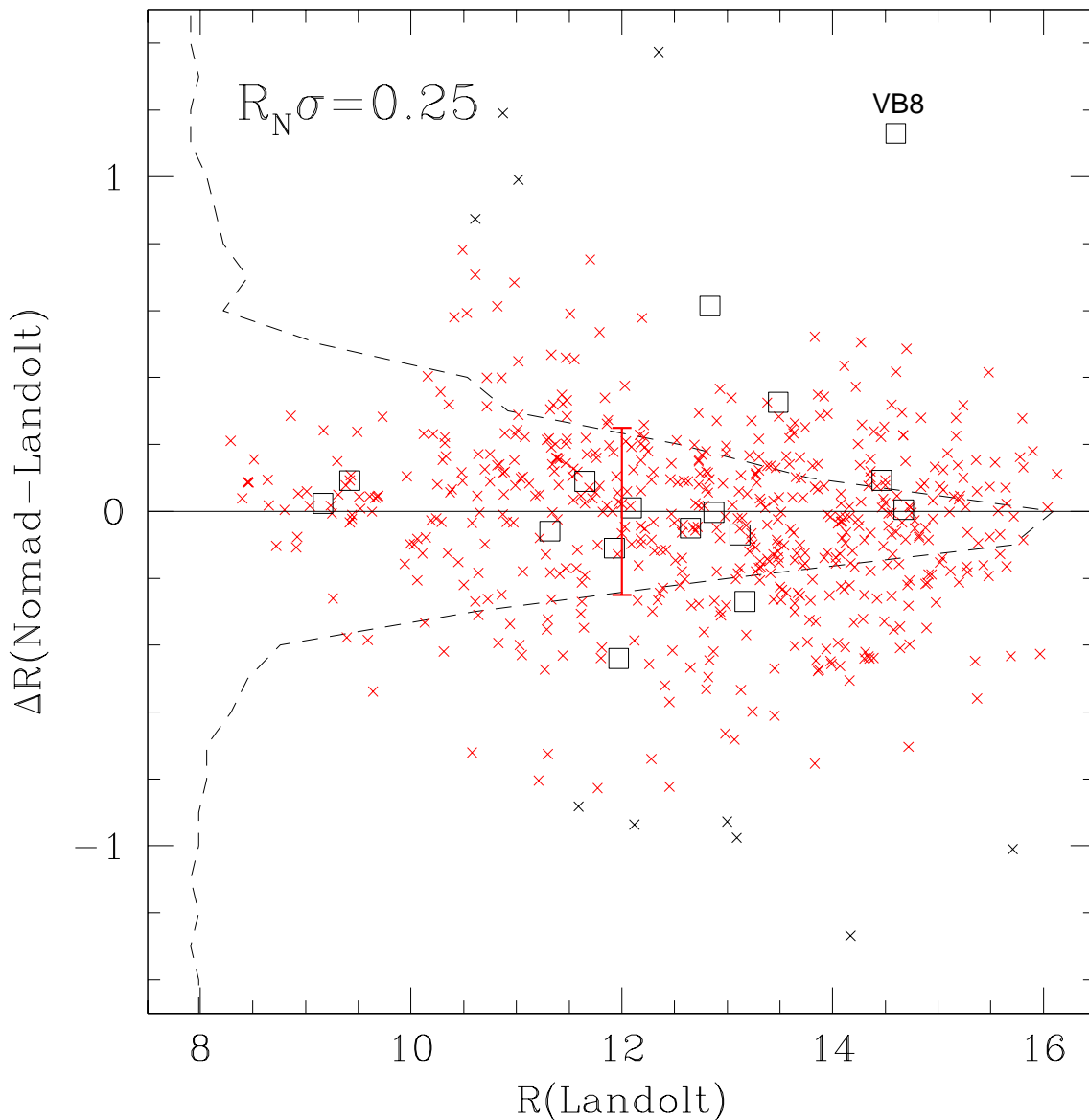


Fig. 9.— Comparison of NOMAD and Landolt R-band data plotted as the difference  $R_N - R_{Landolt}$  vs.  $R_{Landolt}$  (crosses) and CALSPEC standards (squares); VB8 is identified. Black crosses show about 10 points rejected by a  $3\sigma$  clip, and grey crosses (red in the color version) those remaining. The resulting  $1\sigma$  dispersion of 0.25 mag is indicated. The dashed histogram of all the stars shows the distribution of these differences plotted with increasing number to the right against the magnitude delta on the ordinate.

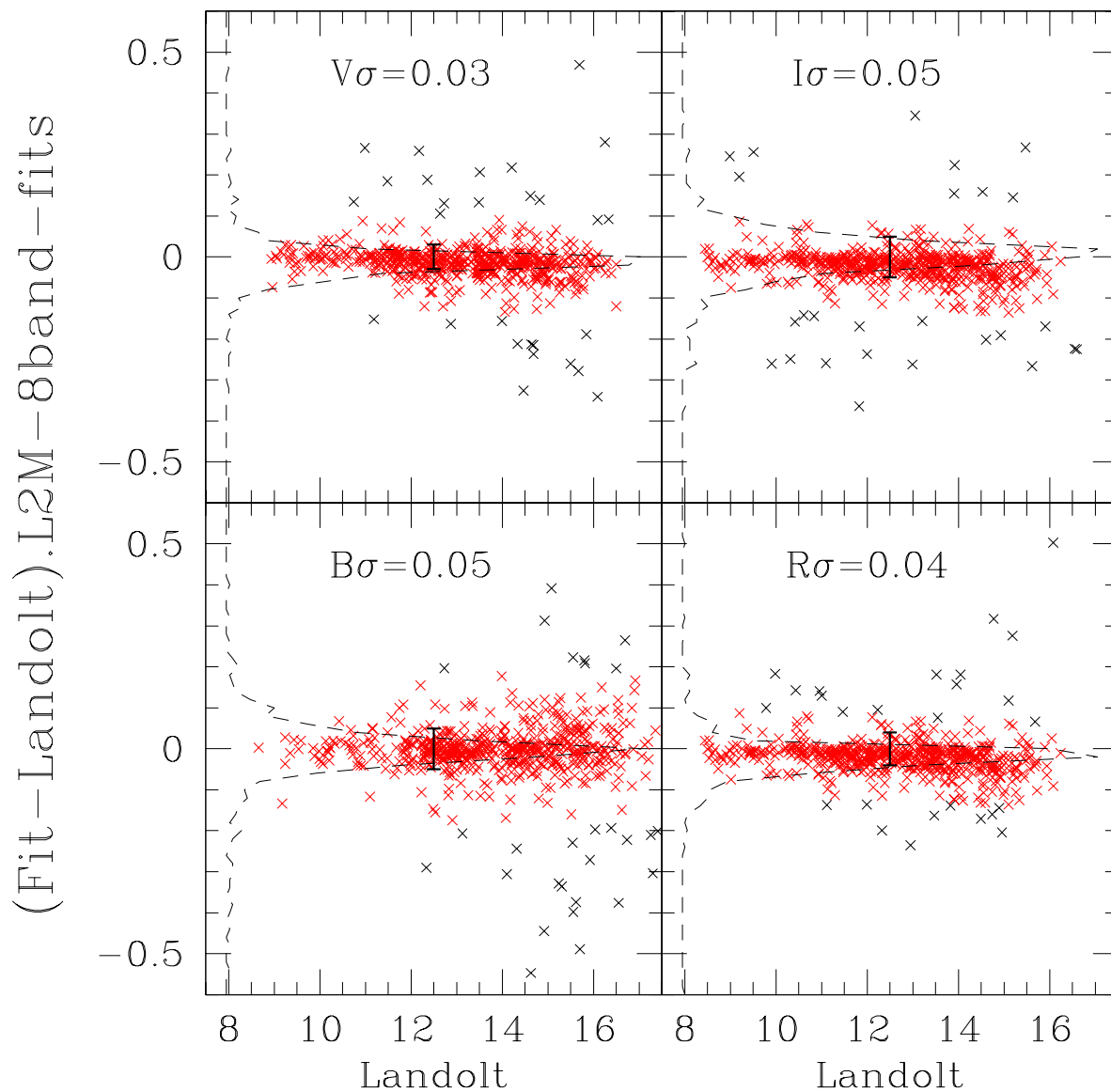


Fig. 10.—  $BVRI$  fits with eight L2M  $UBVRI - JHK_{2/S}$  bands for 594 Landolt standards. The data are plotted as magnitude differences  $\text{Fit} - \text{Landolt}$  on the ordinate vs. Landolt catalog magnitudes on the abscissa. Black crosses indicate points excluded by sigma clipping; the scaling excludes a few outliers discussed in the text. Grey (red) points indicate those remaining after sigma clipping. The dashed histograms plotted vertically in each panel illustrate the number distribution of all the points about the zero-delta (horizontal) line. Clipped  $\pm 1\sigma$  errors are indicated in each panel caption, and by the vertical error bars.

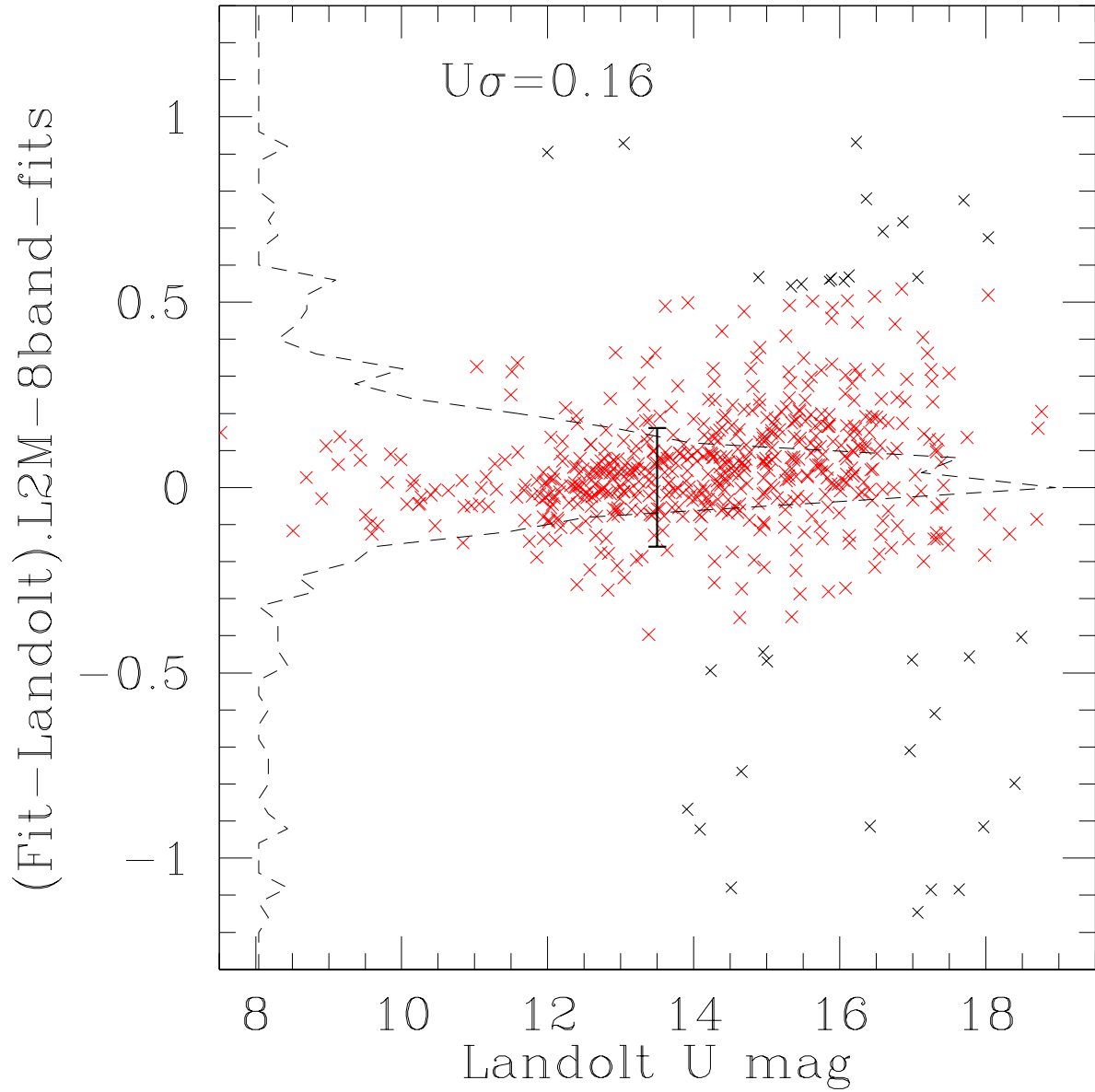


Fig. 11.— U-band fits with eight L2M  $UBVRI - JHK_{2/S}$  bands plotted as  $Fit - Landolt$  for 594 Landolt standards. Grey (red) crosses indicate points retained after sigma clipping, and the dashed histogram illustrates the number distribution of all the points around the zero-delta line. The sigma is 0.12 mag to  $U < 16$ , increasing for fainter stars.

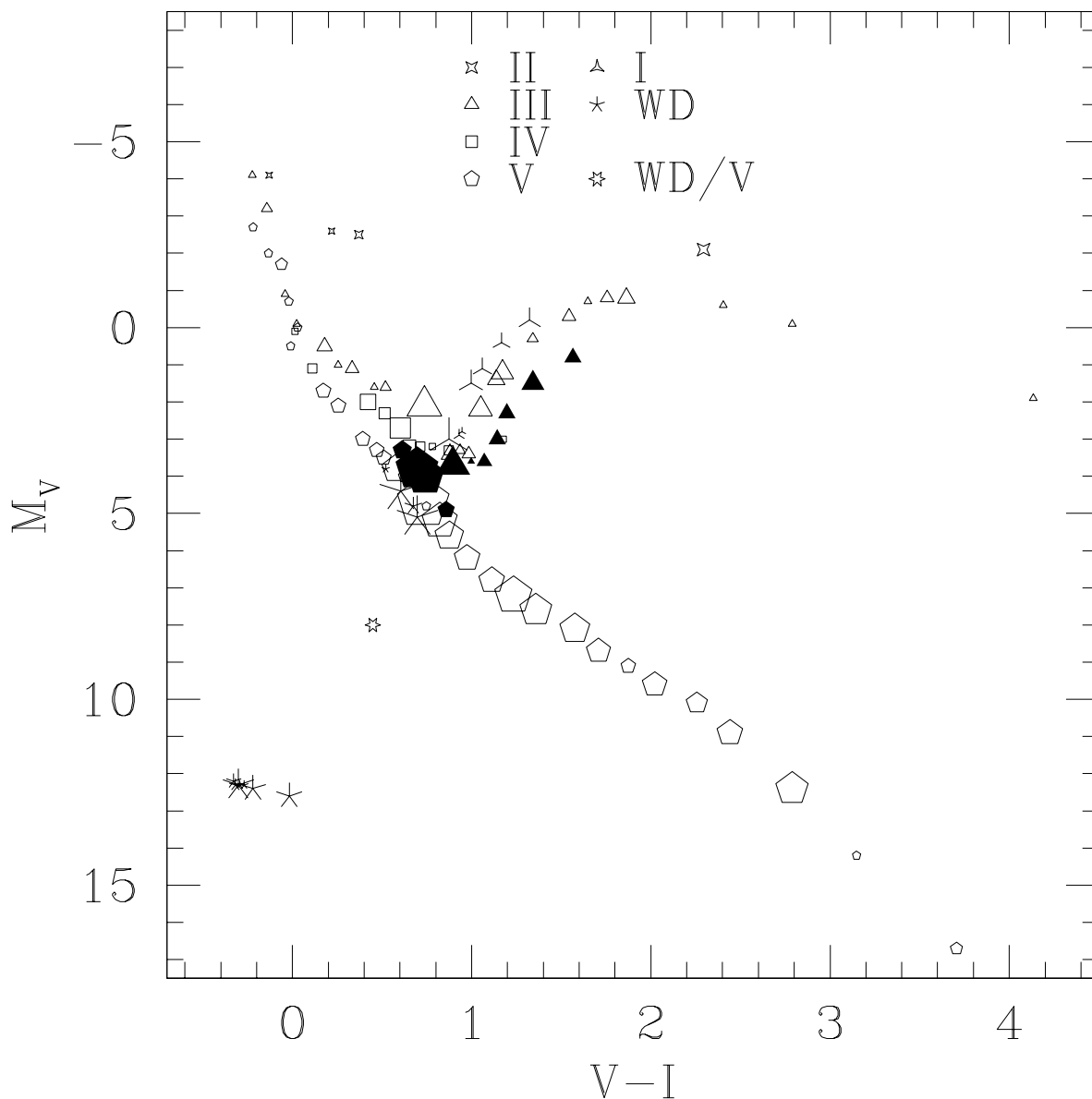


Fig. 12.— HR diagram for 594 Landolt standards shows our fitted types as absolute  $V$  magnitudes vs. spectral library  $V - I$  colors. Dwarfs are represented as pentagons, subgiants as squares, giants as triangles, Luminosity class II and I as four-point and 3-point stars respectively. White dwarfs are shown as 5-point crosses. Metal-weak dwarfs and giants are shown as 5 or 3 sided crosses, metal-rich components as 5 or 3 sided filled symbols. The area of each symbol is proportional to the frequency that library spectrum was selected. The 6-starred symbol at (0.45,8) represents the DA1/K4V double spectral type, fitted to Feige 24, PG1530+057A and SA107-215.

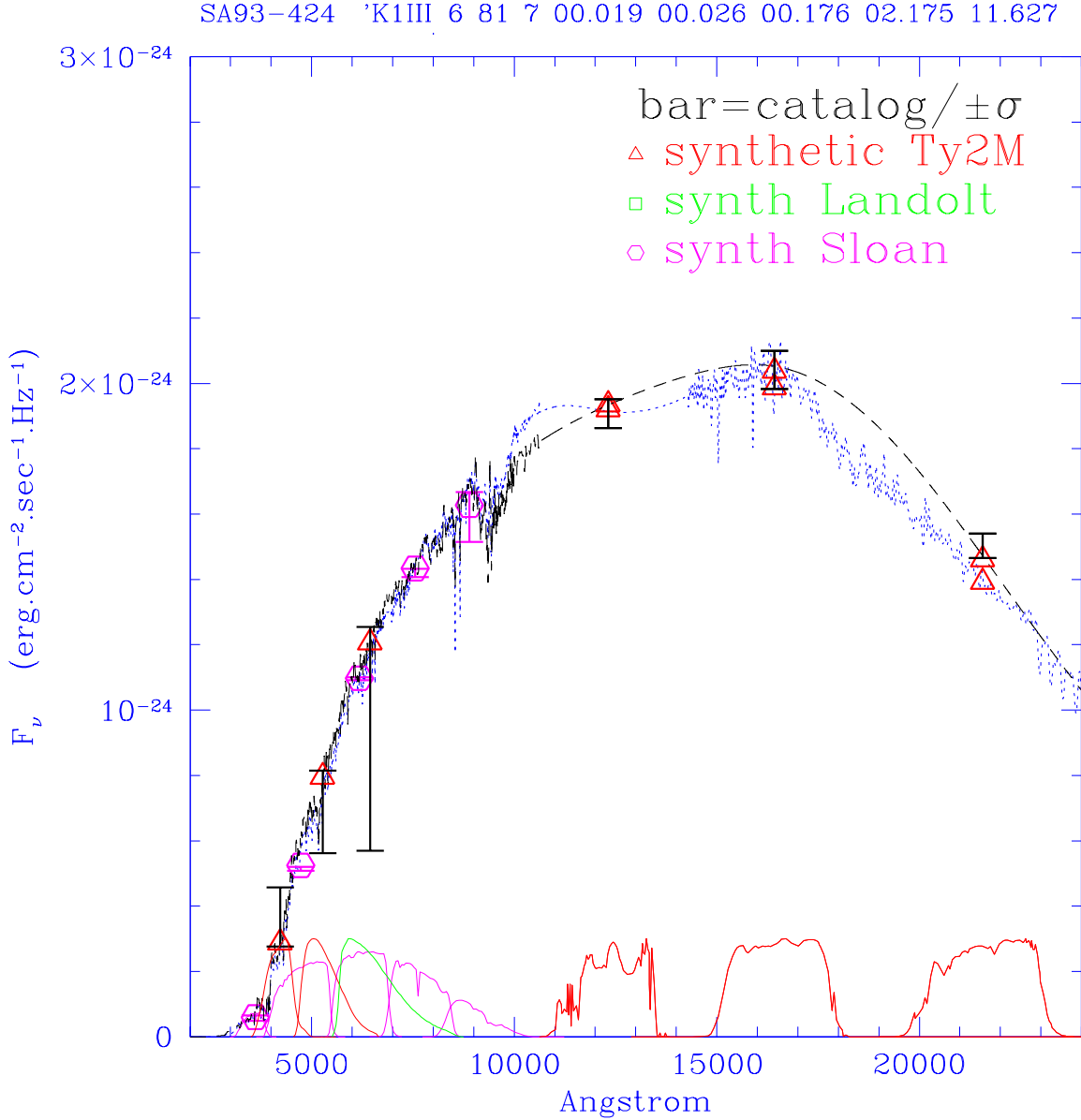


Fig. 13.— The Sloan/2MASS (8-band, S2M) K1 III fit for SA93-424 is shown (fainter, blue dotted trace) as  $F(\nu)$  vs. wavelength. Electronic versions of these figures are in color. The Sloan filter profiles are shown in magenta, the Tycho2/2MASS profiles in red and the R profile (matched here to NOMAD  $R_N$  in green). Black, green and magenta bars identify the Tycho2/2MASS, Landolt (and  $R_N$ ) and Sloan catalog magnitudes and errors. Red triangles, green squares and magenta circles identify fitted synthetic fluxes and magnitudes in the same systems. The overlaid black dashed spectrum is the rK0III fit obtained with 6 Tycho2/ $R_N$ /2MASS (TNM) bands. The long vertical black bar represents the  $R_N$  catalog error, scaled by a factor 1.5, on the second fit. The catalog fluxes are at the center of each bar, and the synthesized fluxes are marked by the symbols.

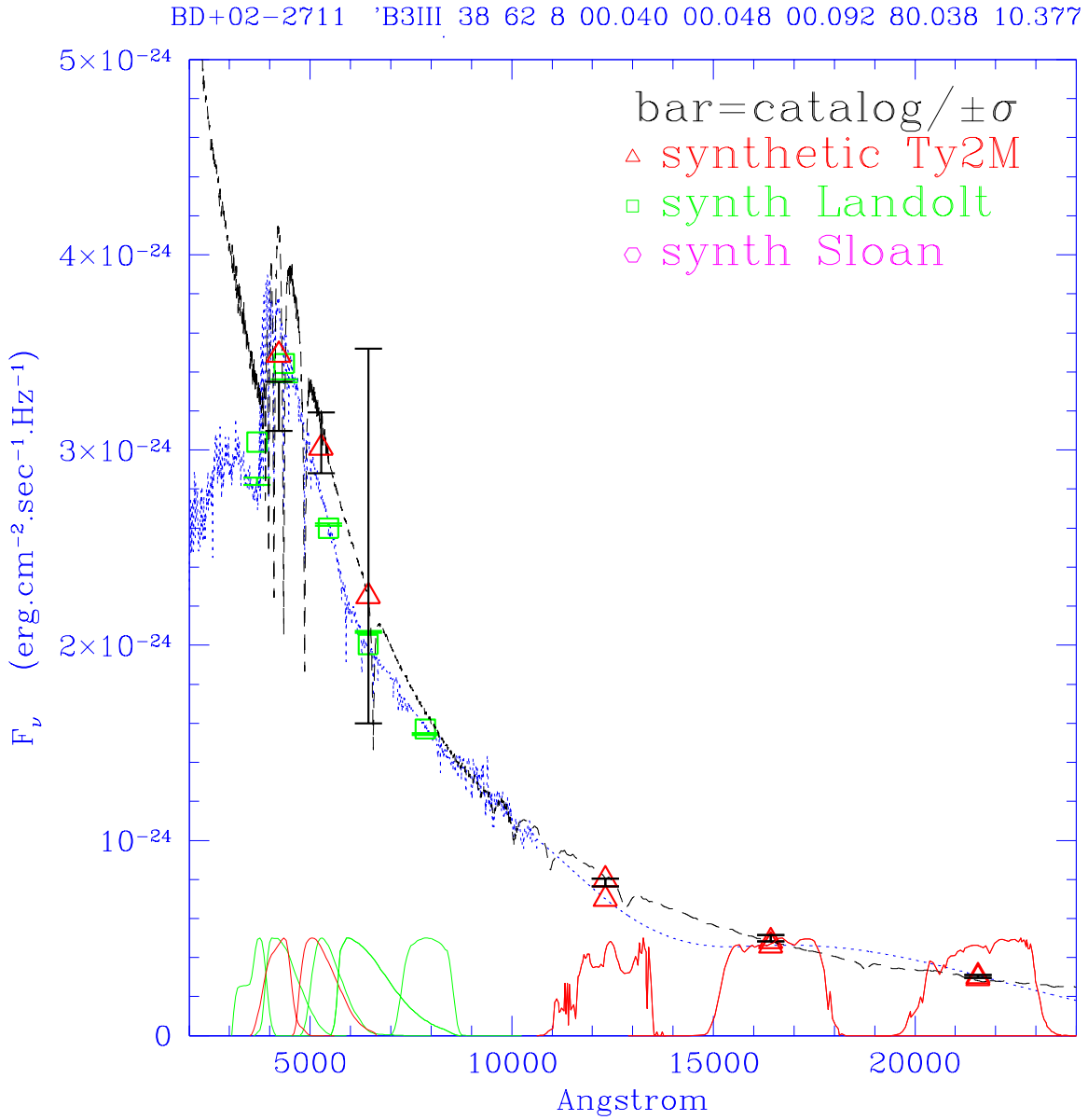


Fig. 14.— The Landolt/2MASS (8-band, L2M) B3III fit is shown (lower, blue dotted line) as  $F(\nu)$  vs. wavelength. The Tycho2/ $R_N$ /2MASS (6-band, TNM) DA3-WD fit is shown as the overlaid black-dashed trace. The long vertical black bar represents the NOMAD  $R_N$  magnitude (in its center) and error for the TNM fit, with red triangle symbol for the synthesized flux. The green bar (above the fitted green square) represents the Landolt R catalog magnitude and error for this star. Symbols as before.

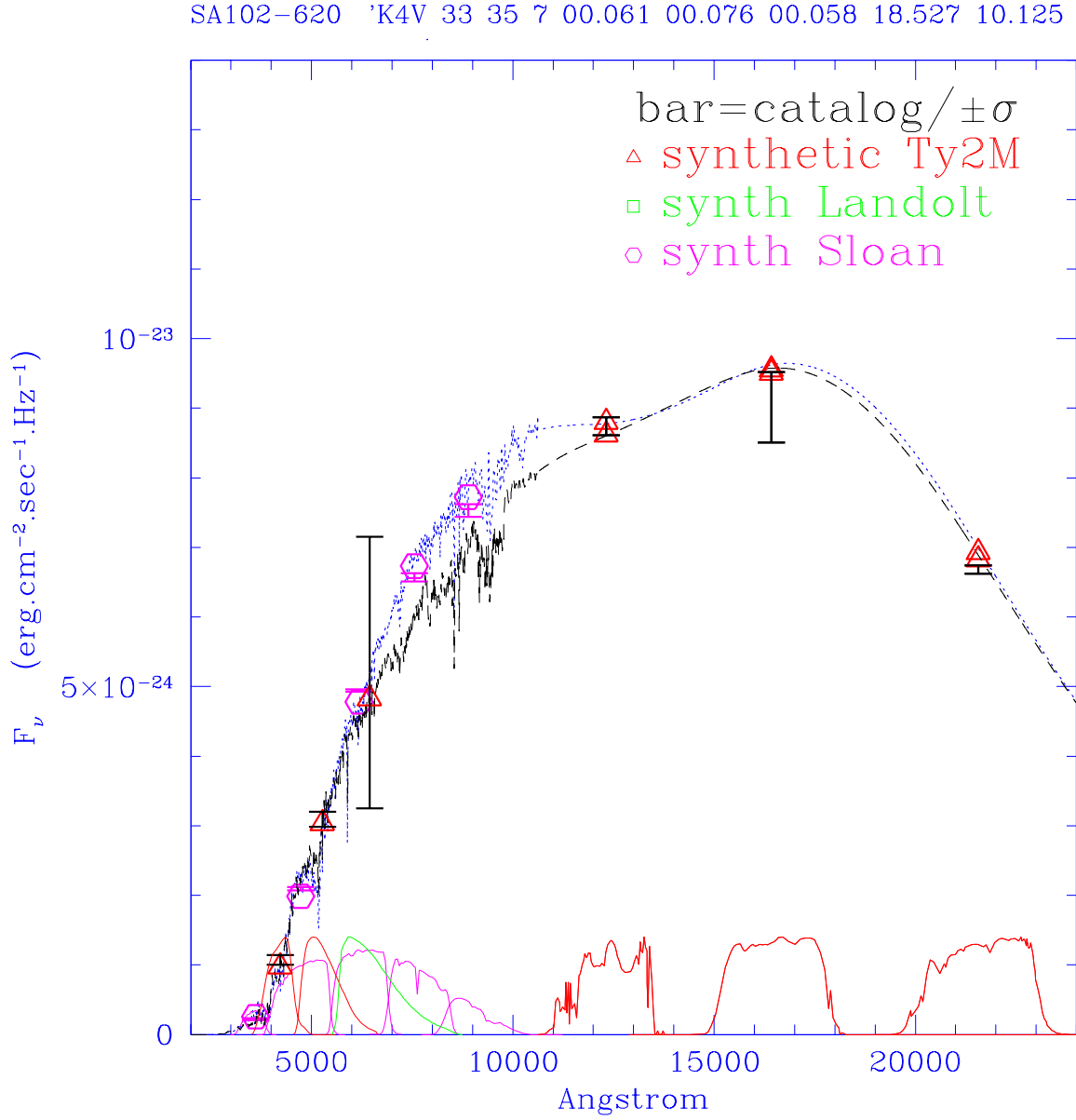


Fig. 15.— The Sloan/2MASS (8-band, S2M) K4V fit for SA102-620 is shown (blue dotted line) as  $F(\nu)$  vs. wavelength. The overlaid black dashed spectrum is the rK1 III fit obtained with 6 Tycho2/ $R_N$ /2MASS bands. Symbols as before.

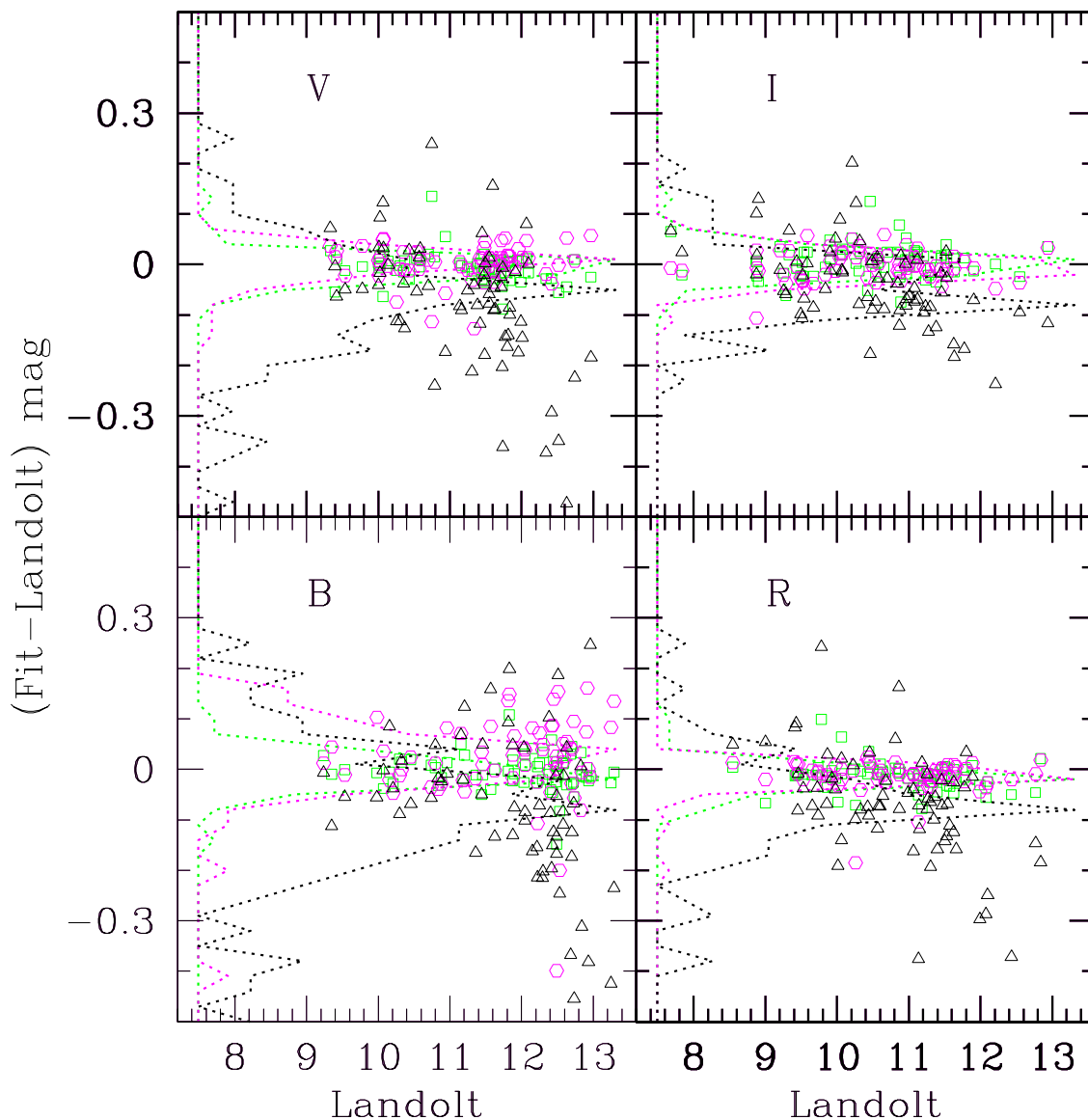


Fig. 16.— Landolt  $BVRI$  fits for 65 stars with Landolt, Sloan, Tycho2, NOMAD and 2MASS standard magnitudes. The fitted  $BVRI$  magnitudes on the ordinate are plotted as  $Fit - Landolt$  vs. the catalog values on the abscissa.  $U$  fits are not shown. Green squares and histogram indicate the L2M fits obtained with five Landolt and three 2MASS magnitudes, magenta circles and histogram indicate the S2M fits obtained with five Sloan and three 2MASS magnitudes, and black triangles and the wider histogram indicate the TNM fits obtained with  $B_T V_T R_N$  and three 2MASS magnitudes. The green and magenta histograms are narrow, indicating good fits to the zero-delta line. The black histogram is wider as expected for these TNM fits.

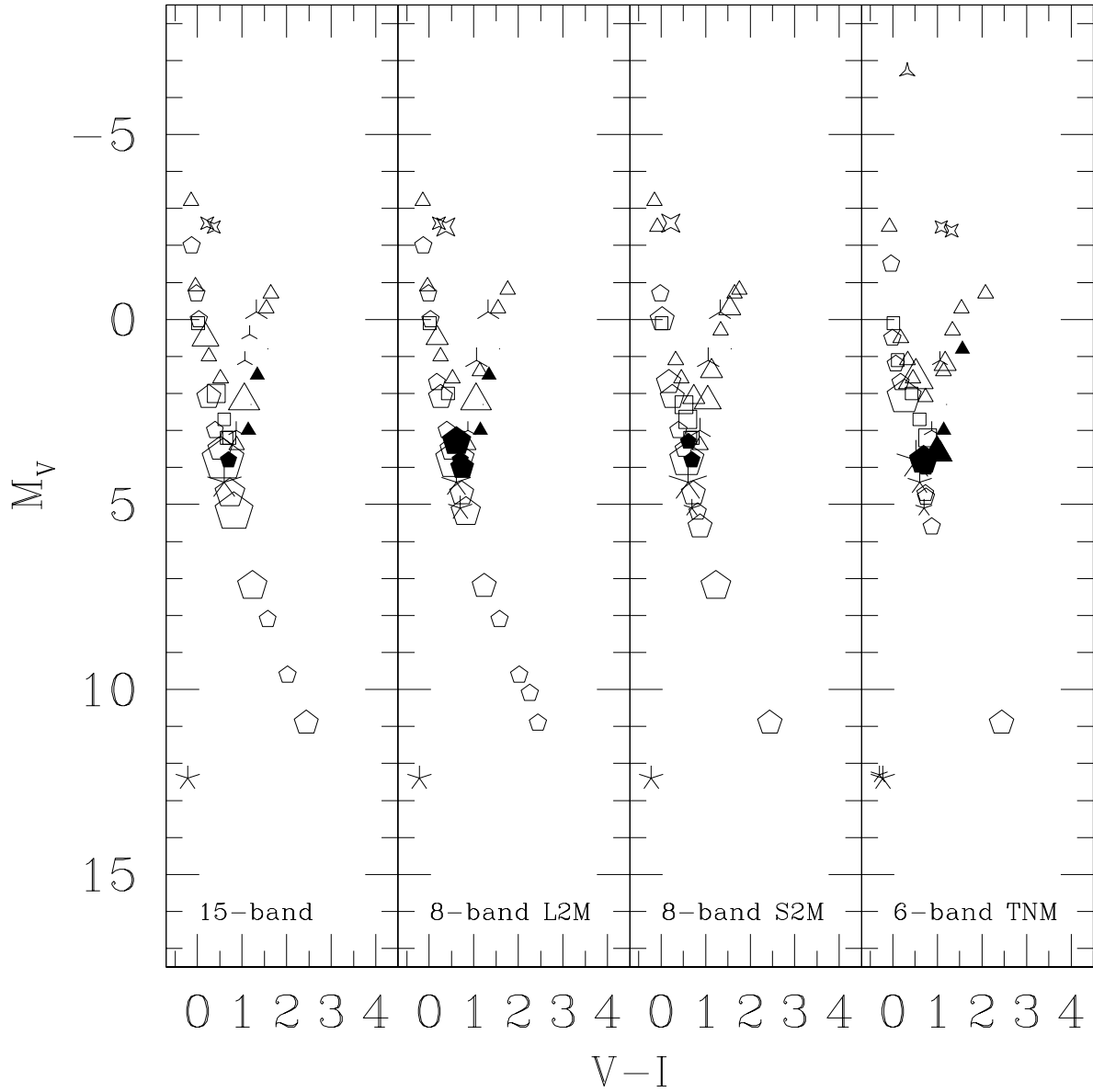


Fig. 17.— HR diagram for 65 Landolt/Sloan standards shows our fitted types as adopted absolute  $V$  magnitudes vs. spectral library  $V-I$  colors, for four different fits. Same symbols as fig 12. The area of each symbol is proportional to the frequency that library spectrum was selected.

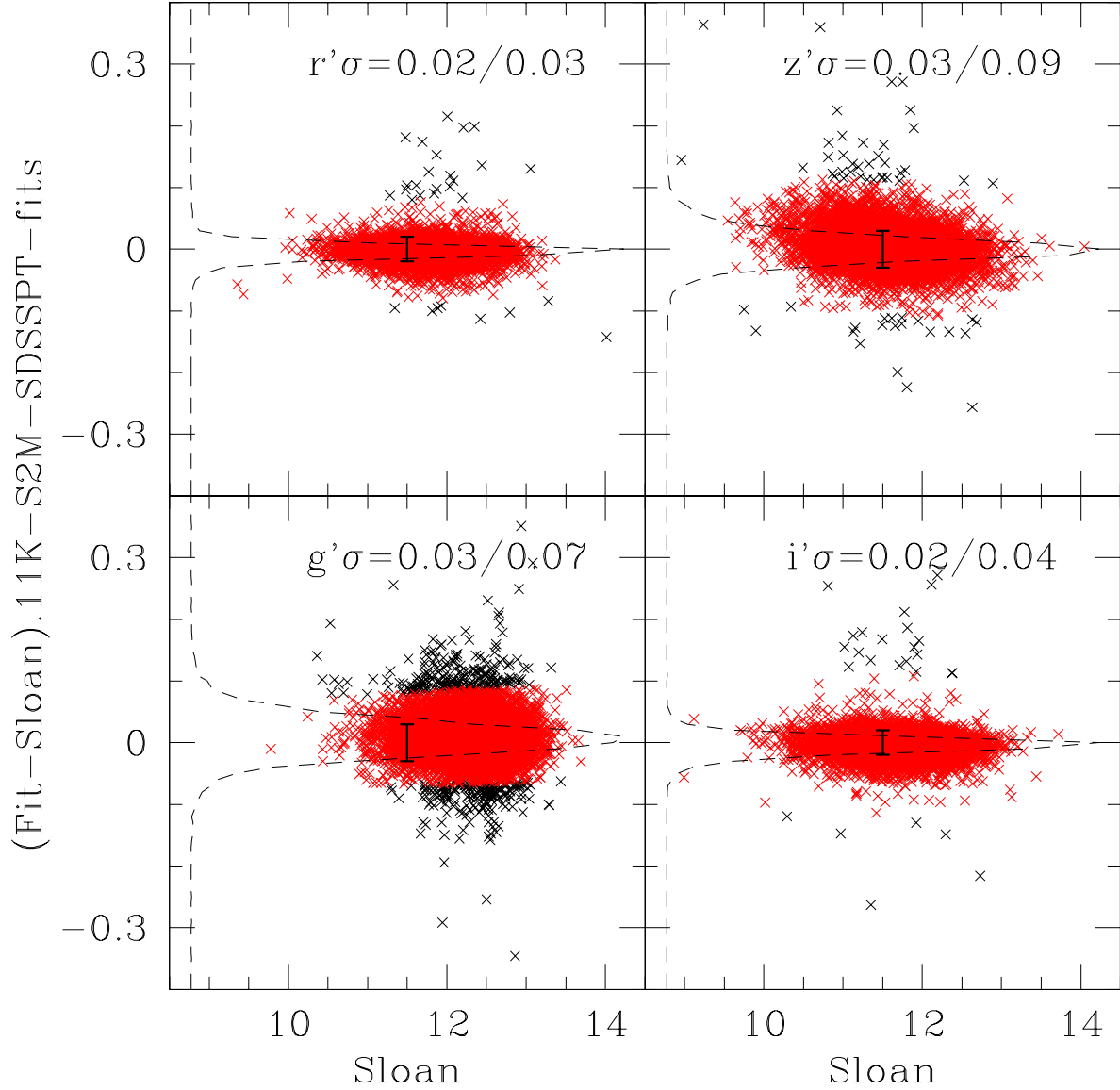


Fig. 18.— S2M fits with seven  $g'r'i'z' - JHK_{2/S}$  bands for  $\sim 11,000$  SDSS PT standards with 2MASS, Nomad & Tycho2 photometry, plotted as (Fit-Sloan) vs. Sloan magnitudes. Black crosses are points rejected by the sigma clipping, and grey (red) points are those remaining after sigma clipping. The clipped points overlap, but the number distributions for all the points about the zero-delta line are indicated by the dashed histograms. The sigmas indicated in the panel captions are for the clipped / and all the stars in each band, with  $\pm 1\sigma$  error bars drawn for the former.

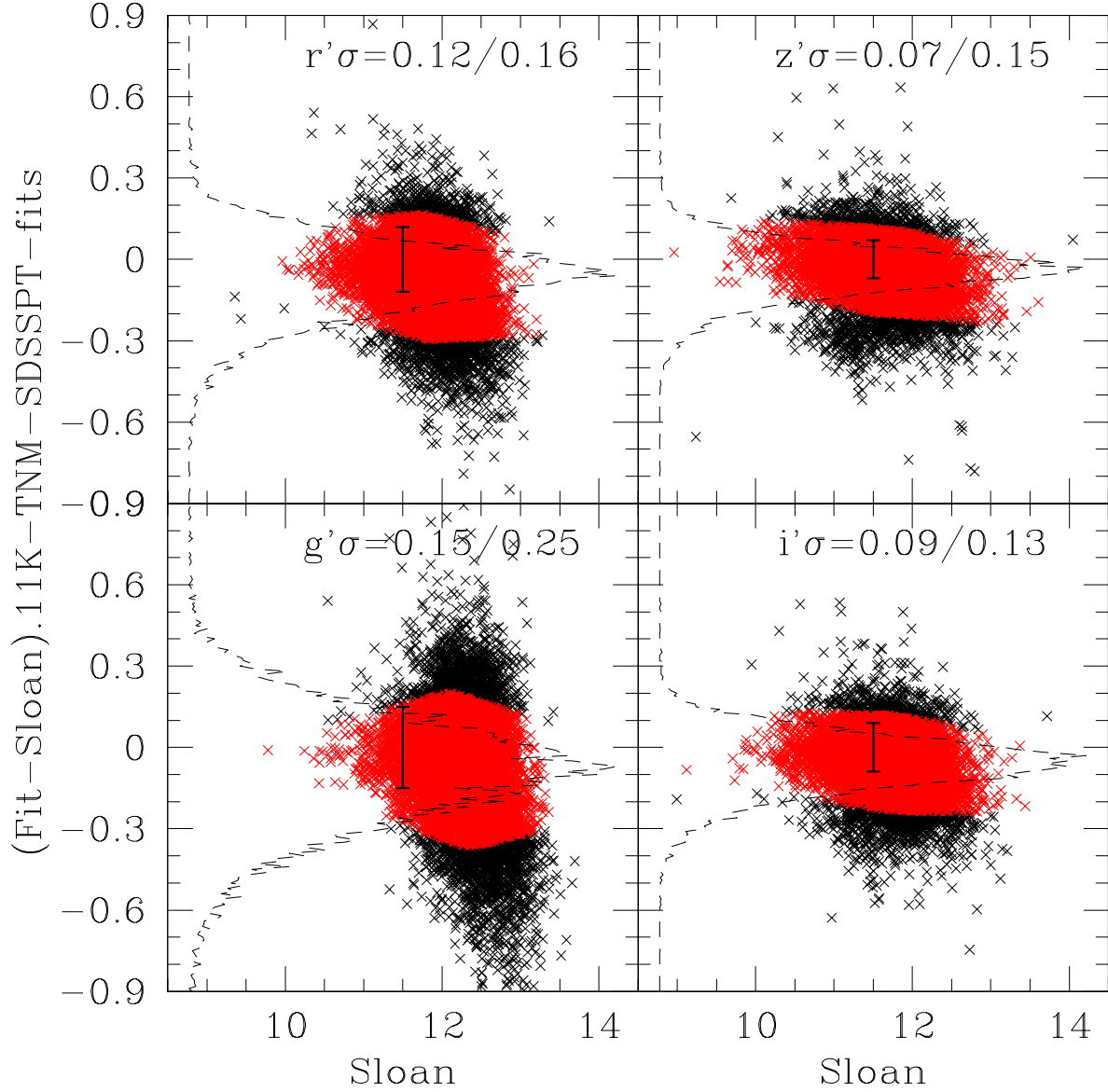


Fig. 19.— TNM fits with six  $B_T V_T R_N - JHK_{2/S}$  bands for the same  $\sim 11,000$  SDSS-PT standards plotted as (Fit-Sloan) vs. Sloan magnitudes. Note the vertical scale change from the previous figure. Black crosses show all the stars. The grey points in the middle (red in the electronic version) show 80–90% of stars remaining after sigma clipping. Sigmas after and before clipping are indicated. The histograms show the number distribution of errors about the mean for all the points. There may be some bias towards brighter fitted magnitudes in at least the  $g'r'$  bands, but the errors are dominated here by the input Tycho2/Nomad catalog accuracies.

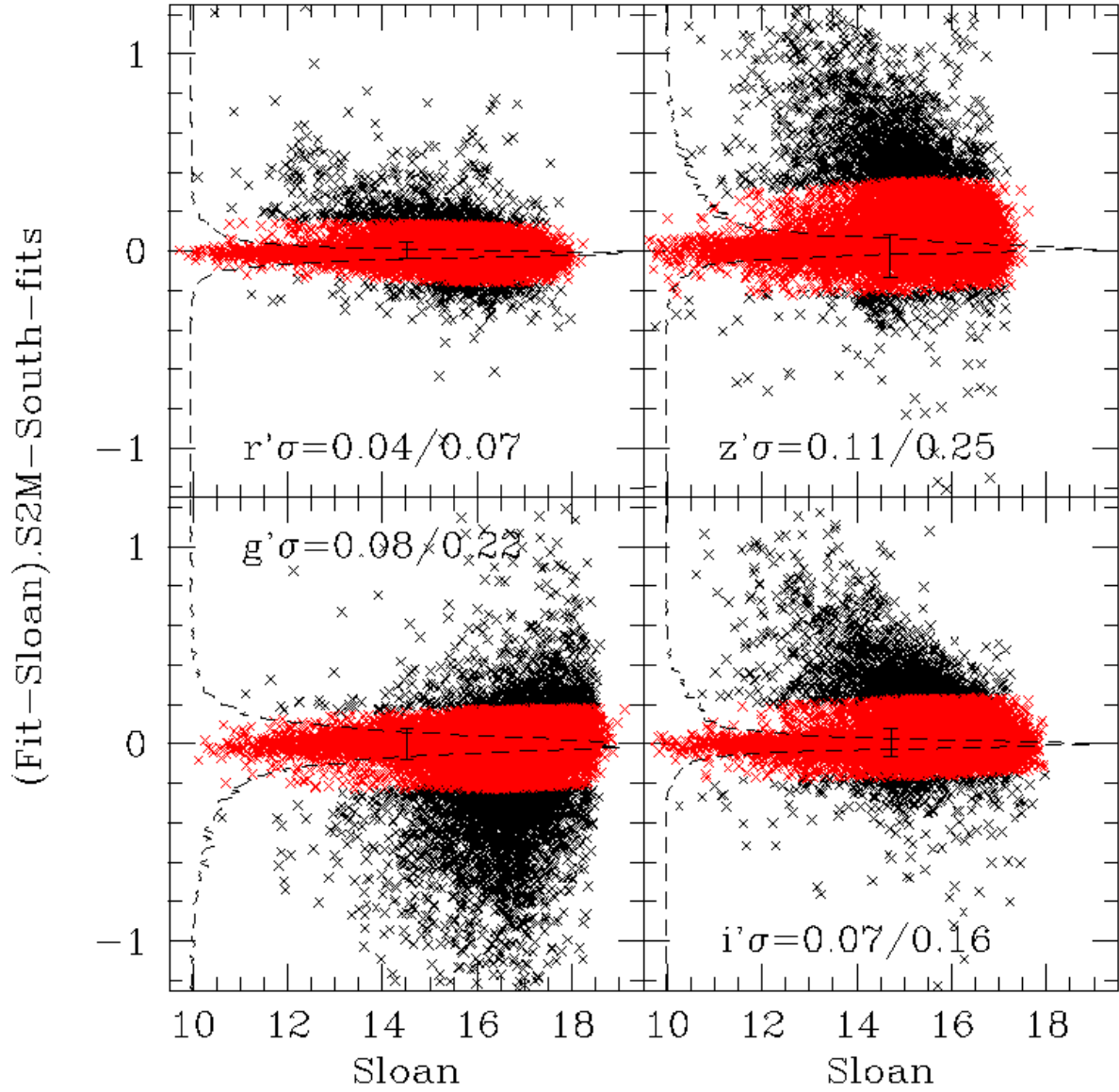


Fig. 20.— S2M fits with eight  $ugriz - JHK_{2/S}$  bands for  $\sim 16,000$  Southern SDSS standards, to  $g' \sim 19$  mag. Clipped/unclipped sigmas, histograms and error bars as before.

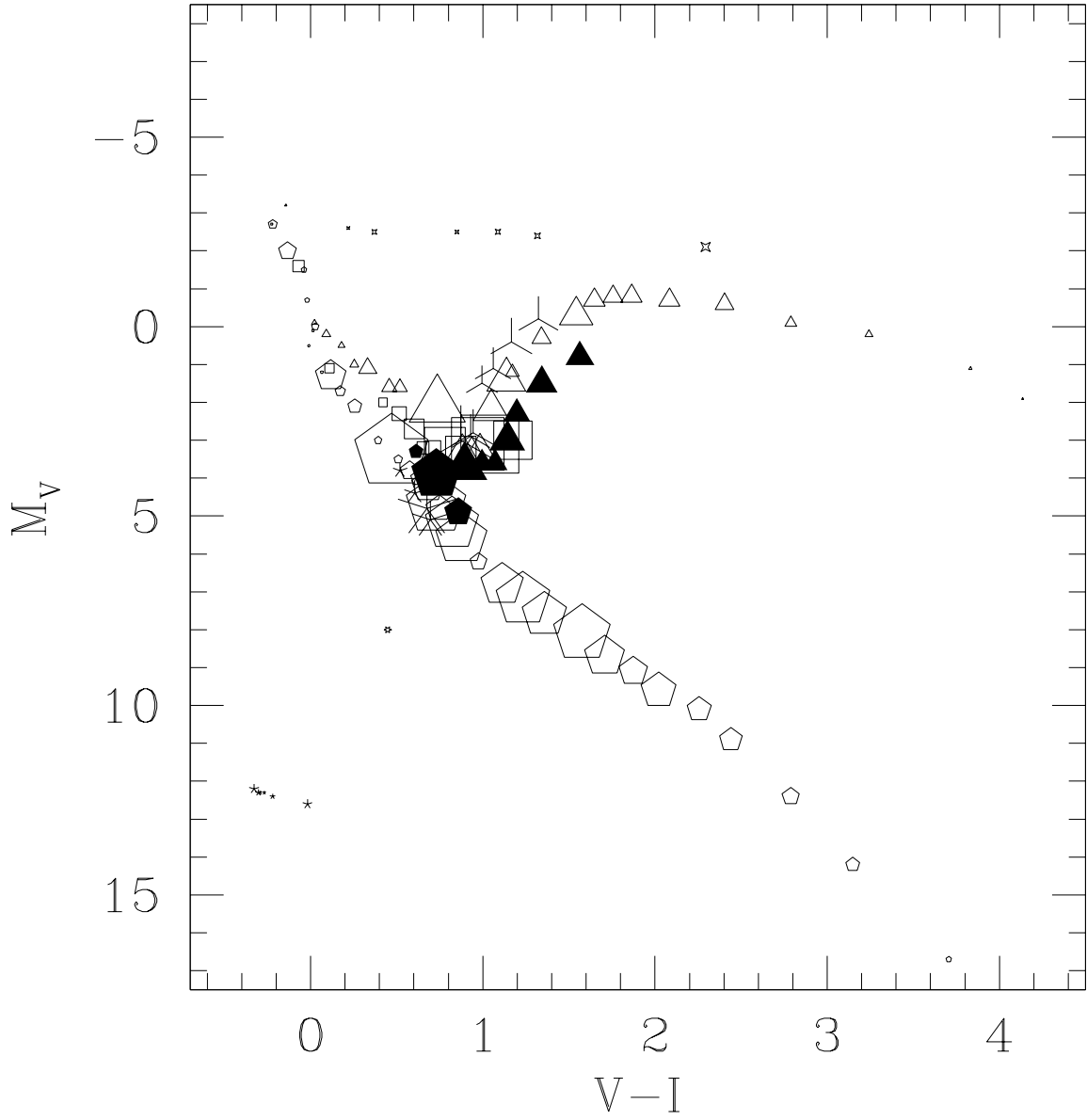


Fig. 21.— HR diagram for  $\sim 16,000$  SDSS Southern standards. Same symbols as fig 12

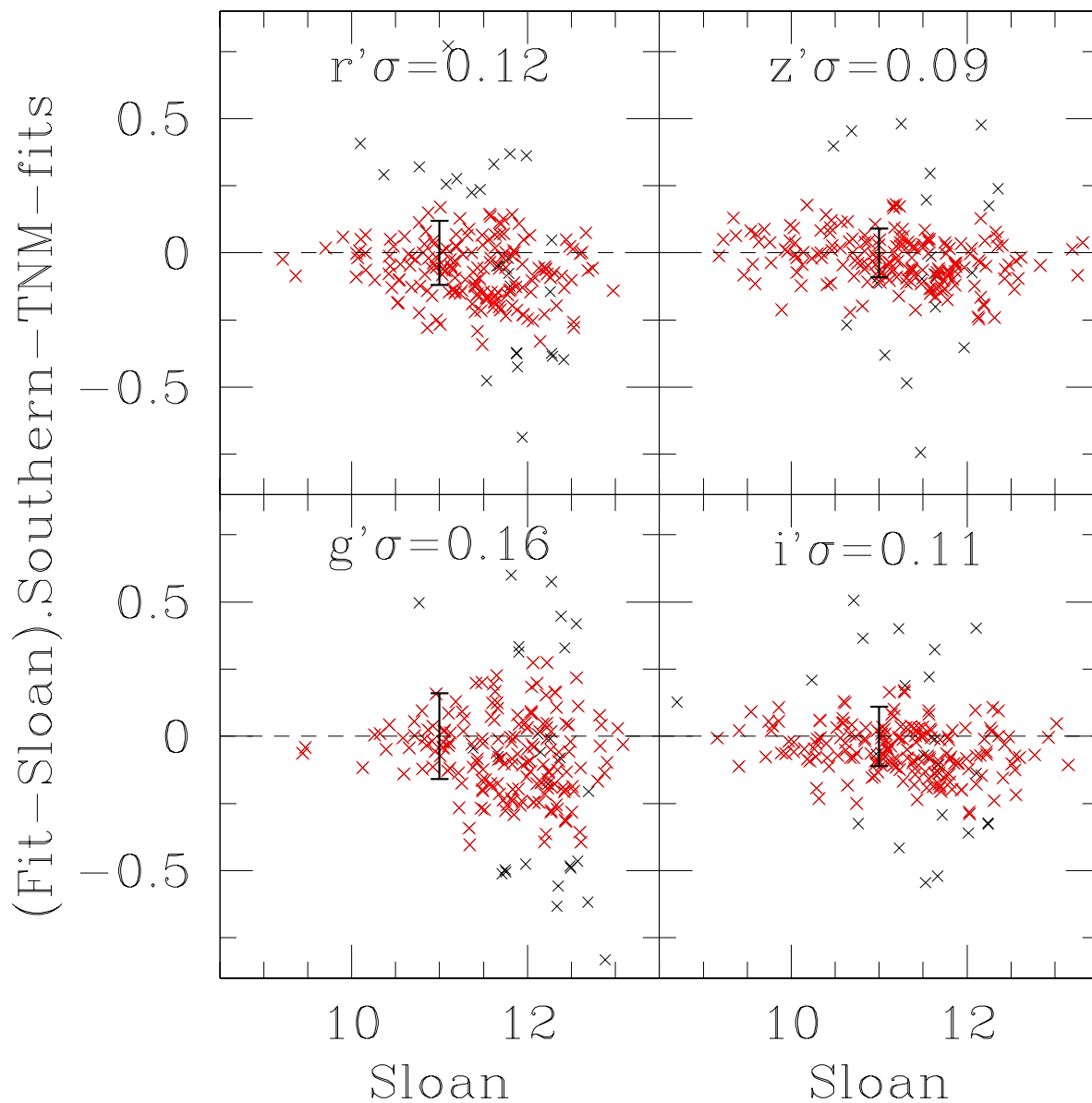


Fig. 22.— TNM fits with six  $B_T V_T R_N - JHK_{2/S}$  bands for 201 Southern SDSS standards with Nomad & Tycho2 magnitudes. The fits for  $g'r'i'z'$  are plotted as (Fit-Sloan) vs. Sloan magnitudes, with the clipped data shown as grey (red) crosses, with their clipped sigmas indicated in the panels, and as error bars. The black crosses were rejected by the sigma clipping process.

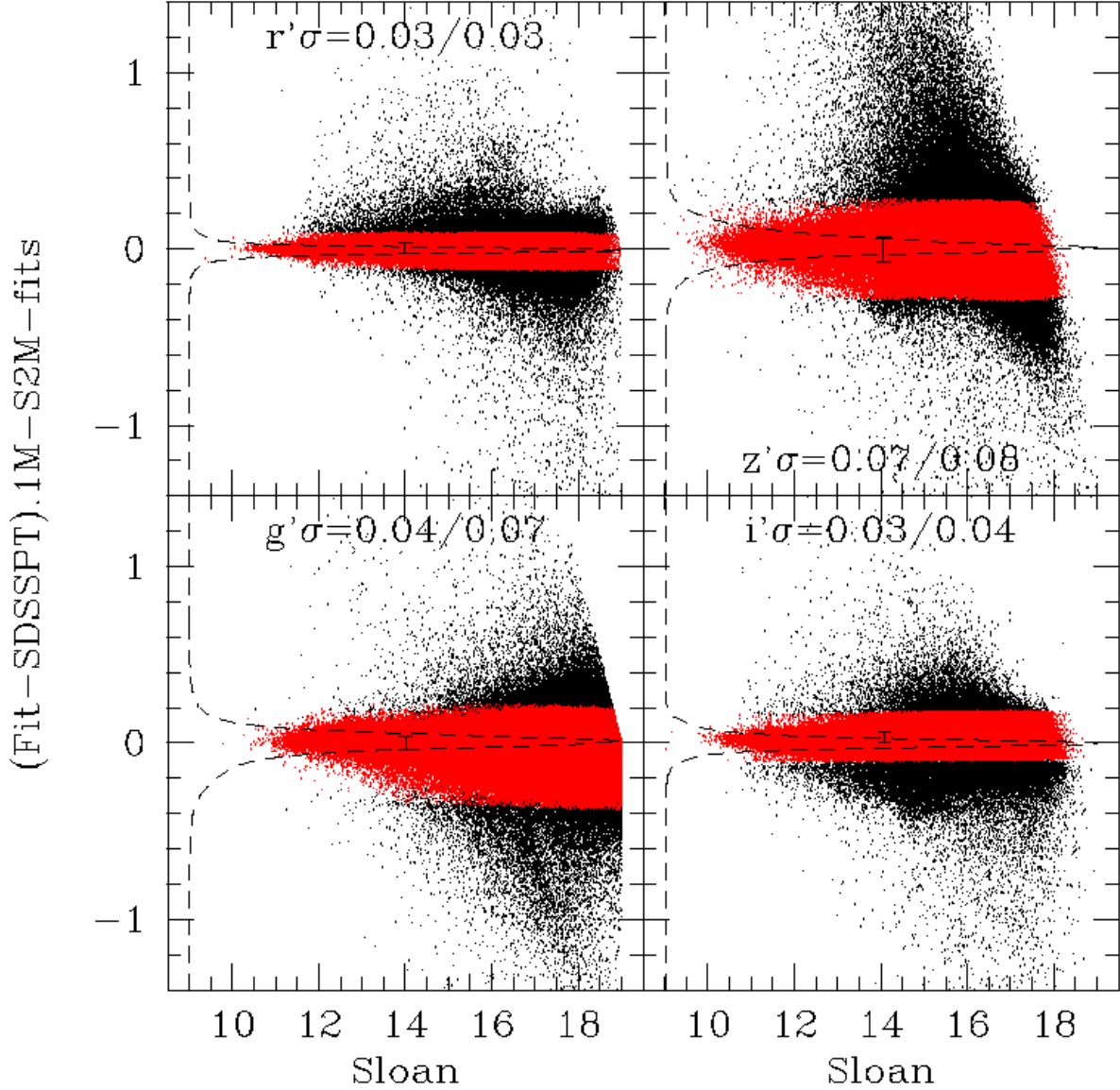


Fig. 23.— S2M fits with seven  $g'r'i'z'JHK_{2/s}$  bands for  $\sim 1$  M SDSS-PT standards with 2MASS magnitudes, to  $g' \sim 19$  mag. plotted as (Fit-SDSSPT) vs. SDSSPT magnitudes in separate panels for  $g'r'i'z'$ . Black dots show all the rejected stars. The grey bands through the middle (red in the electronic version) shows 91% of stars left after sigma clipping in  $g'$  and  $>95\%$  of stars left in  $r'i'z'$ . The dashed histograms show the number distribution of errors about the mean for all the stars. The annotated sigmas are to a limiting magnitude of 16 in each band / and for the full magnitude range.



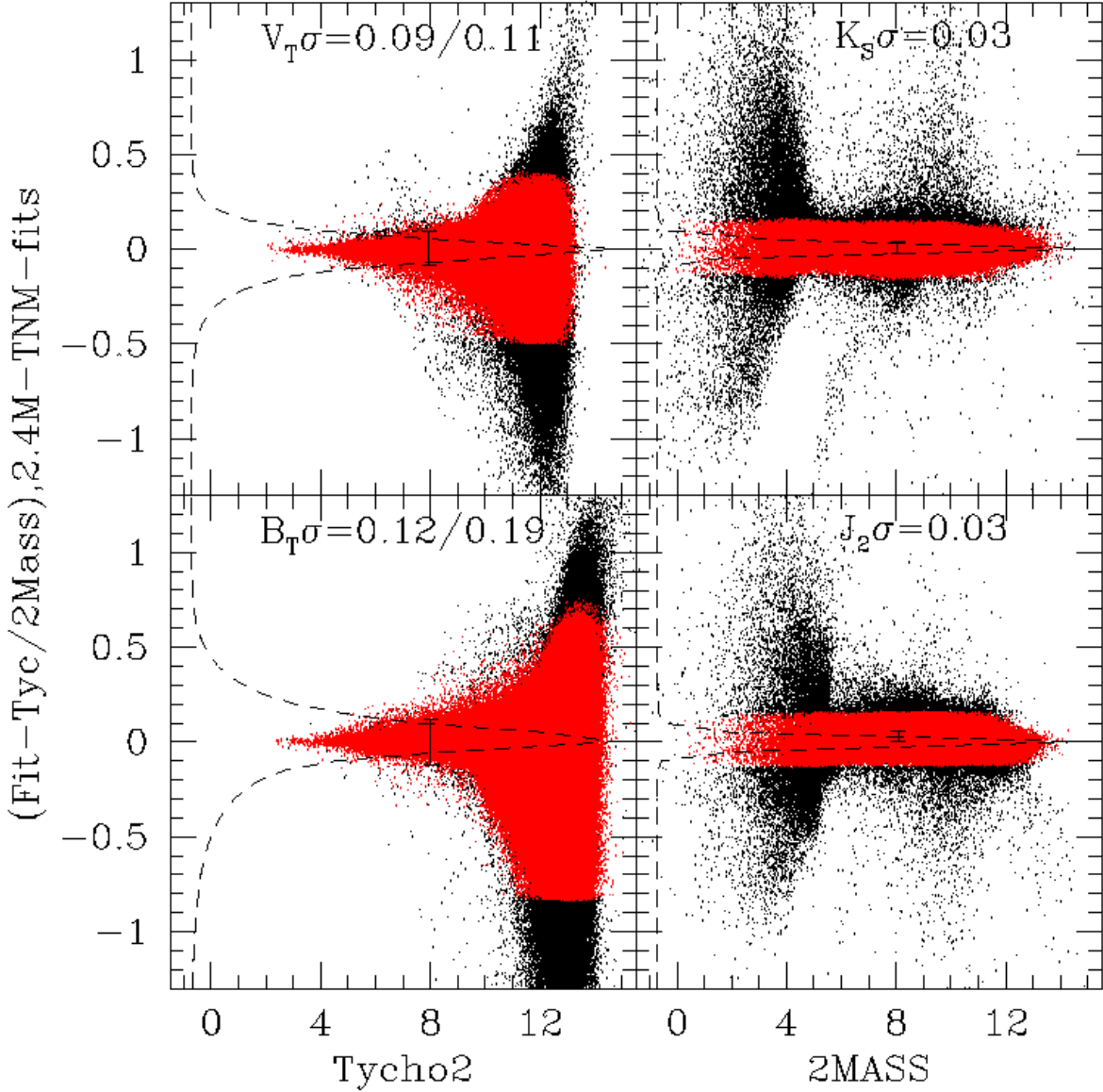


Fig. 25.— TNM fits with six  $B_T V_T R_N J_2 H_2 K_2$  bands for  $\sim 2.4$  M Tycho2 stars with NOMAD  $R_N$  and 2MASS  $JHK_2$  magnitudes, plotted as (Fit-catalog) vs. Tycho/2MASS catalog values on the abscissa. The Tycho2 catalog magnitudes vary between  $\sim 2.4$  to 16.5 mag. The 2MASS magnitudes reach as bright as -4.5 mag, but with significant errors there. Black dots show all the stars rejected by a  $3\sigma$  clip to give the fitted dispersions shown. The grey bands through the middle (red in the electronic version) show 95%, 96%, 99% and 99% of all stars left after sigma clipping in  $B_T V_T J_2 K_2$  respectively. The dashed histograms, which show the number distributions of errors about the zero delta line for all the stars, are quite strongly peaked around this line. The histograms are only slightly affected by the rejected points as there are comparatively few of them. The annotated sigmas are to a limiting magnitude of 13 & 12.5 mag in  $B_T V_T /$  and for the full magnitude range in each band.

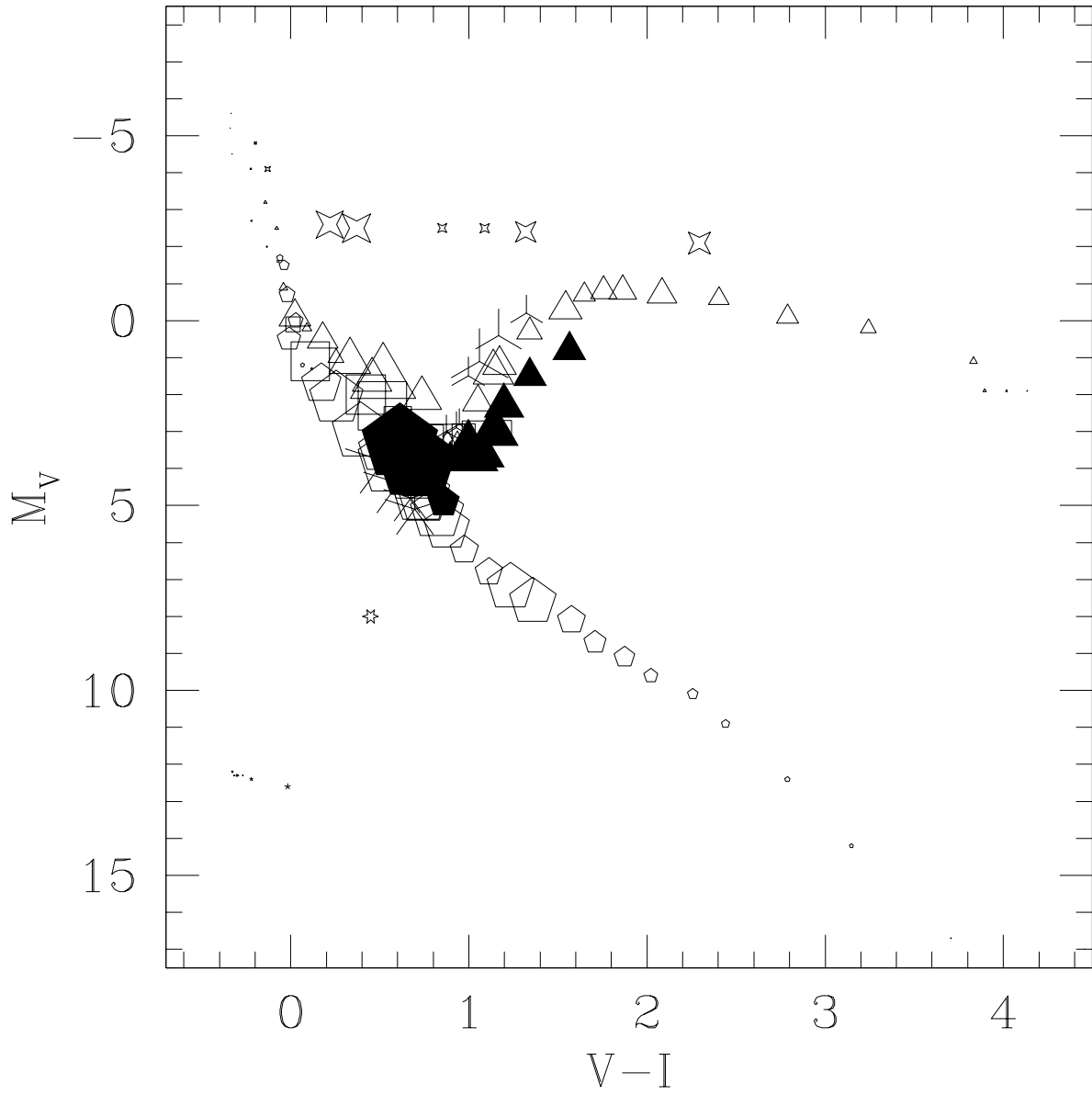


Fig. 26.— HR diagram for  $\sim 2.4 M$  Tycho2 stars. Same symbols as fig 12

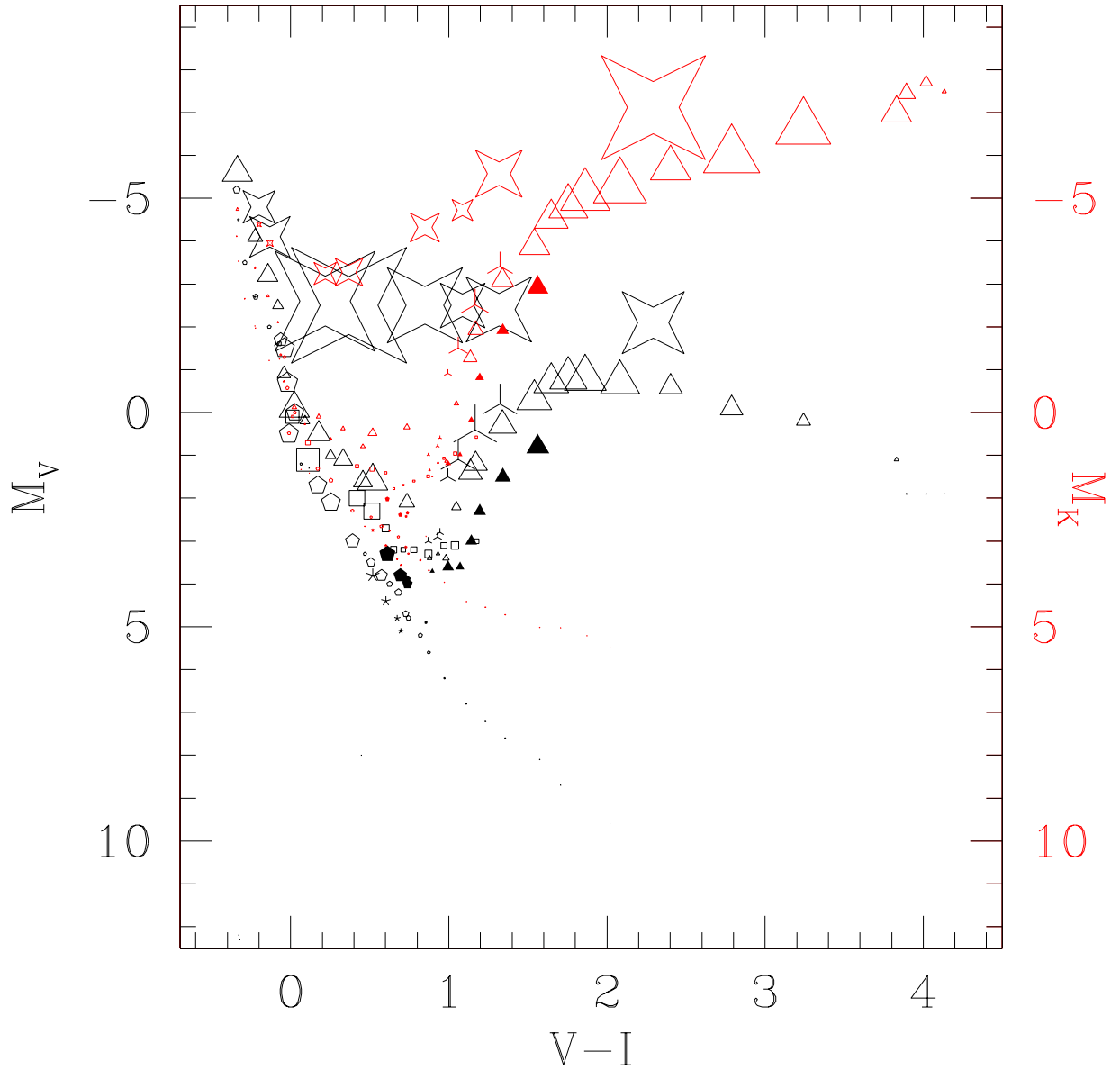


Fig. 27.— HR diagram for  $\sim 2.4M$  Tycho2 stars: The black symbols show the 141 library types plotted as  $M_V$  vs.  $V - I$ , where the area of the symbols is proportional to the V-light emitted by the stellar types. The grey symbols (red in the electronic version) occur on the same vertical line, and are plotted as  $M_K$  (on the right ordinate) vs.  $V - I$ , and the area of the symbols is proportional to the K-light emitted by the stellar types. Symbols as before.

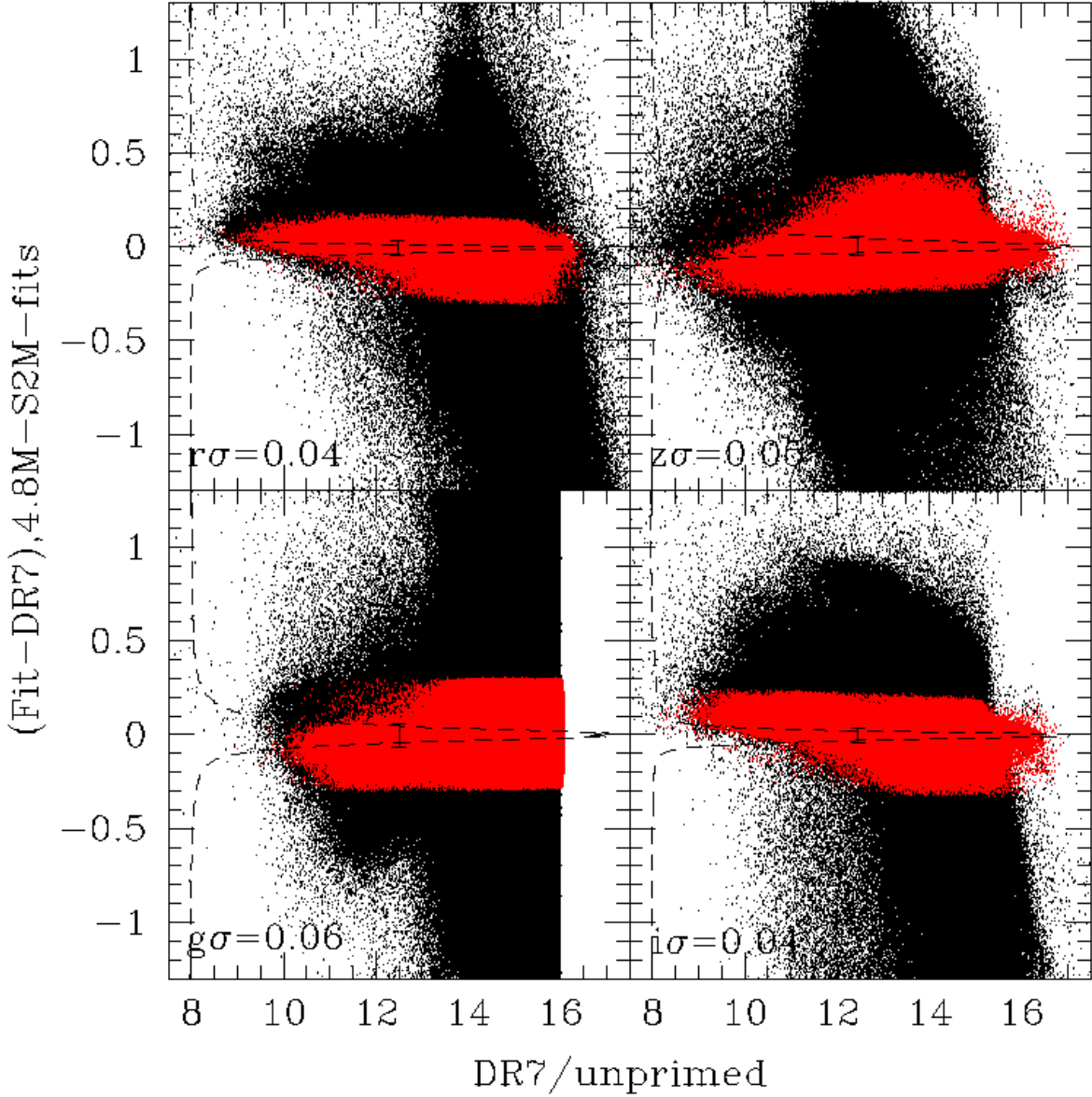


Fig. 28.— S2M fits with eight  $ugrizJHK_2$  bands for  $\sim 4.8$  M SDSS stars to  $g < 16$  with unprimed  $ugriz$  and 2MASS  $JHK_2$  magnitudes, plotted as (Fit-DR7) values on the ordinate and DR7 values on the abscissa. Black dots show all the stars rejected by an Rgz &  $3\sigma$  clip to give the fitted dispersions shown. The grey bands through the middle (red in the electronic version) show about 70% of stars left after Rgz & sigma clipping, The dashed histograms show the number distributions of errors. They are reasonably well peaked about the zero delta line, but there are a surprisingly large number of discrepant points at relatively bright magnitudes, and near the zero-delta line.

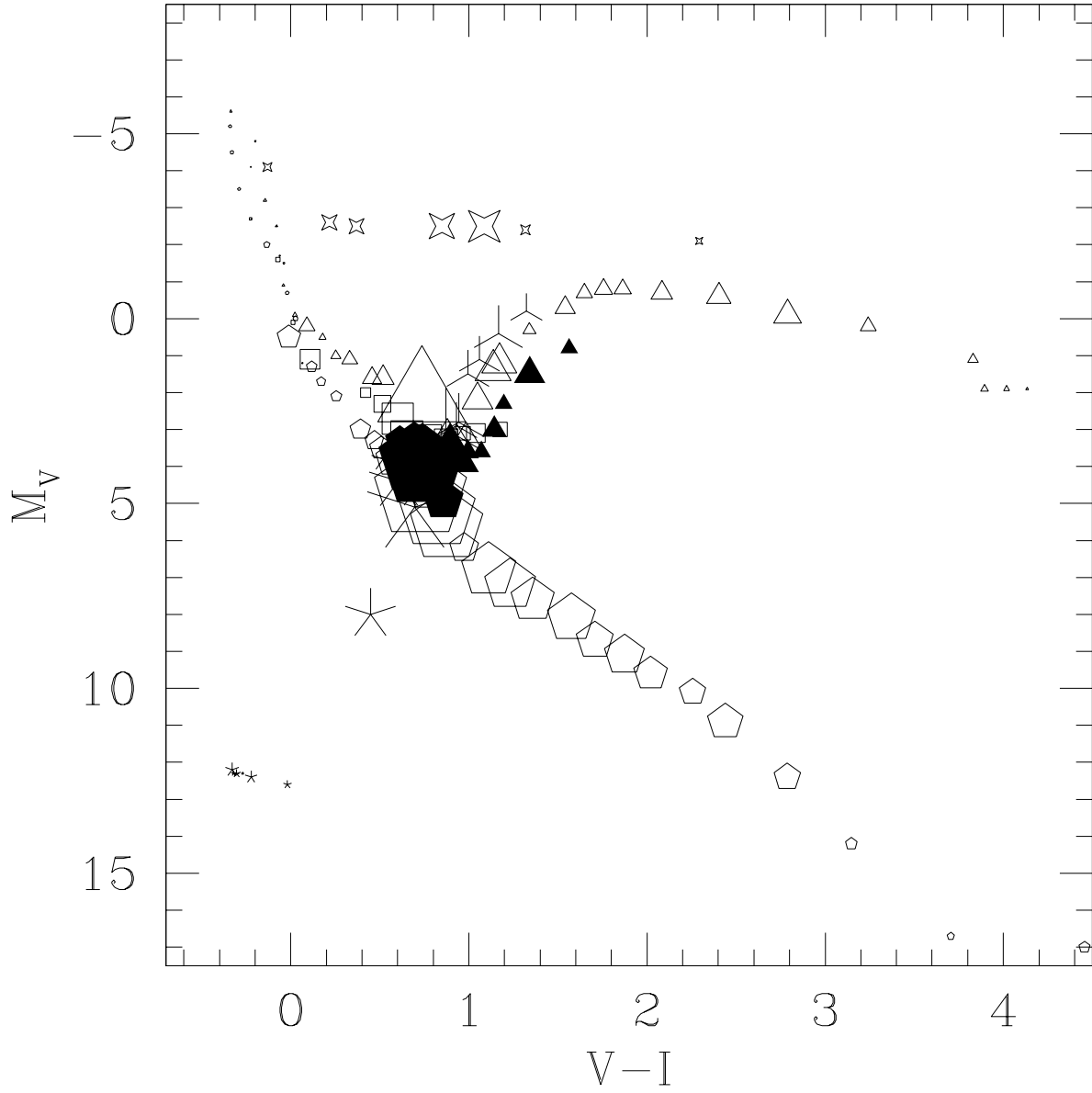


Fig. 29.— HR diagram for  $\sim 4.8 M$  SDSS stars to  $g < 16$ . Same symbols as fig 12, with symbol area proportional to number of occurrences.

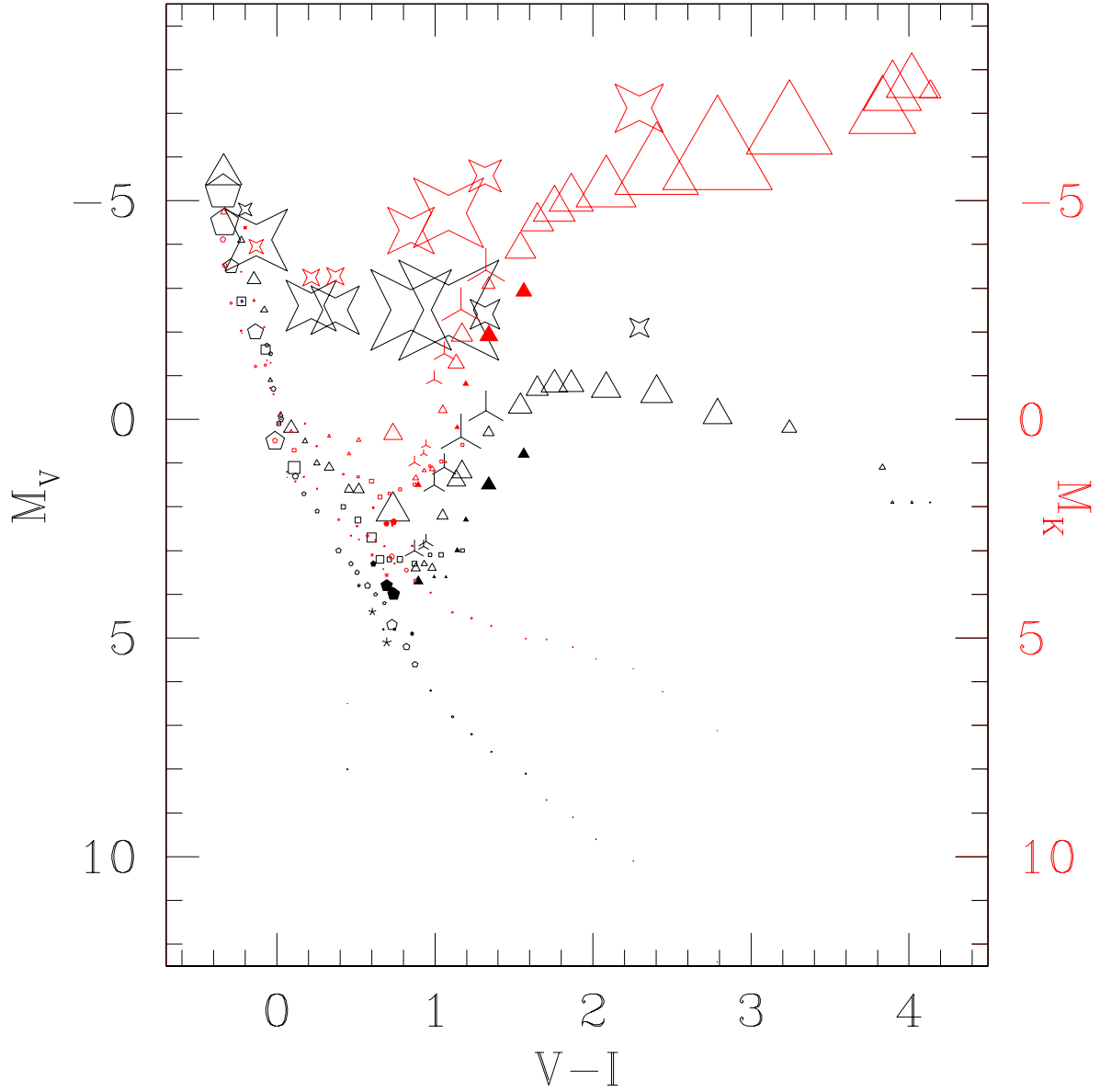


Fig. 30.— HR diagram for  $\sim 4.8$  M SDSS stars to  $g < 16$ : Symbols as before, with black symbols plotted as  $M_V$  vs.  $V - I$ , grey (red) symbols plotted as  $M_K$  vs.  $V - I$ , and symbol area proportional to the V-light or K-light emitted by the stellar types.

Table 1. Photometric Data for STIS\_NIC\_003 Calspec Standards

| StdName          | G191B2B | GD 153  | GD 71   | BD+17 4705 | AGK+81 266 | GRW+70 5824 | LDS 749B | F110   | HD209458 | VB8     | P041C   | P177D   | P330E   |
|------------------|---------|---------|---------|------------|------------|-------------|----------|--------|----------|---------|---------|---------|---------|
| Type             | DA0     | DA0     | DA1     | sdF8       | sdO        | DA3         | DBQ4     | D0p    | G0V      | M7V     | G0V     | G0V     | G0V     |
| B-V              | -0.33   | -0.29   | -0.25   | 0.44       | -0.34      | -0.09       | -0.04    | -0.31  | 0.59     | 1.92    | 0.62    | 0.66    | 0.64    |
| V-I              | -0.33   | -0.3:   | -0.3:   | 0.62       | -0.35      | -0.21       | -0.2:    | -0.31  | 0.7:     | 4.6     | 0.7:    | 0.7:    | 0.7:    |
| <b>Tycho</b>     |         |         |         |            |            |             |          |        |          |         |         |         |         |
| $B_T$            | 11.354  |         |         | 9.969      | 11.482     |             |          | 11.440 | 8.334    |         | 13.00:  |         |         |
| $V_T$            | 11.65:  |         |         | 9.505      | 11.89:     |             |          | 11.49: | 7.699    |         | 12.24:  |         |         |
| <b>Landolt</b>   | LU      | HB      | L09     | LU         | LU         | LU          | LU       | LU     |          | B91     | cal/lib | cal/lib | cal/lib |
| U                | 10.250  | 11.860  | 11.675  | 9.724      | 10.392     | 11.807      | 13.717   | 10.360 |          |         |         |         |         |
| B                | 11.455  | 13.060  | 12.785  | 9.907      | 11.596     | 12.682      | 14.634   | 11.527 |          | 18.7:   | 12.62:  | 14.13:  | 13.64:  |
| V                | 11.781  | 13.346  | 13.033  | 9.464      | 11.936     | 12.773      | 14.674   | 11.832 |          | 16.78   | 12.00:  | 13.47:  | 13.00:  |
| R                | 11.930  | 13.484  | 13.171  | 9.166      | 12.090     | 12.873      | 14.675   | 11.970 |          | 14.60   | 11.65:  | 13.12:  | 12.65:  |
| I                | 12.108  | 13.665  | 13.337  | 8.846      | 12.281     | 12.979      | 14.676   | 12.145 |          | 12.31   | 11.28:  | 12.75:  | 12.28:  |
| <b>2MASS</b>     |         |         |         |            |            |             |          |        |          |         |         |         |         |
| $J_2$            | 12.543  | 14.012  | 13.728  | 8.435      | 12.692     | 13.248      | 14.894   | 12.548 | 6.591    | 9.776   | 10.864  | 12.245  | 11.781  |
| $H_2$            | 12.669  | 14.209  | 13.901  | 8.108      | 12.844     | 13.357      | 15.050   | 12.663 | 6.366    | 9.201   | 10.592  | 11.932  | 11.453  |
| $K_2/S$          | 12.764  | 14.308  | 14.115  | 8.075      | 12.985     | 13.451      | 15.217   | 12.796 | 6.308    | 8.816   | 10.526  | 11.861  | 11.432  |
| <b>UKIRT</b>     |         |         |         |            |            |             |          |        |          |         |         |         |         |
| $Z_V$            |         | 13.642  | 13.398  |            |            |             |          |        |          |         |         |         |         |
| $Y_V$            |         | 13.929  | 13.657  |            |            |             |          |        |          |         |         |         |         |
| $J_{MKO}$        |         | 14.085  | 13.710  |            |            |             |          |        |          | 9.86    |         | 12.212  | 11.772  |
| $H_{MKO}$        |         | 14.165  | 13.805  |            |            |             |          |        |          | 9.22    |         | 11.920  | 11.455  |
| $K_{MKO}$        |         | 14.296  | 13.899  |            |            |             |          |        |          | 8.85    |         | 11.865  | 11.419  |
| <b>Stromgren</b> |         | LF/HM   | W       |            |            | HM          | W/HM     | LF/HM/ |          |         |         |         |         |
| $u_s$            |         | 12.881  | 12.686  |            |            | 12.858      | 14.750   | 11.400 |          |         |         |         |         |
| $v_s$            |         | 13.194  |         |            |            | 12.890      | 14.793   | 11.650 |          |         |         |         |         |
| $b_s$            |         | 13.214  | 12.897  |            |            | 12.700      | 14.722   | 11.720 |          |         |         |         |         |
| $y_s$            |         | 13.350  | 13.120  |            |            | 12.800      | 14.687   | 11.860 |          |         |         |         |         |
| <b>Sloan-air</b> | HB      | HB/PT   | HB      | std        |            |             | convrtd  |        | convrtd  | PT      | PT      | PT      |         |
| $u'$             | 11.033  | 12.700  | 12.438  | 10.560     |            |             | 14.507   |        | 19.287   |         | 15.112  | 14.533  |         |
| $g'$             | 11.470  | 13.047  | 12.752  | 9.640      |            |             | 14.560   |        | 17.607   | 12.260  | 13.745  | 13.280  |         |
| $r'$             | 12.007  | 13.567  | 13.241  | 9.350      |            |             | 14.802   |        | 15.929   | 11.844  | 13.300  | 12.841  |         |
| $i'$             | 12.388  | 13.938  | 13.612  | 9.250      |            |             | 15.034   |        | 16.106   | 11.719  | 13.158  | 12.701  |         |
| $z'$             | 12.740  | 14.287  | 13.973  | 9.230      |            |             | 15.245   |        | 11.767   | 11.703  | 13.125  | 12.674  |         |
| <b>Sloan-vac</b> | convrtd | convrtd | convrtd | convrtd    |            |             | DR7      |        | DR7      | convrtd | convrtd | convrtd |         |
| u                | 11.033  | 12.700  | 12.438  | 10.560     |            |             | 14.507   |        | 19.287   |         | 15.112  | 14.533  |         |
| g                | 11.444  | 13.022  | 12.729  | 9.664      |            |             | 14.551   |        | 17.714   | 12.291  | 13.778  | 13.313  |         |
| r                | 11.996  | 13.557  | 13.231  | 9.356      |            |             | 14.797   |        | 16.027   | 11.851  | 13.308  | 12.849  |         |
| i                | 12.364  | 13.914  | 13.588  | 9.245      |            |             | 15.016   |        | 16.095   | 11.716  | 13.155  | 12.698  |         |
| z                | 12.740  | 14.287  | 13.973  | 9.230      |            |             | 15.245   |        | 11.767   | 11.703  | 13.125  | 12.674  |         |

Note. — References: B91: Bessell (1991); HB: Holberg & Bergeron (2006); HM: Hauck & Mermilliod (1998); LF: Lacombe & Fontaine (1981); L09: Landolt (2009); LU: Landolt & Uomoto (2007), W: Wegner (1983); PT: SDSS-PT secondary standard; DR7: SDSS DR7 release; convrtd: Converted with equations in section 3.6.

Notes: BD+17 4708 is an astrometric binary (Lu et al 1987).

Table 2. Photometric Data for NIC\_001, IUE\_004, Oke/Gunn and STIS\_001 Calspec Standards

| StdName          | KF08T3  | KF06T1  | G93-48  | GD 50   | G158-100 | BD+26 2606 | F34     |
|------------------|---------|---------|---------|---------|----------|------------|---------|
| Type             | K0.5III | K1.5III | DA3     | DA2     | dG/sdG   | sdF        | DA      |
| B-V              | 0.95    | 1.07    | -0.01   | -0.28   | 0.68     | 0.39       | -0.34   |
| V-I              | 0.98    | 1.09    | -0.2:   | -0.19   | 0.84     | 0.62       | -0.28   |
| <b>Tycho</b>     |         |         |         |         |          |            |         |
| $B_T$            |         |         | 12.24:  |         |          | 10.193     | 10.834  |
| $V_T$            |         |         | 13.20:  |         |          | 9.779      | 11.102  |
| <b>Landolt</b>   | est     | est     | L09     | L09     | LU       | LU         | LU      |
| U                |         |         | 11.942  | 12.596  | 15.511   | 9.910      | 9.613   |
| B                | 14.25:  | 14.59:  | 12.732  | 13.787  | 15.572   | 10.152     | 10.838  |
| V                | 13.30:  | 13.52:  | 12.743  | 14.063  | 14.891   | 9.714      | 11.181  |
| R                | 12.80:  | 12.96:  | 12.839  | 14.210  | 14.467   | 9.418      | 11.319  |
| I                | 12.32:  | 12.44:  | 12.938  | 14.388  | 14.051   | 9.109      | 11.464  |
| <b>2MASS</b>     |         |         |         |         |          |            |         |
| $J_2$            | 11.585  | 11.538  | 13.203  | 14.747  | 13.488   | 8.676      | 11.643  |
| $H_2$            | 11.090  | 10.987  | 13.286  | 14.863  | 13.117   | 8.934      | 11.563  |
| $K_{2/S}$        | 10.987  | 10.872  | 13.397  | 15.120  | 13.016   | 8.352      | 11.540  |
| <b>UKIRT</b>     |         |         |         |         |          |            |         |
| $Z_V$            |         |         | 12.937  | 14.396  | 13.808   |            |         |
| $Y_V$            |         |         | 13.143  | 14.688  | 13.738   |            |         |
| $J_{MKO}$        |         |         | 13.215  | 14.802  | 13.427   |            |         |
| $H_{MKO}$        |         |         | 13.255  | 14.878  | 13.059   |            |         |
| $K_{MKO}$        |         |         | 13.330  | 14.990  | 12.984   |            |         |
| <b>Stromgren</b> |         |         | W/HM    |         |          |            | W/HM    |
| $u_s$            |         |         | 12.945  |         |          |            | 10.585  |
| $v_s$            |         |         | 12.930  |         |          |            | 10.901  |
| $b_s$            |         |         | 12.722  |         |          |            | 11.026  |
| $y_s$            |         |         | 12.785  |         |          |            | 11.191  |
| <b>Sloan-air</b> |         |         | std     | convrtd | std      | std        | std     |
| $u'$             |         |         | 12.760  | 13.372  | 16.302   | 10.761     | 10.406  |
| $g'$             |         |         | 12.653  | 13.764  | 15.201   | 9.891      | 10.915  |
| $r'$             |         |         | 12.961  | 14.283  | 14.691   | 9.604      | 11.423  |
| $i'$             |         |         | 13.268  | 14.651  | 14.469   | 9.503      | 11.770  |
| $z'$             |         |         | 13.529  | 14.980  | 14.377   | 9.486      | 12.035  |
| <b>Sloan-vac</b> |         |         | convrtd | DR6     | convrtd  | convrtd    | convrtd |
| u                |         |         | 12.760  | 13.372  | 16.302   | 10.761     | 10.406  |
| g                |         |         | 12.641  | 13.738  | 15.238   | 9.914      | 10.891  |
| r                |         |         | 12.953  | 14.273  | 14.701   | 9.610      | 11.414  |
| i                |         |         | 13.247  | 14.628  | 14.469   | 9.499      | 11.747  |
| z                |         |         | 13.529  | 14.980  | 14.377   | 9.486      | 12.035  |

Note. — References: HM: Hauck & Mermilliod (1998); L09: Landolt (2009); LU: Landolt & Uomoto (2007), W: Wegner (1983); DR6: SDSS DR6 release; convrtd: Converted with equations in section 3.6.

Notes: BD +26 2606 is a spectroscopic binary, possibly variable, but at a level not significant here (Landolt & Uomoto 2007)

Table 3: ZeroPoints, Zero-Mag fluxes and Selected System/Filter bandpasses

| Filter              | $\lambda_{pivot}$<br>(nm) | Filter ZeroPoints |        |       |         | Vega STIS_005 |              | 0-Mag        | Selected |
|---------------------|---------------------------|-------------------|--------|-------|---------|---------------|--------------|--------------|----------|
|                     |                           | Nstd              | Mean   | Sigma | Adopted | Mag           | $F_\nu$ (Jy) | $F_\nu$ (Jy) | BandPass |
| <b>Tycho</b>        |                           |                   |        |       |         |               |              |              |          |
| $B_T$               | 419.6                     | 7                 | -0.108 | 0.045 | -0.11   | 0.046         | 3821         | 3985         | *        |
| $V_T$               | 530.6                     | 5                 | -0.030 | 0.020 | -0.03   | 0.016         | 3689         | 3746         | *        |
| <b>Landolt</b>      |                           |                   |        |       |         |               |              |              |          |
| $U_L$               | 354.6                     | 13                | 0.761  | 0.038 | +0.76   | 0.096         | 1609         | 1758         |          |
| $B_L$               | 432.6                     | 17                | -0.103 | 0.076 | -0.10   | -0.004        | 3979         | 3962         |          |
| $V_L$               | 544.5                     | 17                | -0.014 | 0.021 | -0.014  | 0.013         | 3646         | 3688         |          |
| $R_L$               | 652.9                     | 14                | 0.153  | 0.039 | +0.15   | 0.040         | 3079         | 3195         |          |
| $I_L$               | 810.4                     | 14                | 0.404  | 0.066 | +0.40   | 0.050         | 2407         | 2520         |          |
| <b>UBVRI</b>        |                           |                   |        |       |         |               |              |              |          |
| $U_M$               | 358.9                     | 13                | 0.763  | 0.027 | +0.76   | 0.005         | 1748         | 1755         | *        |
| $U_3$               | 364.6                     | 13                | 0.770  | 0.050 | +0.77   | -0.050        | 1830         | 1748         |          |
| $B_M$               | 437.2                     | 17                | -0.116 | 0.020 | -0.12   | 0.012         | 4003         | 4048         | *        |
| $B_3$               | 440.2                     | 17                | -0.124 | 0.024 | -0.12   | 0.012         | 4006         | 4050         |          |
| $V_M$               | 547.9                     | 17                | -0.014 | 0.010 | -0.014  | 0.019         | 3626         | 3690         |          |
| $V_C$               | 549.3                     | 17                | -0.014 | 0.008 | -0.014  | 0.021         | 3619         | 3691         | *        |
| $R_C$               | 652.7                     | 14                | 0.165  | 0.014 | +0.17   | 0.023         | 3066         | 3131         | *        |
| $R_p$               | 658.7                     | 13                | 0.192  | 0.030 | +0.19   | 0.025         | 2988         | 3058         |          |
| $I_C$               | 789.1                     | 14                | 0.386  | 0.016 | +0.39   | 0.031         | 2470         | 2542         | *        |
| <b>2MASS</b>        |                           |                   |        |       |         |               |              |              |          |
| $J_2$               | 1239.0                    | 15                | 0.913  | 0.022 | +0.91   | -0.016        | 1601         | 1577         | *        |
| $H_2$               | 1649.5                    | 15                | 1.352  | 0.024 | +1.35   | 0.018         | 1034         | 1050         | *        |
| $K_2/S$             | 2163.8                    | 15                | 1.830  | 0.018 | +1.83   | 0.008         | 670.3        | 674.9        | *        |
| <b>UKIRT</b>        |                           |                   |        |       |         |               |              |              |          |
| $Z_V$               | 877.6                     | 5                 | 0.583  | 0.038 | +0.58   | -0.069        | 2268         | 2128         | *        |
| $Y_V$               | 1020.8                    | 4                 | 0.607  | 0.031 | +0.61   | -0.011        | 2092         | 2072         | *        |
| $J_{MKO}$           | 1248.8                    | 4                 | 0.936  | 0.020 | +0.94   | -0.027        | 1570         | 1531         | *        |
| $H_{MKO}$           | 1673.0                    | 5                 | 1.395  | 0.022 | +1.40   | -0.014        | 1019         | 1006         | *        |
| $K_{MKO}$           | 2200.0                    | 5                 | 1.851  | 0.038 | +1.85   | 0.017         | 653.0        | 663.1        | *        |
| $E_{bol}$           | 1006.1                    | -                 | -      | -     | +1.40   | -0.194        | 1195         | 1000         |          |
| <b>Stromgren</b>    |                           |                   |        |       |         |               |              |              |          |
| $u_s$               | 346.1                     | 7                 | -0.290 | 0.035 | -0.29   | 1.431         | 1267         | 4734         | *        |
| $v_s$               | 410.7                     | 6                 | -0.316 | 0.012 | -0.32   | 0.189         | 4094         | 4871         | *        |
| $b_s$               | 467.0                     | 7                 | -0.181 | 0.024 | -0.18   | 0.029         | 4175         | 4288         | *        |
| $y_s$               | 547.6                     | 7                 | -0.041 | 0.030 | -0.04   | 0.046         | 3612         | 3768         | *        |
| <b>Sloan Air</b>    |                           |                   |        |       |         |               |              |              |          |
| $u'$                | 355.2                     | 12                | -0.033 | 0.021 | -0.03   | 0.974         | 1500         | 3680         | *        |
| $g'$                | 476.6                     | 14                | -0.009 | 0.027 | 0.00    | -0.093        | 3970         | 3643         | *        |
| $r'$                | 622.6                     | 14                | 0.004  | 0.020 | 0.00    | 0.148         | 3182         | 36y48        | *        |
| $i'$                | 759.8                     | 13                | 0.008  | 0.023 | 0.00    | 0.372         | 2587         | 3644         | *        |
| $z'$                | 890.6                     | 14                | 0.009  | 0.018 | 0.00    | 0.513         | 2263         | 3631         | *        |
| <b>Sloan Vacuum</b> |                           |                   |        |       |         |               |              |              |          |
| $u$                 | 355.7                     | 12                | -0.034 | 0.019 | -0.03   | 0.961         | 1517         | 3676         | *        |
| $g$                 | 470.3                     | 14                | -0.002 | 0.036 | 0.00    | -0.101        | 3994         | 3640         | *        |
| $r$                 | 617.6                     | 14                | 0.003  | 0.019 | 0.00    | 0.142         | 3197         | 3645         | *        |
| $i$                 | 749.0                     | 13                | 0.011  | 0.022 | 0.00    | 0.356         | 2624         | 3641         | *        |
| $z$                 | 889.2                     | 14                | 0.007  | 0.019 | 0.00    | 0.513         | 2263         | 3631         | *        |